University of Alberta

MODELING MOVEMENT, COMPETITION, AND INFECTION OF BACTERIA

by

Silogini Thanarajah

A thesis submitted to the Faculty of Graduate Studies and Research
in partial fulfillment of the requirements for the degree of

Doctor of Philosophy

in

Applied Mathematics

Department of Mathematical and Statistical Sciences

Fall 2013

Edmonton, Alberta

Abstract

Partial differential equations (PDEs) have been used to model the movement of bacteria, phages, and animals. Species movement and competition exist in many interesting practical applications such as dental plaque, animal movement, and infectious diseases. This dissertation consists of three main sections: bacterial competition in a petri dish, bacteria-phage interaction in a petri dish, and animal movements.

Competition of motile and immotile bacterial strains for nutrients in a homogeneous nutrient environment is dependent on the relevant bacterial movement properties. To study undirected bacterial movement in a petri dish, we modify and extend the bacterial competition model used in Wei et al. (2011) to obtain a group of more realistic PDE models. Our model suggests that in agar media the motile strain is more competitive than the immotile strain, while in liquid media both strains are equally competitive. Furthermore, we find that in agar as bacterial motility increases, the extinction time of the motile bacteria decreases without competition, but increases with competition. In addition, we show the existence of traveling-wave solutions mathematically and numerically.

To study the role of bacteriophage in controlling the bacterial population, we construct a group of bacteria-phage petri dish models. We present rigorous mathematical results and obtain insightful numerical results. The analysis of these models leads to an elegant explanation of species long term behavior, patient recovery time, and the most important factors affecting the growth rate of bacteria. Our results can potentially provide some guidance for future

phage therapy.

Motivated by the evolution of animal movement, we study competition of fast and slow moving animals by extending our bacteria model to incorporate a resource renewal term. We use linear and nonlinear resource uptake functions to run and test simulations. Conclusions from our linear model are consistent with Lotka-Volterra type models. Interestingly, our nonlinear model exhibits two new outcomes. If we further assume the fast mover has a larger resource uptake rate than the slow mover, it is possible that the slow mover is excluded by the fast mover.

Acknowledgements

Many people contributed to this dissertation in numerous ways, and I am grateful to all of them. First and foremost, I would like to acknowledge my supervisor, Prof. Hao Wang, for his consistent encouragement during my studies at University of Alberta. It has been an honor to be his first Ph.D. student. I appreciate all his contributions of time, ideas, and funding to make my Ph.D. experience productive and stimulating. Without his support, this project would not have been possible. His encouragement and enthusiasm were important for the completion of this project. Furthermore, I would like to thank the members of my supervisory committee for participating in my candidacy and final defence examination, and my thesis committee for reading this dissertation. Prof. Michael Li, Prof. Gerda de Vries, Prof. Henry J.J. Van Roessel, Prof. Bingtuan Li and Prof. Fangliang He provided valuable discussions and suggestions during my candidacy and final examination. Likewise, I would like to thank Dr. Aditya Raghavan, Dr. Qihua Huang, and Xihui Lin for encouraging and in-depth discussions on my research and programming. Also, I would like to thank the external committee member Prof. Bingtuan Li for his time and effort. Special thanks go to the center of mathematical biology (CMB) and all the CMB fellow members for a pleasant and friendly atmosphere.

I would like to thank the PIMS International Graduate Training Center (IGTC) in Mathematical Biology and the Department of Mathematical and Statistical Sciences at the University of Alberta for financial support.

Finally, I thank my family and friends for their support and affiliation during my graduate program.

Table of Contents

List of Tables

List of Figures

Chapter 1

Introduction

In the study of mathematical biology, researchers have been discussing the competition and interaction of microorganisms or animals that have different movement strategies in the presence of diffusive resources. The movement of microorganisms and animals is an important aspect of ecology. To uncover the outcomes of competing strategies, we construct a group of reaction diffusion models that incorporate movement, competition for diffusive resources, and viral infections. These reaction diffusion models provide a better understanding of the effect of spatial heterogeneity on population dynamics.

1.A Bacteria and Their Motility

How do bacteria swim towards or detect food? And how do they control this movement? With the help of flagella, bacteria can swim with pili by extending and retracting them inside the cell body. Depending on the rotation direction, several flagella either form a bundle or allow forward swimming or they "repel" each other and block swimming. For example, E. coli bacteria move by switch-

ing directions such as runs and random tumble motions. Bacterial chemotaxis is the movement toward (an attractant) or away from (a repellent) a chemical. In the absence of a chemical attractant, the bacterial strain swims randomly in runs, changing direction during tumbles. In the presence of an attractant, runs become biased, and the bacterial strain moves up the gradient of the attractant.

A few studies have been done to discuss the role of random motility on bacterial competition. The first bacterial competition model was developed in 1983 by Lauffenburger et al. (15) to study the effects of random motility in competition between two bacterial species in a non-mixed environment. They consider two populations of bacterial cells in a finite one-dimensional region of length L. They suggested that the effects of random motility are important in their own right, for system will exist where the nutrients present are not chemotactic stimuli. Here b_1 and b_2 are respectively, the densities of species 1 and species 2 and s is the substrate concentration. The model is given in the regin $0 < x < L$:

$$\begin{aligned} \frac{\partial b_1}{\partial t} &= \mu_1 \frac{\partial^2 b_1}{\partial x^2} + \left[f_1(s) - k_{e1}\right] b_1, \\ \frac{\partial b_2}{\partial t} &= \mu_2 \frac{\partial^2 b_2}{\partial x^2} + \left[f_2(s) - k_{e2}\right] b_2, \\ \frac{\partial s}{\partial t} &= D \frac{\partial^2 s}{\partial x^2} - \frac{1}{\gamma_1} f_1(s) b_1 - \frac{1}{\gamma_2} f_2(s) b_2. \end{aligned} \tag{1.1}$$

The boundary conditions are

$$x = 0; \quad \frac{\partial b_1}{\partial x} = \frac{\partial b_2}{\partial x} = \frac{\partial s}{\partial x} = 0$$

$$x = L; \quad \frac{\partial b_1}{\partial x} = \frac{\partial b_2}{\partial x} = 0 \quad s = s_0$$

where $f_i(s) = \frac{k_i s}{K_i + s}$; k_i is the maximum specific growth rate constant, K_i is the Monod saturation constant, k_{ei} is the specific death rate constant, γ_i is the yield coefficient, μ_i is the diffusion coefficient of bacterial species, $i = 1, 2$ and D is the diffusion coefficient of substrate.

Their goal was to provide the competition results of bacterial species that are differing in growth kinetics and motility properties, which species should survive or coexist and at what level or and in what proportion. The study found that cell motility properties have more effect on the steady state relative population sizes.

Results:

(1) There may be as many as three possible non-trivial steady state: only species 1 survives, only species 2 survives or both species coexist.

(2) The coexistence state can exist even though one species possesses a smaller intrinsic growth rate constant at all nutrient concentrations, if that same species is significantly less motile than the other species.

(3) The species with the smaller maximum specific growth rate may grow to a larger population than other.

In 1988, Kelly et al. (11) modified the previous model by using a simple unstructured model for cell growth and death to study the effect of chemotaxis on dynamics of microbial competition for a single rate-limiting nutrient in a confined nonmixed reign. They examined both transient and steady-state of competing species, mainly focusing on the effect of the cell random motility, and the cell chemotaxis. They found that, in general, there are four possi-

ble steady-state outcomes and in contrast to well-mixed systems, the slower-growing population can coexist and even exist alone if it possesses sufficiently superior motility and cheomotaxis properties. Further more, there is a minimum value of chemotaxis coefficient necessary for a chemotactic population to have a competitive advantage over an immotile population in a confined nonmixed system.

The above two models assume that bacterial growth is limited by a diffusing substrate from an adjacent phase not accessible to the bacteria, but our model has zero flux boundary conditions. Also, we assume that both species are genetically identical except for their motility properties.

The first bacterial competition in a petri dish model was developed in 2011 by Wei et al. (28) to study the existence of undirected motility in bacteria. Their focus was on what are the selection pressures responsible for the evolution and maintenance of undirected motility in bacteria. The two-dimensional model is provided by

$$\begin{aligned}
\frac{\partial b_M}{\partial t} &= D_M \left(\frac{\partial^2 b_M}{\partial x^2} + \frac{\partial^2 b_M}{\partial y^2} \right) + \frac{\alpha r}{r+k} b_M, \\
\frac{\partial b_N}{\partial t} &= D_N \left(\frac{\partial^2 b_N}{\partial x^2} + \frac{\partial^2 b_N}{\partial y^2} \right) + \frac{\alpha r}{r+k} b_N, \\
\frac{\partial r}{\partial t} &= D_r \left(\frac{\partial^2 r}{\partial x^2} + \frac{\partial^2 r}{\partial y^2} \right) - \frac{\nu r}{r+k} (b_M + b_N),
\end{aligned} \tag{1.2}$$

where $b_M = b_M(x, y, t)$ and $b_N = b_N(x, y, t)$ are respectively, the densities of the motile and a nonmotile bacteria, M and N, at a point (x, y) at a time t and $r = r(x, y, t)$ is the corresponding concentration of the resource. The monod constant k, the maximum per-capita rate ν, D_M, D_N and D_r are, respectively, the diffusion coefficients for the M and N bacteria and resource.

Their work was motivated by lab experimental results testing their theoretical predictions. They used different nutrient media such as agar and liquid in their experiments and a combination of mathematical models to generate and test a parsimonious and ecologically general hypothesis for the existence of undirected motility in bacteria: it enables bacteria to move away from each other and thereby obtain greater individual shares of resources in physically structured environment.

The main difference between the model of Lauffenburger et al. and Wei et al. is that Lauffenburger et al. model has different maximum specific growth rate for bacterial strains but same for Wei et al model. Also, Wei et al. model (28) assumes that the rate of bacterial mortality is negligible but it can be significant for long-term behavior of solutions, so we incorporate it into our model. We modify and study their model numerically and mathematically in chapter 2.

1.B Bacteriophages

What role does bacteriophage (phage) infection play in controlling the abundance of bacteria? Bacteriophages, viruses which infect and destroy bacteria, have been referred to as bacterial parasites, with each phage type replicating on a specific strain of host bacteria. There are two types of phage infection that are lytic and lysogenic. In the process of lytic phage infection, initially, a phage pierces the outer surface of a bacterium and injects viral DNA. Then, the DNA will take over the inner part of the bacterial cell and force them to make many copies of the phage. After the latent period, the bacterial cell breaks apart, releasing new phages that start the search for bacteria all over

again (43). The process of phage replication can be used to understand how phages have influenced the control of the bacterial density.

Some preliminary studies have discussed phage infection on host bacteria. In 2012, Jones et al. (40) proposed a reaction diffusion system to study virus spread on bacteria on an agar plate. They proved that an interval of possible spreading speeds for virus infection is established and traveling wave solutions are shown to exist. In 2011, Smith et al. (41) modified the previous model by incorporating virus mortality to study the virus infection in bacteria. They studied the model in its natural setting of a bounded domain which in the applications is the surface of a Petri dish. Their model can be reduced to a single delayed partial differential equation. They both assume that host bacteria in agar do not grow or diffuse but our model, introduced in chapter 3, is more realistic because we assume bacteria in agar grow and diffuse. The main departure of our model from theirs is that we incorporate nutrient dynamics explicitly. The Smith et al. (41) model is provided by

$$\begin{aligned} V_t &= d\Delta V - kBV + \beta kB(t-\tau,x)V(t-\tau,x) - \alpha V, \\ B_t &= -kBV \quad x \in \Omega,\, t > \tau, \\ I_t &= kBV - kB(t-\tau,x)V(t-\tau,x), \end{aligned} \tag{1.3}$$

where virus density is denoted by V, bacteria density is denoted by B, infected bacteria density is denoted by I, $\alpha \geq 0$ denotes virus decay rate, k denotes virus adsorption rate and the virus latent period is assumed to have duration exactly τ units of time.

In 2005, Weitz (48) introduced a chemostat model to study the co-evolutionary arms races between bacteria and bacteriophage. We introduce this model to

show the study of bacteria-phage interaction without using time delay. The model equations are provided by

$$\begin{aligned}
\frac{dR}{dt} &= -\omega(R - R_0) - \omega\gamma\frac{RN}{R+K}, \\
\frac{dN}{dt} &= -\omega N + \gamma\frac{RN}{R+K} - \phi NV, \\
\frac{dV}{dt} &= -\omega V + \beta\phi NV,
\end{aligned} \tag{1.4}$$

where nutrient density is denoted by R, bacteria density is denoted by N, virus density is denoted by V, φ is the adsorption constant, γ is the maximum growth rate, ω is a wash out rate, ϵ is a resource conversion rate, R_0 is the resource density, β is called the burst size, and K is the half-saturation constant.

1.C Slow and Fast Moving Animals

Why do animals move? Animals move for many reasons such as to access food, escape from predators, competition and other interactions. The choice between fast and slow movement involves a proportion between benefits and risks and the structure of landscape. Animal species live in landscapes where resources are renewable and diffusible. A species' competency may increase or decrease by their movement across landscape.

In 1998, Dockery et al. (34) proposed a reaction-diffusion model to study the evolution of slow dispersal rates. They considered n phenotypes of a species in a continuous but heterogeneous environment and the phenotypes differ only in their diffusion rates. Their focus was on the effect of spatial variability on its own by considering a haploid model of species where the only phenotypic

difference is the dispersal rate. The model is provided by

$$\frac{\partial u_i}{\partial t} = d_i \Delta u_i + u_i \left(a(x) - \sum_{j=1}^{n} u_j \right) + \epsilon \sum_{j=1}^{n} M_{ij} u_j \qquad (1.5)$$

$$\text{on} \qquad \Omega \times R_+ \qquad (1 \leq i \leq n),$$

where Δ is the Laplacian. Zero Neumann conditions $\frac{\partial u_i}{\partial v} = 0$ (where $\frac{\partial}{\partial v}$ signifies differentiation in the direction of the outward normal) are imposed on the boundary $\partial\Omega$ of Ω, representing the condition of no migration across $\partial\Omega$. When $\epsilon = 0$, i.e, there is no mutation. They showed that there is a strong evolutionary force causing the phenotype with the slowest diffusion rate to be favored.

Even though the Lotka-Volterra model is often blamed for its unrealistic assumptions, it provides a useful starting point for the development of a more mechanistic model of fast and slow moving animals. Our model differs from their Lotka- Volterra model in the important way that we incorporate nutrients explicitly. A reaction diffusion model which incorporates this new assumption is presented in chapter 4.

1.D Outline

In chapter 2, we present a reaction diffusion model to illustrate the effects of random motility on bacterial competition in a petri dish. This model was proposed by Wei (28) and employed a numerical approach. We expand it by adding the mathematical approach. The main difference between ours and Wei model is that we incorporate the mortality rate of bacteria. Similar

to Wei (28), we assume a homogeneous nutrient environment. Furthermore, a mathematical and numerical analysis provides unambiguous results such as steady states, traveling wave solutions, extinction time, and long term behavior regarding bacterial competition.

In chapter 3, we present a combination of reaction diffusion models to study the interaction between bacteria and phage in a petri dish. It is built on previous model proposed by Smith (41), but we incorporate nutrient explicitly to make our model more realistic. Also, mathematical and numerical analyses obtain more plausible results such as long term behavior, travelling wave solution, the effect of burst size and the effect of threshold value of burst size. In addition, we introduce two models that incorporate infected bacteria and resistant bacteria to study our model to fit the reality.

In chapter 4, we present a mechanistic extension of Dockery et al. model (34) to study the competition of fast and slow moving animals for renewable and diffusive resources. The main difference between our model and Dockery et al. (34) model is that we incorporate nutrients explicitly and include nonlinear resource uptake functions. Furthermore, we show more realistic results than other previous model results such as slow mover exclude fast mover or both coexist in oscillatory way.

In chapter 5, we compile and discuss our results, and suggest potential future work.

Chapter 2

Competition of Motile and Immotile Bacterial Strains in a Petri Dish

2.A Introduction

Bacteria are a major domain of single-celled microorganisms and play an essential role in the maintenance of energy and nutrients throughout our world. In most natural environments, bacteria compete with neighbors for space and nutrients (19). Bacteria can be beneficial or harmful to us when they grow and reproduce. Bacterial strains are recognized by their appearance, the types of nutrients they can grow on, the types of substances they produce, etc. Motile bacteria can move using flagella or glide over surfaces by movement mechanisms (30; 25). The majority of bacteria can display self-propelled movement (motility) under suitable conditions (4; 8). The most well studied bacterial cell movements are recognized as directed (runs) and undirected (tumbles).

When a bacterial cell moves towards a chemical (attractants) or directly away from a chemical (repellents), this process is called chemotaxis (22; 10; 30). In some cases, chemotaxis climbs a chemical gradient because of the chemical distribution. On the other hand, bacteria with flagella and other mechanisms can move in random directions (28). In the absence of chemotaxis, a species with a small enough random motility can grow to a larger population size than a second population with a greater growth rate (15).

Many existing theoretical studies assume that bacteria have to move in the direction of nutrients (19; 18; 5; 6). However, there have been a few papers that do not assume directional movement of motile bacteria (28; 14; 45). The recent PNAS paper (28) suggests that undirected movement has been overlooked in literature. In most cases, flagella evolved after motility was in place (28). Some types of bacteria, such as E.coli, move in a random direction when the coordinated motion of the flagella stops because the flagella has turned in the opposite direction (31; 32). In this theoretical work, we assume that bacteria have undirected movement to reach nutrients. Recent studies showed that motility provides a selective compensation in the unshaken cultures because motile cells could move actively to acquire growth-limiting nutrients (29). In addition, undirected motility can be more important in resource-homogeneous environments or when the chemicals are not chemotactic stimuli.

Our work is motivated by the experimental observations of Wei (28). We extend a Wei (28) model by including mortality rates to study the competitive results of motile and immotile bacterial strains in a finite one and two-dimensional, non-mixed region. They presented their results numerically but we will present mathematically and numerically. Our motivation is to test whether the model is suitable for elucidating bacterial random motility by

comparing numerical results with the experimental results of Wei (28). Thus, on the basis of the work in (28), section 2.B aims at presenting the general reaction diffusion model for agar case. In section 2.C, we will study mathematical results such as steady states, traveling wave solutions, and long term behavior for single bacterial strain compete for nutrients. In section 2.D, We will introduce the model for liquid case and study the will discuss the numerical results in section 2.F.3. In section 2.E, we will obtain an additional results for extinction time (for long term competition) of bacteria. In section 2.F, we will introduce the reaction diffusion model for two competing bacterial strains. Also, we will present the mathematical results for agar case and will present the numerical results for agar and liquid cases.

Our focus in this chapter is to use bacteria as a model organism to study the competition of two strains in a petri dish. The assumption for our model is that there are two kinds of bacterial strains: the motile strain that moves quickly and the immotile strain that moves very slowly (27; 17). Nutrient media varies from agar to liquid by changing the nutrient diffusion rate. We apply this theoretical framework to verify the existence of undirected motility in bacterial movement and discuss the role of motility and nutrient medium types in determining bacterial competition. Our model address this issue by include only random motility for bacteria. Our simulation results exhibit that the role of undirected motility is preferred by bacteria in the agar case because it increases the chance of getting nutrients. We run one-dimensional spatial simulations to compute extinction times, traveling-wave solutions and the total densities of both bacterial strains, and we run two-dimensional spatial simulations to exhibit pattern formation. We present rigorous mathematical analysis of steady states, asymptotical behaviors of solutions, and traveling-wave so-

lutions. Our PDE model can elucidate and validate petri dish experimental result which is undirected motility enables bacteria to move away from each other and thereby obtain greater individual shares of resources in physically structured environments (28).

2.B Mathematical Model for Agar Case

In literature, many papers have considered the directed and undirected movements of bacteria (28; 45; 14; 19; 18). We extend the existing model (28) to incorporate mortality rates and general diffusion terms (especially in polar coordinates for the disk shape of petri dish). With these new components in the theoretical framework, we can discuss the long term behavior of solutions such as steady states, asymptotic behavior and extinction time.

Agar is a gelatinous substance made from red algae. It is used as a solid culture media for bacteria and other microorganisms. We consider the reaction-diffusion competition model for agar media as follows:

$$\begin{aligned} \frac{\partial B_i}{\partial t} &= D_i \Delta B_i + \left[h_i(N) - \delta_i\right] B_i, \\ \frac{\partial N}{\partial t} &= -\sum_i \frac{1}{\gamma_i} h_i(N) B_i, \end{aligned} \tag{2.1}$$

where Δ is Laplacian, $i = 1, 2, \cdots, m$, $x \in \Omega$ and the consumption function $h_i(N)$ satisfies the conditions $h_i(0) = 0$, $h_i'(t) > 0$, and $h_i''(t) \leq 0$, for example, $h_i(N) = \alpha_i N/(k_i + N)$ or $h_i(N) = \alpha_i N$. Here m is a positive integer representing the number of competing bacterial species. The model has initial conditions: $N(0, x) = N_0$ for $x \in \Omega$, $B_i(0, x) = B_0$ (small and supported in a small disk) for each i on Ω, and Neumann boundary conditions (zero flux):

$\nabla B \cdot n = 0$ on $\partial\Omega$, where n is a outward normal vector to the boundary $\partial\Omega$. Here $B_i(t,x)$, $N(t,x)$ represent the density of ith bacterial strain and the density of nutrients respectively, with diffusion coefficients D_i. Ω is a bounded domain in $[0,L] \subseteq \mathbb{R}$ or $\mathbb{R}^2$, δ_i is a mortality rate, and γ_i is the yield constant ($1/\gamma_i$ units of nutrient are consumed in producing one unit of bacterial biomass). All parameters are nonnegative constants.

In the next few sections, we establish the case of a single bacterial strain (no competition) and the case of two competing bacterial strains (motile versus immotile). The liquid media case will be introduced for a comparison with the agar media case. Mathematical results will only be provided for agar models, which are our main focus.

2.C Single Bacterial Species

First, we consider the model for a single bacterial strain in one-dimensional and two-dimensional spaces. We perform rigorous mathematical analysis including uniform and non-uniform steady states, traveling-wave solutions, extinction of bacteria, and non-extinction of nutrients. Finally, we compute the extinction time of bacteria and determine its dependence on key parameters.

2.C.1 Mathematical Analysis

The single species model is provided by

$$\begin{aligned} \frac{\partial B}{\partial t} &= D\Delta B + (h(N) - \delta)B, \\ \frac{\partial N}{\partial t} &= -\frac{1}{\gamma}h(N)B, \qquad \text{where } \gamma < 1 \text{ is the yield constant,} \end{aligned} \tag{2.2}$$

the initial conditions are

$$B(0,x) = B_0 \quad \text{(small and supported in a small disk)},$$
$$N(0,x) = N_0,$$

and the boundary conditions are

$$\frac{\partial B}{\partial x}(t,0) = \frac{\partial B}{\partial x}(t,L) = 0 \quad \text{on} \quad \partial\Omega.$$

Our first theorem states steady state results for one-dimensional and two-dimensional (disk case) spaces.

Theorem 2.1: *The system (2.2) with Neumann boundary conditions admits infinitely many steady states* $(0, \overline{N})$ *where* $\overline{N} \geq 0$.

Proof: We consider the one-dimensional space case and the two-dimensional space (disk petri dish) case separately.

For spatially uniform steady states where solutions are independent of time and space, we have the following algebraic equations

$$\begin{aligned} (h(N) - \delta)B &= 0, \\ -\frac{1}{\gamma}h(N)B &= 0. \end{aligned} \tag{2.3}$$

The second equation of (2.3) implies $B = 0$ or $N = 0$.

If $B = 0$, then $N \geq 0$.

If $N = 0$, substituting it into the first equation of (2.3) leads to $B = 0$.

For spatially non-uniform steady states, where solutions are independent of

time, we have the following equations

$$\begin{aligned} D\frac{d^2B}{dx^2} + (h(N) - \delta)B =& 0, \\ -\frac{1}{\gamma}h(N)B =& 0. \end{aligned} \tag{2.4}$$

The second equation of (2.4) implies $B = 0$ or $N = 0$.

If $B = 0$, then $N \geq 0$.

If $N = 0$, then substituting it into the first equation of (2.4) leads to

$$D\frac{d^2B}{dx^2} - \delta B = 0. \tag{2.5}$$

From steady states we can see that $B(x) = 0$ is always a solution of the above equation. Therefore we shall look for solutions other than the trivial zero solution. Let $B = e^{wx}$, where w is a constant ready to be determined, then the equation (2.5) leads to $w^2 - \frac{\delta}{D} = 0$, and thus the solution is

$$B = C_1 e^{wx} + C_2 e^{-wx}. \tag{2.6}$$

One important characteristic of a boundary value problem is that it may not have a solution, while the initial value problem always has a solution and the solution is unique. For the equation (2.5), there is no solution when $\delta/D > 0$. We can prove this as follows: Suppose there is a solution, then it must be

$$B = C_1 e^{\sqrt{\frac{\delta}{D}}x} + C_2 e^{-\sqrt{\frac{\delta}{D}}x} \tag{2.7}$$

for some constants C_1 and C_2 and we can solve the constants using boundary conditions $\frac{\partial B}{\partial x}(0,t) = \frac{\partial B}{\partial x}(L,t) = 0$. Thus $C_1 = C_2 = 0$. Therefore the equation

(2.5) has only zero solution ($\delta > 0$, $D > 0$). $\square$

Now we consider the single species model in a petri dish $\Omega = \mathbb{R}^2$ (disk shape)

$$\begin{aligned} \frac{\partial B}{\partial t} =& D(B_{xx} + B_{yy}) + (h(N) - \delta)B, \\ \frac{\partial N}{\partial t} =& -\frac{1}{\gamma}h(N)B, \end{aligned} \tag{2.8}$$

or equivalently in polar coordinates

$$\begin{aligned} \frac{\partial B}{\partial t} &= D\left(B_{rr} + \frac{1}{r}B_r + \frac{1}{r^2}B_{\theta\theta}\right) + (h(N) - \delta)B, \\ \frac{\partial N}{\partial t} &= -\frac{1}{\gamma}h(N)B. \end{aligned} \tag{2.9}$$

Spatially uniform steady states are similar to the one-dimensional space case.

Now we discuss spatially non-uniform steady states.

The second equation of (2.9) implies $B = 0$ or $N = 0$.

If $B = 0$ then $N \geq 0$.

If $N = 0$ then

$$B_{rr} + \frac{1}{r}B_r + \frac{1}{r^2}B_{\theta\theta} - \frac{\delta}{D}B = 0, \tag{2.10}$$

That is,

$$\begin{aligned} \Delta B = \frac{\delta}{D}B \quad \text{in} \quad \Omega, \\ \frac{\partial B}{\partial n} = 0 \quad \text{in} \quad \partial\Omega, \end{aligned} \tag{2.11}$$

then the equation (2.11) has only zero solution. $\square$

From spatially uniform steady states and spatially non-uniform steady states,

we conclude that for both one-dimensional and two-dimensional cases, if $B = 0$ then $N \geq 0$ and if $N = 0$ then $B = 0$.

We study traveling-wave solutions for a system of two equations representing a single bacterial strain and nutrient. For simplicity, we only discuss one-dimensional space case. The influence of growth and random movement in a homogeneous environment affects the bacterial population generating a colony, leading to the formation of a traveling wave. Now we discuss the existence of traveling-wave solutions and their minimum traveling wave speed.

We are looking for traveling wave solutions to the reaction-diffusion model (2.2) in a homogeneous nutrient environment. Thus, we seek some solution $B(t, x)$, $N(t, x)$, that satisfies the following conditions:

(i) $B(t, x)$ tends to a solitary wave (see (9)) such that

$$B_x \to 0 \qquad \text{as} \qquad x \to \pm\infty,$$

$$B \to 0 \qquad \text{as} \qquad x \to \pm\infty,$$

and (ii) $N(t, x)$ tends to a transition wave (see (9)) such that

$$N \to 1 \qquad \text{as} \qquad x \to +\infty,$$

$$N \to n(-\infty)(= n) \qquad \text{as} \qquad x \to -\infty.$$

Note that $n(-\infty) = n$ is an unknown constant. Based on the above conditions, we have the following theorem.

Theorem 2.2: *The model (2.2) admits traveling-wave solutions of the form* $B(t,x) = \bar{B}(x-ct)$ *and* $N(t,x) = \bar{N}(x-ct)$ *connecting two steady states* $(0,n)$ *and* $(0,1)$ *if* $c \geq c^* = 2(\frac{D\sigma(1)}{\gamma})^{1/2}$ *such that* $N(-\infty) = n$ *and* $N(+\infty) = 1$, *where* $\sigma(\bar{N}_s) = -h(\bar{N}_s)\phi'(\bar{N}_s)$, $\phi(\bar{N}) = \gamma\left(1 - \bar{N} - \delta\int_{\bar{N}}^{1}\frac{d\bar{n}}{h(\bar{n})}\right)$. *The parameter* c *is the traveling wave speed.*

Proof: We look for traveling-wave solutions of the form

$$B(t,x) = \bar{B}(\eta), \qquad N(t,x) = \bar{N}(\eta),$$

where $\eta = x - ct$. With this specific form of traveling waves, the PDE system becomes an ODE system

$$\begin{aligned} -c\frac{d\bar{B}}{d\eta} &= D\frac{d^2\bar{B}}{d\eta^2} + (h(\bar{N}) - \delta)\bar{B}, \\ -c\frac{d\bar{N}}{d\eta} &= -\frac{1}{\gamma}h(\bar{N})\bar{B}. \end{aligned} \tag{2.12}$$

Letting $\frac{d\bar{B}}{d\eta} = R$, the equation (2.12) can be written as a system of first-order ODEs as follows

$$\begin{aligned} \frac{d\bar{B}}{d\eta} &= R, \\ \frac{dR}{d\eta} &= -\frac{c}{D}R - \frac{h(\bar{N}) - \delta}{D}\bar{B}, \\ \frac{d\bar{N}}{d\eta} &= \frac{1}{\gamma c}\bar{B}h(\bar{N}), \end{aligned} \tag{2.13}$$

and the critical points are all points on the $\bar{N}$ axis.

Integrating (2.12) from $-\infty$ to $+\infty$ implies

$$-c[\bar{B}]_{-\infty}^{+\infty} = D\left[\frac{dB}{d\eta}\right]_{-\infty}^{+\infty} + \int_{-\infty}^{+\infty}(h(\bar{N}) - \delta)\bar{B}d\eta,$$

$$\int_{-\infty}^{+\infty}(h(\bar{N})-\delta)\bar{B}d\eta=0 \qquad (\text{ since } B\to 0 \text{ as } x\to\pm\infty), \tag{2.14}$$

$$-c[\bar{N}]_{-\infty}^{+\infty}=-\frac{1}{\gamma}\int_{-\infty}^{+\infty}h(\bar{N})\bar{B}d\eta,$$

$$-c(1-n)=-\tfrac{1}{\gamma}\textstyle\int_{-\infty}^{+\infty}h(\bar{N})\bar{B}d\eta \tag{2.15}$$

(since $N\to 1$ as $x\to+\infty$, $N\to n$ as $x\to-\infty$).

$\frac{(2.14)}{\gamma}+$ (2.15) implies

$$c(1-n)=\tfrac{1}{\gamma}\textstyle\int_{-\infty}^{+\infty}\delta\bar{B}d\eta=c\delta\displaystyle\int_{n}^{1}\frac{d\bar{n}}{h(\bar{n})}$$

(replace $\bar{N}$ with $\bar{n}$ for integral).

From equation (2.13), we have

$$\frac{dR}{d\eta}=-\frac{c}{D}\frac{d\bar{B}}{d\eta}-\frac{\gamma c}{D}\frac{d\bar{N}}{d\eta}+\frac{\delta\gamma c}{D}\frac{1}{h(\bar{N})}\frac{d\bar{N}}{d\eta}.$$

Integrating it from $-\infty$ to $+\infty$ to get

$$\frac{D}{c}R=\phi(\bar{N})-\bar{B}, \tag{2.16}$$

where

$$\phi(\bar{N}) = \gamma\left(1 - \bar{N} - \delta\int_{\bar{N}}^{1}\frac{d\bar{n}}{h(\bar{n})}\right). \tag{2.17}$$

Obviously, we have $\phi(1) = 0$, and from equation (2.17), we have

$$\phi(n) = \gamma\left(1 - n - \delta\int_{n}^{1}\frac{d\bar{n}}{h(\bar{n})}\right) = \gamma(1 - n - (1 - n)) = 0.$$

This defines an invariant manifold for the system. If a trajectory starts on it, it stays on it, and since

$$\phi(n) = \phi(1) = 0,$$

$(0, 0, n)$, $(0, 0, 1)$ are both on it, we can reduce (2.13) to the planar system

$$\begin{aligned}\frac{d\bar{B}}{d\eta} &= \frac{c}{D}(\phi(\bar{N}) - \bar{B}),\\ \frac{d\bar{N}}{d\eta} &= (\gamma c)^{-1}\bar{B}h(\bar{N}).\end{aligned} \tag{2.18}$$

We need to look for eigenvalues at the critical points $(0, \bar{N}_s)$. The Jacobian matrix of the system (2.18) is

$$\begin{bmatrix}\bar{B}'\\ \bar{N}'\end{bmatrix} = \begin{bmatrix}-\frac{c}{D} & \frac{c}{D}\phi'(\bar{N}_s)\\ \frac{h(\bar{N}_s)}{\gamma c} & 0\end{bmatrix}\begin{bmatrix}\bar{B}\\ \bar{N}\end{bmatrix},$$

which leads to the characteristic equation at $(0, \bar{N}_s)$

$$\lambda^2 + \frac{c}{D}\lambda - \frac{1}{\gamma D}\phi'(\bar{N}_s)h(\bar{N}_s) = 0.$$

The set of eigenvalues for the above matrix is given by

$$\lambda_1 = \frac{-c + \sqrt{c^2 - \frac{4D}{\gamma}\sigma(\bar{N}_s)}}{2D},$$
$$\lambda_2 = \frac{-c - \sqrt{c^2 - \frac{4D}{\gamma}\sigma(\bar{N}_s)}}{2D},$$

where $\sigma(\bar{N}_s) = -h(\bar{N}_s)\phi'(\bar{N}_s)$.

The trajectory representing a wave must approach $(0, 0, n)$ as $\eta \to -\infty$, so it is necessary that one of the eigenvalues has positive real part if $-\sigma(n) < 0$. If this is the case, λ_1 and λ_2 are real. Similarly, the trajectory must approach $(0, 0, 1)$ as $\eta \to \infty$. We have the restriction on the wave speed that $c \geq 2(\frac{D\sigma(1)}{\gamma})^{1/2} \equiv c^*$. We see that $c \geq c^*$ is only the necessary condition. Hence the minimum traveling-wave speed is $c^* \equiv 2(\frac{D\sigma(1)}{\gamma})^{1/2} \leq c$, where $\sigma(\bar{N}_s) = -h(\bar{N}_s)\phi'(\bar{N}_s)$. Biologically, the bacterial population creates a symbiosis with nutrient source directing to the formation of traveling wave. In our case, the bacterial population invades a region of the petri dish where the nutrient is sufficient.
In Fig.2.1, we numerically show spreading speed for different diffusion rates of motile bacteria with long and short time periods. As the motility of motile bacteria increases, traveling waves propagate faster, thus it takes less time for motile bacteria to occupy the non-centered region of the petri dish. □

It follows from the second equation of (2.2) that for fixed $x \in \Omega$, the nutrient density $N(t, x)$ is monotone decreasing in t with the limit $N_\infty(x)$. Based on these results, we have the following theorems.

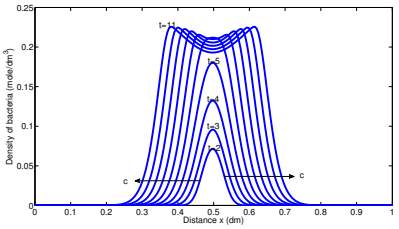

(a) Diffusion $D_1 = 0.0002$, $t = 11$

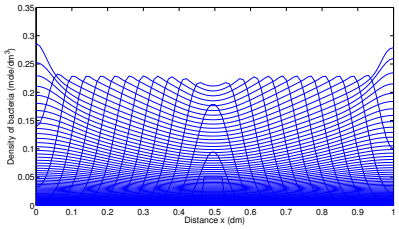

(b) Diffusion $D_1 = 0.0002$, $t = 101$

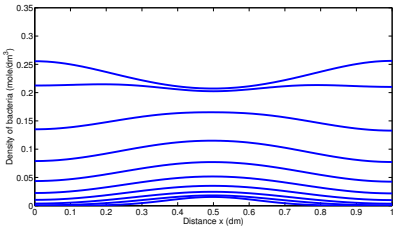

(c) Diffusion $D_1 = 0.008$, $t = 11$

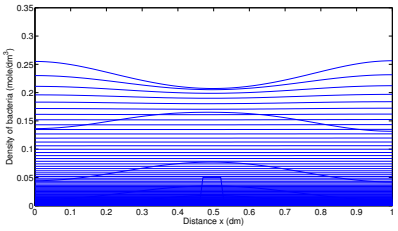

(d) Diffusion $D_1 = 0.008$, $t = 101$

Figure 2.1: Numerical simulations show the existence of traveling-wave solutions for the system (2.2) with $D_1 = 0.0002$ or $D_1 = 0.008$. We run simulations for the shorter time ($t = 11$) and the longer time ($t = 101$). Different curves represent different times. The details of panels (b), (c), (d) are similar to panel (a). The parameter c is the traveling wave speed. If we make a cross-section, the distances between any two consecutive curves are the same.

We define the total population of bacteria and nutrient as follows:

$$\widetilde{B}(t) = \int_\Omega B(t,x)dx \qquad \text{and} \qquad \widetilde{N}(t) = \int_\Omega N(t,x)dx.$$

Theorem 2.3: *The bacteria become extinct as $t \to \infty$. More precisely,*

$$\lim_{t\to\infty} \widetilde{B}(t) = 0.$$

Proof: Differentiating $\widetilde{B}(t)$ yields

$$\frac{d\widetilde{B}(t)}{dt} = \int_\Omega D\triangle B dx - \delta\widetilde{B}(t) - \gamma\frac{d\widetilde{N}(t)}{dt}.$$

The integral is zero by the zero flux hypothesis and Stoke's theorem. We thus obtain the ODE

$$\frac{d\widetilde{B}(t)}{dt} + \delta\widetilde{B}(t) = -\gamma\widetilde{\frac{dN(t)}{dt}}.$$

By the Method of Variation of Parameters, the solution can be written as

$$\widetilde{B}(t) = \widetilde{B}(0)e^{-\delta t} - \gamma\int_0^t e^{-\delta(t-s)}\frac{d\widetilde{N}(s)}{ds}ds. \tag{2.19}$$

We decompose the integral from 0 to t into two sub integrals $[0,\sqrt{t}]$ and $[\sqrt{t},t]$. Integrating by parts we obtain

$$-\int_0^{\sqrt{t}} e^{-\delta(t-s)}d\widetilde{N}(s)dsds = -e^{-\delta(t-\sqrt{t})}\widetilde{N}(\sqrt{t}) + e^{-\delta t}\widetilde{N}(0) + \delta\int_0^{\sqrt{t}}\widetilde{N}(s)e^{-\delta(t-s)}ds.$$

Since $N(t,x)$ is monotone decreasing in t, it follows that $\widetilde{N}(t)$ is also monotone

decreasing in t, and thus

$$-\int_0^{\sqrt{t}} e^{-\delta(t-s)}\frac{d\widetilde{N}(s)}{ds}ds \leq -e^{-\delta(t-\sqrt{t})}\widetilde{N}(\sqrt{t}) + e^{-\delta t}\widetilde{N}(0) + \delta\sqrt{t}\widetilde{N}(0)e^{-\delta(t-\sqrt{t})}.$$

All terms on the right hand side approach zero as $t \to \infty$. Estimating the second sub integral is even easier, since

$$-\int_{\sqrt{t}}^{t} e^{-\delta(t-s)}\frac{d\widetilde{N}(s)}{ds}ds \leq -\int_{\sqrt{t}}^{t}\frac{d\widetilde{N}(s)}{ds}ds = -(\widetilde{N}(t) - \widetilde{N}(\sqrt{t})).$$

Since the limits of $\widetilde{N}(t)$ and $\widetilde{N}(\sqrt{t})$ as t approaches infinity coincide, the difference is zero, and thus the second sub integral approaches zero as $t \to \infty$.

Theorem 2.4: *When the consumption function $h(N)$ takes natural forms αN or $\frac{\alpha N}{k+N}$, then nutrient never gets completely consumed at any position. More precisely, if $N(0,x) > 0$, then $N_\infty(x) = \lim_{t\to\infty} N(t,x) > 0$.*

Proof: The claim follows if we can prove that

$$\int_0^\infty B(t,x)dt < \infty.$$

Let

$$\mathcal{B}(t,x) = \int_0^t B(s,x)ds.$$

Since $\partial\mathcal{B}/\partial t = B$, we can rewrite (2.2) as

$$\frac{\partial^2\mathcal{B}}{\partial t^2} = (D\triangle - \delta)\frac{\partial\mathcal{B}}{\partial t} - \gamma\frac{\partial N}{\partial t}, \tag{2.20}$$

which can be rewritten as

$$\frac{\partial}{\partial t}\left(\frac{\partial \mathcal{B}}{\partial t} - (D\triangle - \delta)\mathcal{B}(t,x) + \gamma N(t,x)\right) = 0.$$

Integrating it to obtain

$$\frac{\partial \mathcal{B}(t,x)}{\partial t} - (D\triangle - \delta)\mathcal{B}(t,x) + \gamma N(t,x) = A(x), \tag{2.21}$$

for some smooth function $A(x)$. By the sophisticated version of the Method of Variation of Parameters, the solution can be written as

$$\mathcal{B}(t,x) = \int_0^t e^{(D\triangle-\delta)(t-s)}(A(x) - \gamma N(s,x))ds \leq \int_0^t e^{(D\triangle-\delta)(t-s)}A(x)ds$$

$$= \left(\int_0^t e^{(D\triangle-\delta)(t-s)}ds\right)A(x) < \infty.$$

Integrating the second equation of (2.2) yields

$$\int_0^t \frac{1}{h(N)}\frac{\partial N}{\partial s}\partial s = \int_0^t -\frac{1}{\gamma}B(s,x)\partial s.$$

For the case $h(N) = \alpha N$:

$$\int_0^t \frac{\partial N}{N} = \int_0^t -\frac{\alpha}{\gamma}B\partial t = -\frac{\alpha}{\gamma}\mathcal{B},$$

which leads to

$$N(t,x) = N(0,x)e^{-\frac{\alpha}{\gamma}\mathcal{B}},$$

that causes a contradiction when $N \to 0$.

For the case $h(N) = \frac{\alpha N}{k+N}$:

$$\int_0^t \frac{k+N}{N} \partial N = -\frac{\alpha}{\gamma}\mathcal{B},$$

which leads to

$$k(\log N(t,x) - \log N(0,x)) + N(t,x) - N(0,x) = -\frac{\alpha}{\gamma}\mathcal{B} > -\infty.$$

When $N \to 0$, the left hand side goes to $-\infty$ but the right hand side never goes to $-\infty$, it is a contradiction.

Remark: Even though the function $h(N)$ satisfies the conditions $h(0) = 0$, $h'(t) > 0$, and $h''(t) \leq 0$, we cannot reach theorem 2.4. Counter example: If $h(N) = \sqrt{N}$, then $h'(N) = \frac{1}{2}N^{-\frac{1}{2}} > 0$ and $h''(N) = -\frac{1}{4}N^{-\frac{3}{2}} < 0$. Hence, we have

$$\int_0^t N^{-\frac{1}{2}} \partial N = -\frac{1}{\gamma}\mathcal{B},$$

$$2(N(t,x)^{\frac{1}{2}} - N(0,\vec{x})^{\frac{1}{2}}) = -\frac{1}{\gamma}\mathcal{B}.$$

When $N \to 0$, the left hand side goes to zero and the right hand side also goes to zero. We cannot obtain Theorem 2.4 using the same approach.

2.D Mathematical Model for Liquid Case

Chemically defined basal liquid media are used to provide nutrients for cell growth in research (simply made by nutrient soup). Our model is developed to study competition in agar media. We use the following liquid model to compare with agar case because the experiment was performed to test both

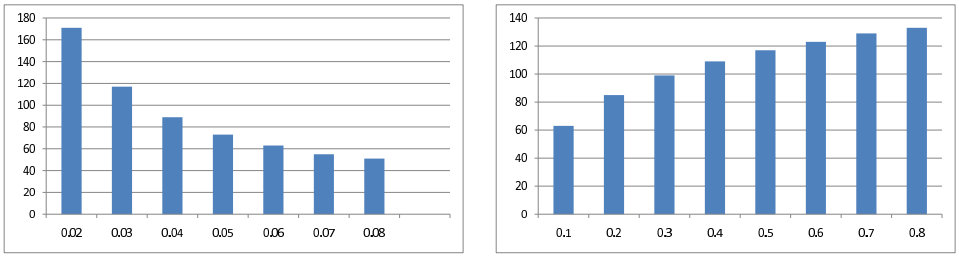

(a) T_0 vs δ (b) T_0 vs γ

Figure 2.2: Extinction time (T_0) vs. mortality rate (δ) and yield constant (γ).

cases. The single species model for liquid media is provided by

$$\frac{\partial B}{\partial t} = D\frac{\partial^2 B}{\partial x^2} + (h(N) - \delta)B,$$
$$\frac{\partial N}{\partial t} = D_3\frac{\partial^2 B}{\partial x^2} - \frac{1}{\gamma}h(N)B,$$

where D_3 is a diffusion coefficient of nutrient,

the initial conditions are

$$B(0, x) = B_0 \quad \text{(small and supported in a small disk)},$$
$$N(0, x) = N_0,$$

and the boundary conditions are

$$\frac{\partial B}{\partial x}(t, 0) = \frac{\partial B}{\partial x}(t, L) = 0 \quad \text{on} \quad \partial\Omega,$$

$$\frac{\partial N}{\partial x}(t, 0) = \frac{\partial N}{\partial x}(t, L) = 0 \quad \text{on} \quad \partial\Omega.$$

The two species model for liquid media is presented in section 2.*F*.3.

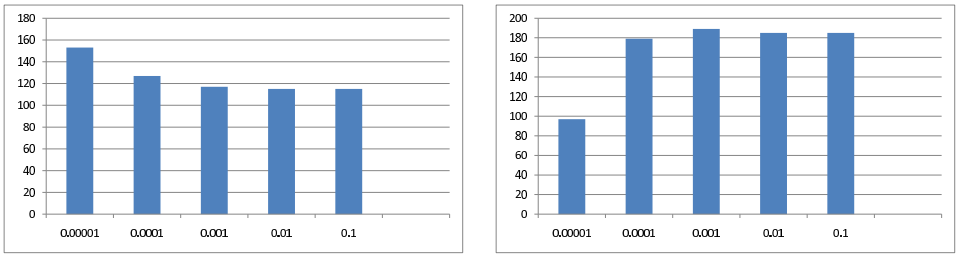

(a) single strain case (b) competition case

Figure 2.3: Extinction time (T_0) vs. motility (D)-agar case.

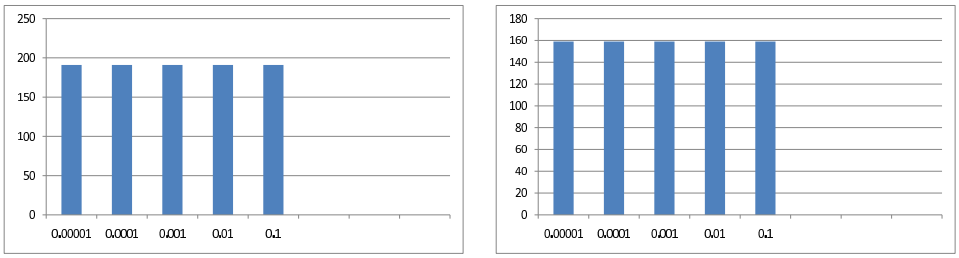

(a) single strain case (b) competition case

Figure 2.4: Extinction time (T_0) vs. motility rate (D)-liquid case.

2.E Computation of Extinction Time

Extinction is the end of an organism or group of species. The extinction threshold ϵ_0 is defined as the minimum total density of bacteria, below which bacteria go extinct. We define the extinction time T_0 as the maximum time for the total density of bacteria to stay above the extinction threshold. We analyze the dependence of the extinction time T_0 on δ (mortality rate) (see Fig.2.2(a)), γ (yield constant) (see Fig.2.2(b)) and D (motility rate) (see Figs.2.3-2.4). The total density of bacteria over the space is defined as $\widetilde{B}(.) = \int_\Omega B(., \overline{x}) d\overline{x}$.

Fig.2.2 directly follows common sense: when the mortality rate increases, the extinction time decreases (see panel (a)); when the yield constant increases, the extinction time increases (see panel (b)). According to Fig.2.3, for the agar media, larger motility results in shorter survival of a single strain, while larger

motility of motile strain prolongates the extinction time of the motile strain in competition with the immotile strain. In a single species (no competition) case, larger motility is worse for itself, because single strain goes extinct faster if it consumes more nutrients by spreading out. However, in the case of two competing species (two species competition models will be clearly presented in section 2.F), the motile strain gets more nutrient, leading to the earlier extinction of the immotile strain. According to Fig.2.4, for the liquid case, the extinction time is almost independent of motility because liquid nutrients move almost infinitely fast.

2.F Two Competing Bacterial Species in a Petri Dish

We start with two species competing for the same nutrients in one-dimensional space. These species are genetically identical except for their movement speed: the first strain is motile while the second one is immotile. Culture medium ranges from agar to liquid. We perform mathematical analysis including global stability for non-spatial case and the existence of traveling-wave solutions.
We consider the following reaction-diffusion competition spatial model for agar media:

$$\begin{aligned} \frac{\partial B_1}{\partial t} &= D_1 \frac{\partial^2 B_1}{\partial x^2} + \left[h_1(N) - \delta_1\right] B_1, \\ \frac{\partial B_2}{\partial t} &= D_2 \frac{\partial^2 B_2}{\partial x^2} + \left[h_2(N) - \delta_2\right] B_2, \\ \frac{\partial N}{\partial t} &= -\frac{1}{\gamma_1} h_1(N) B_1 - \frac{1}{\gamma_2} h_2(N) B_2, \end{aligned} \tag{2.22}$$

where $h_i(N) = \frac{\alpha_i N}{k_i + N}$ - resource uptake function;

$B_1(t,x)$-density of motile strain; $B_2(t,x)$-density of immotile strain;

D_1-diffusion constant of motile strain; D_2-diffusion constant of immotile strain;

$D_1 >> D_2$;

$\alpha_1 = \alpha_2$ - maximum specific growth rate;

$k_1 = k_2$ - half-saturation constants for resource uptake (representing resource uptake efficiencies);

$\delta_1 = \delta_2$ - bacterial mortality rate;

$\gamma_1 = \gamma_2$ - yield coefficient (mass of viable cells produced per unit of nutrient).

2.F.1 Mathematical Analysis

We first consider the ODE model, which is provided by

$$\begin{aligned} \frac{dB_1}{dt} &= [h_1(N) - \delta_1]\, B_1, \\ \frac{dB_2}{dt} &= [h_2(N) - \delta_2]\, B_2, \\ \frac{\partial N}{\partial t} &= -\frac{1}{\gamma_1} h_1(N) B_1 - \frac{1}{\gamma_2} h_2(N) B_2. \end{aligned} \tag{2.23}$$

We have the following global stability result for ODE model, which state that eventually the nutrient density approaches some positive steady state.

Theorem 2.5: *The equilibrium ray $(0,0,\zeta)$, where ζ is an arbitrary nonnegative number, is globally attracting.*

Proof: It is obvious that any point on the ray $(0,0,\zeta), \zeta \geq 0$ is an equilibrium. We will show that there exists $T > 0$ such that $\delta_1 > h_1(N)$ and $\delta_2 > h_2(N)$ when $t > T$, by contradiction.

If this claim is not true, we have $\delta_1 < h_1(N)$ for all t or $\delta_2 < h_2(N)$ for all t.

Therefore

$$\begin{aligned} \frac{dB_1}{dt} &\geq \epsilon B_1 \qquad \text{for all} \qquad t \qquad \text{or} \\ \frac{dB_2}{dt} &\geq \epsilon B_2 \qquad \text{for all} \qquad t. \end{aligned} \tag{2.24}$$

Integrating them with respect to t implies

$$\begin{aligned} B_1 &\geq ae^{\epsilon t} \qquad \text{for all} \qquad t \qquad \text{or} \\ B_2 &\geq be^{\epsilon t} \qquad \text{for all} \qquad t. \end{aligned} \tag{2.25}$$

When $t \to \infty$, then $B_1 \to \infty$ or $B_2 \to \infty$. On the other hand, if we consider the Lyapunov function

$$\begin{aligned} V(B_1, B_2, N) &= 1/2(B_1^2 + B_2^2 + N^2), \\ \frac{dV}{dt}(B_1, B_2, N) &= B_1 \frac{dB_1}{dt} + B_2 \frac{dB_2}{dt} + N \frac{dN}{dt} \\ &= B_1^2(h_1(N) - \delta_1) + B_2^2(h_2(N) - \delta_2) \\ &\qquad - N\left(\frac{1}{\gamma_1} h_1(N) B_1 + \frac{1}{\gamma_2} h_2(N) B_2\right) \\ &< 0, \qquad \text{for} \qquad t > T, \end{aligned}$$

then any solution approaches some point on the line $(0, 0, \zeta), \zeta \geq 0$, that is, the equilibrium line $(0, 0, \zeta), \zeta \geq 0$ is globally attracting. A contradiction.

For the spatial model, the following theorem summarizes the necessary condition for the existence of traveling-wave solutions for system of equations (2.22).

Theorem 2.6: *If $\delta_1 > \bar{h}_1$ and $\delta_2 > \bar{h}_2$, where $h_1(\zeta) = \bar{h}_1$ and $h_2(\zeta) = \bar{h}_2$ then the necessary condition for existence of traveling-wave solutions that*

connect two steady states $(0,0,\zeta_1)$ *and* $(0,0,\zeta_2)$ *for the agar model (2.22) is*

$$\sqrt{\frac{D_1^2(\delta_2-\bar{h}_2)+D_2^2(\delta_1-\bar{h}_1)}{(D_1+D_2)}} \geq c \geq \frac{\mid D_1(\bar{h}_2-\delta_2)-D_2(\bar{h}_1-\delta_1)\mid}{\sqrt{(D_1+D_2)(\delta_1+\delta_2-\bar{h}_1-\bar{h}_2)}}$$

such that $N(-\infty)=\zeta_1,\ N(+\infty)=\zeta_2$.

Proof: Consider the model

$$\begin{aligned}
\frac{\partial B_1}{\partial t} &= D_1\triangle B_1+(h_1(N)-\delta_1)B_1,\\
\frac{\partial B_2}{\partial t} &= D_2\triangle B_2+(h_2(N)-\delta_2)B_2,\\
\frac{\partial N}{\partial t} &= -\frac{1}{\gamma_1}h_1(N)B_1-\frac{1}{\gamma_2}h_2(N)B_2.
\end{aligned} \tag{2.26}$$

Let $B_1(t,x)=B_1(x-ct)$, $B_2(t,x)=B_2(x-ct)$, and $N(t,x)=N(x-ct)$, then the equations become

$$\begin{aligned}
-cB_1' &= D_1B_1''+(h_1(N)-\delta_1)B_1,\\
-cB_2' &= D_2B_2''+(h_2(N)-\delta_2)B_2,\\
-cN' &= -\frac{1}{\gamma_1}h_1(N)B_1-\frac{1}{\gamma_2}h_2(N)B_2.
\end{aligned} \tag{2.27}$$

Now let $B_1'=B_{11}$ and $B_2'=B_{22}$ implies

$$\begin{aligned}
-cB_{11} &= D_1B_{11}'+(h_1(N)-\delta_1)B_1,\\
-cB_{22} &= D_2B_{22}'+(h_2(N)-\delta_2)B_2,\\
-cN' &= -\frac{1}{\gamma_1}h_1(N)B_1-\frac{1}{\gamma_2}h_2(N)B_2,
\end{aligned} \tag{2.28}$$

and then

$$B_{11}'=\frac{-c}{D_1}B_{11}-\frac{1}{D}(h_1(N)-\delta_1)B_1,$$

$$B_1' = B_{11},$$

$$B_{22}' = \frac{-c}{D_2} B_{22} - \frac{1}{D}(h_2(N) - \delta_2) B_2,$$

$$B_2' = B_{22},$$

$$N' = \frac{1}{c\gamma_1} h_1(N) B_1 + \frac{1}{c\gamma_2} h_2(N) B_2.$$

At the critical point $(0, 0, \zeta)$, $\zeta \geq 0$, let $h_1(\zeta) = \bar{h}_1$ and $h_2(\zeta) = \bar{h}_2$, the Jacobian matrix is

$$\mathrm{J} = \begin{pmatrix} -c/D_1 & -(\bar{h}_1 - \delta_1)/D_1 & 0 & 0 & 0 \\ 1 & 0 & 0 & 0 & 0 \\ 0 & 0 & -c/D_2 & -(\bar{h}_2 - \delta_2)/D_2 & 0 \\ 0 & 0 & 1 & 0 & 0 \\ 0 & \frac{\bar{h}_1}{c\gamma_1} & 0 & \frac{\bar{h}_2}{c\gamma_2} & 0 \end{pmatrix}$$

and thus the characteristic polynomial is given by

$$\chi(\lambda) = \begin{vmatrix} -c/D_1 - \lambda & -(\bar{h}_1 - \delta_1)/D_1 & 0 & 0 & 0 \\ 1 & 0 - \lambda & 0 & 0 & 0 \\ 0 & 0 & -c/D_2 - \lambda & -(\bar{h}_2 - \delta_2)/D_2 & 0 \\ 0 & 0 & 1 & 0 - \lambda & 0 \\ 0 & \frac{\bar{h}_1}{c\gamma_1} & 0 & \frac{\bar{h}_2}{c\gamma_2} & 0 - \lambda \end{vmatrix}.$$

The characteristic equation $\chi(\lambda) = 0$ is

$$\begin{aligned} 0 = \lambda^5 + (c/D_1 + c/D_2)\lambda^4 + (\frac{c^2}{D_1 D_2} + \frac{(\bar{h}_1 - \delta_1)}{D_1} + \frac{(\bar{h}_2 - \delta_2)}{D_2})\lambda^3 \\ + \frac{c}{D_1 D_2}(\bar{h}_1 + \bar{h}_2 - \delta_1 - \delta_2)\lambda^2 + \frac{(\bar{h}_1 - \delta_1)(\bar{h}_2 - \delta_2)}{D_1 D_2}\lambda. \end{aligned}$$

We apply the Routh-Hurwitz criterion to obtain the following

$$\begin{bmatrix} 1 & \frac{c^2}{D_1D_2}+\frac{(\bar{h}_1-\delta_1)}{D_1}+\frac{(\bar{h}_2-\delta_2)}{D_2} & \frac{(\bar{h}_1-\delta_1)(\bar{h}_2-\delta_2)}{D_1D_2} \\ \frac{c}{D_1}+\frac{c}{D_2} & \frac{c}{D_1D_2}(\bar{h}_1+\bar{h}_2-\delta_1-\delta_2) & 0 \end{bmatrix},$$

$$b_1 = \frac{c^2(D_1+D_2)+D_1^2(\bar{h}_2-\delta_2)+D_2^2(\bar{h}_1-\delta_1)}{D_1D_2(D_1+D_2)} \qquad b_2 = \frac{(\bar{h}_1-\delta_1)(\bar{h}_2-\delta_2)}{D_1D_2},$$

$$c_1 = \frac{c}{D_1D_2}\frac{\big([D_1(\bar{h}_2-\delta_2)-D_2(\bar{h}_1-\delta_1)]^2+c^2(D_1+D_2)(\bar{h}_1+\bar{h}_2-\delta_1-\delta_2)\big)}{c^2(D_1+D_2)-D_1^2(\delta_2-\bar{h}_2)-D_2^2(\delta_1-\bar{h}_1)},$$

and $d_1 = b_2$.

If $b_2 > 0$ and $c_1 < 0$ then $(0, 0, \zeta)$ is unstable.

If $b_2 < 0$ and $c_1 > 0$ then $(0, 0, \zeta)$ is unstable.

If $b_2 > 0$ and $c_1 > 0$ then $(0, 0, \zeta)$ is locally asymptotically stable, which imply

$$\frac{(\bar{h}_1-\delta_1)(\bar{h}_2-\delta_2)}{D_1D_2} > 0 \tag{2.29}$$

and

$$\frac{c}{D_1D_2}\frac{[D_1(\bar{h}_2-\delta_2)-D_2(\bar{h}_1-\delta_1)]^2+c^2(D_1+D_2)(\bar{h}_1+\bar{h}_2-\delta_1-\delta_2)}{c^2(D_1+D_2)-D_1^2(\delta_2-\bar{h}_2)-D_2^2(\delta_1-\bar{h}_1)} > 0. \tag{2.30}$$

The first condition (2.29) leads to two cases:

(i) $(\bar{h}_1-\delta_1) > 0$ and $(\bar{h}_2-\delta_2) > 0$;

(ii) $(\bar{h}_1-\delta_1) < 0$ and $(\bar{h}_2-\delta_2) < 0$.

For the case (i) $(\bar{h}_1-\delta_1) > 0$ and $(\bar{h}_2-\delta_2) > 0$, we have $b_1 > 0$. Thus $(0, 0, \zeta)$ is locally asymptotically stable.

On the other hand, if $(\bar{h}_1-\delta_1) > 0$ and $(\bar{h}_2-\delta_2) > 0$, then there exists $\xi > 0$

(small enough) such that

$$\begin{aligned}
\frac{\partial B_1}{\partial t} &= D_1 \Delta B_1 + (h_1(N) - \delta_1) B_1 \geq D_1 \Delta B_1 + \epsilon B_1, \\
&\qquad \text{for} \quad (B_1(0), B_2(0), N(0)) \in \mathbf{B}_\xi((0,0,\zeta)), \\
\frac{\partial B_2}{\partial t} &= D_2 \Delta B_2 + (h_2(N) - \delta_2) B_2 \geq D_2 \Delta B_2 + \epsilon B_2, \\
&\qquad \text{for} \quad (B_1(0), B_2(0), N(0)) \in \mathbf{B}_\xi((0,0,\zeta)).
\end{aligned}$$

Differentiating $\widetilde{B}(t) = \int_\Omega B(t,x)dx$ yields

$$\begin{aligned}
\frac{\partial \widetilde{B_1}}{\partial t} &\geq \int_\Omega D_1 \Delta B_1 dx + \epsilon \widetilde{B_1}, \\
\frac{\partial \widetilde{B_2}}{\partial t} &\geq \int_\Omega D_2 \Delta B_2 dx + \epsilon \widetilde{B_2}.
\end{aligned}$$

The integral is zero due to the zero flux hypothesis and Stoke's theorem. We thus obtain

$$\begin{aligned}
\frac{\partial \widetilde{B_1}}{\partial t} &\geq \epsilon \widetilde{B_1}, \\
\frac{\partial \widetilde{B_2}}{\partial t} &\geq \epsilon \widetilde{B_2}.
\end{aligned}$$

Integrating them with respect to t yields

$$\begin{aligned}
\widetilde{B_1} &\geq a e^{\epsilon \widetilde{B_1}}, \\
\widetilde{B_2} &\geq b e^{\epsilon \widetilde{B_2}}.
\end{aligned}$$

It contradicts the result that $(0,0,\zeta)$ is locally asymptotically stable.

For the case (ii) $(\bar{h}_1 - \delta_1) < 0$ and $(\bar{h}_2 - \delta_2) < 0$, the second condition (2.30) for asymptotic stability leads to

$$[D_1(\bar{h}_2 - \delta_2) - D_2(\bar{h}_1 - \delta_1)]^2 > c^2(D_1 + D_2)(\delta_1 + \delta_2 - \bar{h}_1 - \bar{h}_2)$$

and

$$c^2(D_1 + D_2) > D_1^2(\delta_2 - \bar{h}_2) + D_2^2(\delta_1 - \bar{h}_1),$$

or

$$[D_1(\bar{h}_2 - \delta_2) - D_2(\bar{h}_1 - \delta_1)]^2 < c^2(D_1 + D_2)(\delta_1 + \delta_2 - \bar{h}_1 - \bar{h}_2)$$

and

$$c^2(D_1 + D_2) < D_1^2(\delta_2 - \bar{h}_2) + D_2^2(\delta_1 - \bar{h}_1).$$

They are equivalent to

$$\frac{D_1^2(\delta_2 - \bar{h}_2) + D_2^2(\delta_1 - \bar{h}_1)}{(D_1 + D_2)} < c^2 < \frac{[D_1(\bar{h}_2 - \delta_2) - D_2(\bar{h}_1 - \delta_1)]^2}{(D_1 + D_2)(\delta_1 + \delta_2 - \bar{h}_1 - \bar{h}_2)} \quad (2.31)$$

or

$$\frac{D_1^2(\delta_2 - \bar{h}_2) + D_2^2(\delta_1 - \bar{h}_1)}{(D_1 + D_2)} > c^2 > \frac{[D_1(\bar{h}_2 - \delta_2) - D_2(\bar{h}_1 - \delta_1)]^2}{(D_1 + D_2)(\delta_1 + \delta_2 - \bar{h}_1 - \bar{h}_2)}. \quad (2.32)$$

To show the inequality (2.32)

$$\frac{D_1^2(\delta_2 - \bar{h}_2) + D_2^2(\delta_1 - \bar{h}_1)}{(D_1 + D_2)} \geq \frac{[D_1(h_2 - \delta_2) - D_2(\bar{h}_1 - \delta_1)]^2}{(D_1 + D_2)(\delta_1 + \delta_2 - \bar{h}_1 - \bar{h}_2)},$$

we only need to show that

$$[D_1^2(\delta_2 - \bar{h}_2) + D_2^2(\delta_1 - \bar{h}_1)](\delta_1 + \delta_2 - \bar{h}_1 - \bar{h}_2) \geq [D_1(\bar{h}_2 - \delta_2) - D_2(\bar{h}_1 - \delta_1)]^2.$$

Now

$$LHS = D_1^2(\delta_2 - \bar{h}_2)(\delta_1 - \bar{h}_1) + D_1^2(\delta_2 - \bar{h}_2)^2 + D_2^2(\delta_1 - \bar{h}_1)(\delta_2 - \bar{h}_2) + D_2^2(\delta_1 - \bar{h}_1)^2,$$

$$RHS = D_1^2(\delta_2 - \bar{h}_2)^2 - 2D_1D_2(\delta_1 - \bar{h}_1)(\delta_2 - \bar{h}_2) + D_2^2(\delta_1 - \bar{h}_1)^2.$$

Obviously,

$$LHS \geq RHS.$$

Hence, (2.31) can never be satisfied, and (2.32) is the only choice. Hence, the necessary condition for existence of traveling wave solution is,

$$\sqrt{\frac{D_1^2(\delta_2 - \bar{h}_2) + D_2^2(\delta_1 - \bar{h}_1)}{(D_1 + D_2)}} \geq c \geq \frac{\mid D_1(\bar{h}_2 - \delta_2) - D_2(\bar{h}_1 - \delta_1) \mid}{\sqrt{(D_1 + D_2)(\delta_1 + \delta_2 - \bar{h}_1 - \bar{h}_2)}}.$$

Investigating traveling wave solutions in competition allows us to understand how the nutrients can be ruled by the bacterial strains. Our system admits traveling wave solutions depending on the initial condition. When the nutrients stay at their stable state in the petri dish, adding bacterial strains may result in a "wave of transition" of bacterial strains. We obtain maximum and minimum traveling speeds for traveling-wave solutions.

2.F.2 Numerical Simulations

Numerical simulations provide model predictions to be compared with experimental results. One goal of simulations is to determine whether our theoretical results are consistent to experimental results in (28). We run simulations in one-dimensional and two-dimensional spaces to illustrate the data fitting. Simulation results in one-dimensional space were obtained using MATLAB, and simulation results in two-dimensional space were obtained using COMSOL. For all the simulations, zero flux boundary conditions were used. Furthermore, we compute extinction times of bacteria, and ratios of total densities of the two competing strains.

We start with the simulations on one-dimensional space. We place motile and immotile bacterial strains in the middle of the petri dish and observe competition outcomes (see Fig.2.5). We select parameter values from ranges given in Table 2.1 (1; 3; 14; 19; 26; 13; 11):

$\alpha_1 = \alpha_2 = 0.6$, $k_1 = k_2 = 0.06$, $\delta_1 = \delta_2 = 0.03$, $\gamma_1 = \gamma_2 = 0.5$, $D_1 = 0.002$, $D_2 = 0.0002$, and the initial conditions:

$$B_1(0,x) = \begin{cases} 0.05, |x-0.5| \leq 0.03; \\ 0, \quad |x-0.5| > 0.03; \end{cases}, \; B_2(0,x) = \begin{cases} 0.05, |x-0.5| \leq 0.03; \\ 0, \quad |x-0.5| > 0.03; \end{cases}$$

and $N(0,x) = 0.5$ (high resource) or 0.05 (low resource).

Initially, both strains grow in the middle. After a few hours the motile strain moves out and grows on the boundary, while the immotile strain grows quickly in the middle. And finally both strains die out due to the nutrient-closed system. Fig.2.7 illustrates that the motile strain is dominant in total density (integration of density over the space). After half a day, the ratio of motile

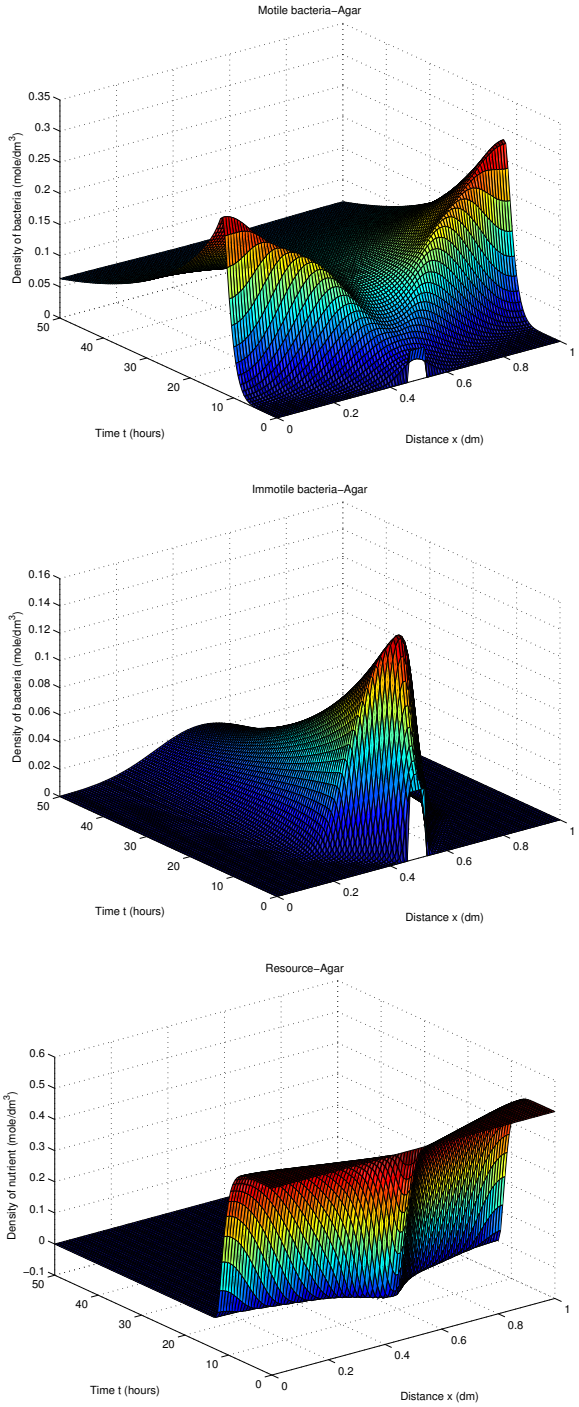

Figure 2.5: One dimensional simulation for the competition of motile and immotile strains in a homogeneous nutrient environment - agar case. Chosen values of parameters are $\alpha_1 = \alpha_2 = 0.6h^{-1}$, $k_1 = k_2 = 0.04(dm)^{-3}$, $\delta_1 = \delta_2 = 0.03h^{-1}$, $\gamma_1 = \gamma_2 = 0.5$, $D_1 = 0.002(dm)^2h^{-1}$, $D_2 = 0.0002(dm)^2h^{-1}$, $N(x,0) = 0.5$.

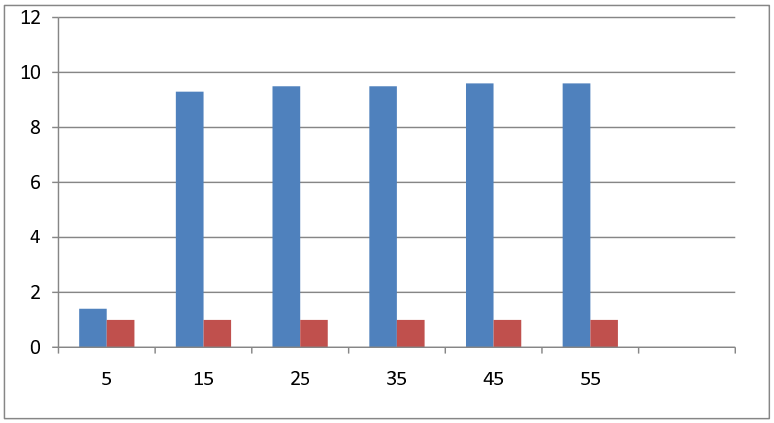

Figure 2.6: Quantitatively fitting the ratio data by computing the total density ratio of motile strain to immotile strain (M/IM) from simulations. The x-axis is time (hrs), and the y-axis is the total density ratio. The first column (blue) at each time plots the ratio for the agar case, and the second column (red) at each time plots the ratio for the liquid case.

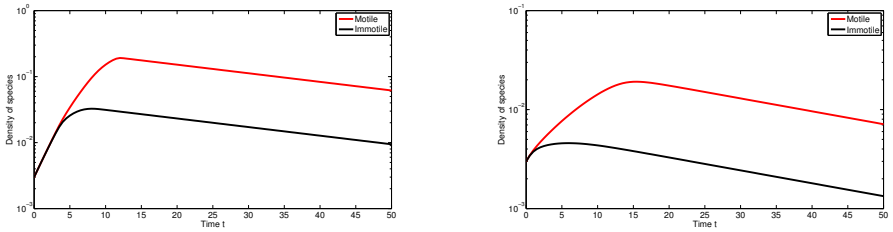

(a) high resource-agar (b) low resource-agar

Figure 2.7: Total density of motile and immotile strains in one dimensional agar case. Red and black colors represent total density of motile and immotile strains. (a) high resource. (b) low resource. Chosen values of parameters are $\alpha_1 = \alpha_2 = 0.6h^{-1}$, $k_1 = k_2 = 0.04(dm)^{-3}$, $\delta_1 = \delta_2 = 0.03h^{-1}$, $\gamma_1 = \gamma_2 = 0.5$, $D_1 = 0.002(dm)^2h^{-1}$, $D_2 = 0.0002(dm)^2h^{-1}$, $N(x, 0) = 0.5$.

strain to immotile strain is around 10 : 1 (see Fig.2.6). This result is qualitatively fit to the experimental data of the agar case (28). Fig.4.6 shows the spatial distributions of both bacterial strains and resource over time.

Now we run simulations on two-dimensional space. We place one drop of motile strain in the middle and one drop of immotile strain a bit away from the middle of the petri dish. We compute the density distributions of both strains and resource over time, and record these spatial distributions at 0hr, 12hrs, 15hrs and 20hrs in Fig.2.8. We select parameter values from ranges given in Table 2.1 (1; 3; 14; 19; 26; 13; 11). Note that the unit of diffusion coefficients in two-dimensional space is different from that in one-dimensional space. We choose the following initial conditions to run simulations in COMSOL:

$$
\begin{aligned}
B_1(0,x,y) &= \exp[(-(x-0.5)^2-(y-0.5)^2)/0.0001], \\
B_2(0,x,y) &= \exp[(-(x-0.4)^2-(y-0.5)^2)/0.0001], \\
N(0,x,y) &= 0.5.
\end{aligned}
$$

We use $B_1(0,x,y)$ and $B_2(0,x,y)$ to mimic one drop of bacteria in the petri dish. Actually after a very short time, one drop will become these initial functions for bacterial densities. Note that these initial conditions are similar to those in one-dimensional space.

To mimic experiments, we start at time $t = 0$ in Fig.2.8. Motile and immotile strains start to grow on the same position as placed, and the density of the immotile strain is higher than the density of the motile strain. After twelve hours, the density of the immotile strain starts to decrease and the density of motile strain starts to increase. After fifteen hours, the motile strain moves out and grows mainly outside the middle region, and a heterogeneous pattern

occurs. After twenty hours, the motile strain grows everywhere and dominates most of the petri dish, the immotile strain has very low density (even in the middle region) due to lack of resources, and most nutrients are used but actually some remain according to Theorem 2.4. However, in real experiments the density of nutrients can be extremely low.

2.F.3 Liquid Case

We consider two bacterial strains, genetically identical except for their motility, in a finite one-dimensional space, with homogeneous diffusible liquid nutrient. The model is provided by

$$\begin{aligned}
\frac{\partial B_1}{\partial t} &= D_1 \frac{\partial^2 B_1}{\partial x^2} + \left[h_1(N) - \delta_1\right] B_1, \\
\frac{\partial B_2}{\partial t} &= D_2 \frac{\partial^2 B_2}{\partial x^2} + \left[h_2(N) - \delta_2\right] B_2, \\
\frac{\partial N}{\partial t} &= D_3 \frac{\partial^2 N}{\partial x^2} - \frac{1}{\gamma_1} h_1(N) B_1 - \frac{1}{\gamma_2} h_2(N) B_2,
\end{aligned} \tag{2.33}$$

where the nutrient diffusion coefficient $D_3 >> D_1 >> D_2$. Pattern formation in liquid is not as interesting as in agar. Numerical simulations in this section show competition results (spatial distribution over time, total densities, extinction times) and will be compared with the agar case.

Now we consider the simulations on one-dimensional space. Similar to the agar case, we place motile and immotile bacterial strains in the middle of the petri dish and observe competition outcomes in Fig.2.9. We select parameter values from ranges given in Table 2.1 (1; 3; 14; 19; 26; 13; 11; 12):

$\alpha_1 = \alpha_2 = 0.6$, $k_1 = k_2 = 0.06$, $\delta_1 = \delta_2 = 0.03$, $\gamma_1 = \gamma_2 = 0.5$, $D_1 = 0.002$, $D_2 = 0.0002$, $D_3 = 4$, and initial conditions:

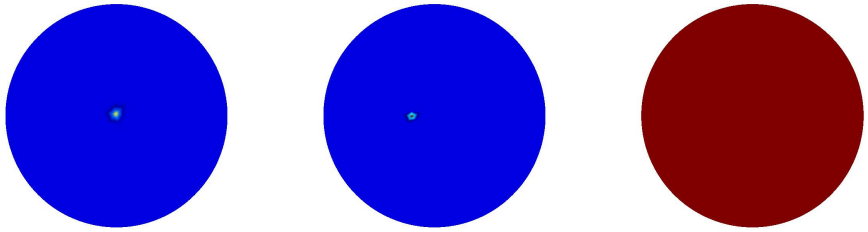

(a) Density of M at $t = 0$ (b) Density of IM at $t = 0$ (c) Density of N at $t = 0$

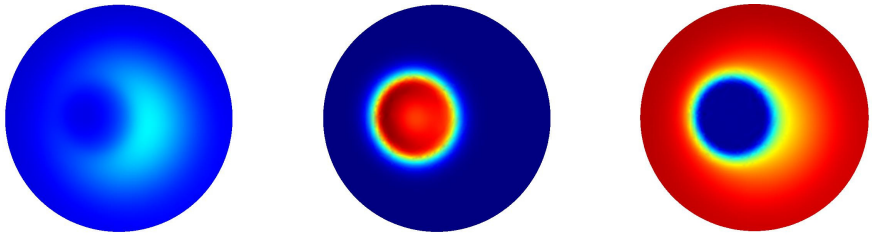

(d) Density of M at $t = 12$ (e) Density of IM at $t = 12$ (f) Density of N at $t = 12$

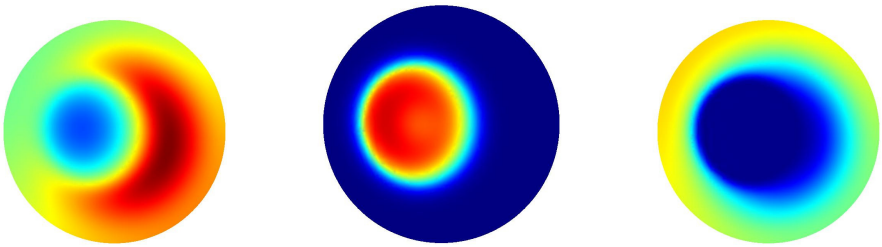

(g) Density of M at $t = 15$ (h) Density of IM at $t = 15$ (i) Density of N at $t = 15$

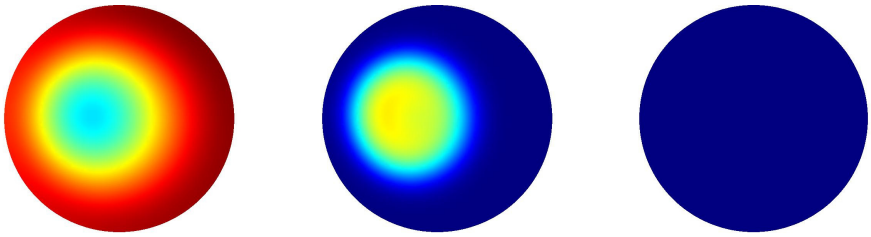

(j) Density of M at $t = 20$ (k) Density of IM at $t = 20$ (l) Density of N at $t = 20$

Figure 2.8: Two dimensional simulations ($2-D$ figures) at $t = 0, 12, 15, 20$. M represents the motile strain, IM represents the immotile strain and N represents the nutrients. In these figures, the color changing from dark red to blue represents the density of bacterial strain changing from high to low.

$$B_1(0,x) = \begin{cases} 0.04, & |x-0.5| \leq 0.03; \\ 0, & |x-0.5| > 0.03; \end{cases}, \; B_2(0,x) = \begin{cases} 0.04, & |x-0.5| \leq 0.03; \\ 0, & |x-0.5| > 0.03; \end{cases},$$

and $N(0,x) = 0.4$ (high resource) or 0.04 (low resource).

The motile strain moves out only a bit more than the immotile strain. Actually, both strains grow around the middle of the petri dish (see Fig.2.9) and have almost the same density (see Fig.2.11). In the liquid case, bacterial motility is irrelevant because liquid nutrients move almost infinitely fast compared to bacterial movement. When the nutrient density becomes low in the middle, liquid nutrient spreads inward to the middle. Thus, the motile strain has no advantage in liquid media (see Fig.2.11). The ratio of motile strain to immotile strain is around $1:1$ (see Fig.2.6). It is almost consistent to the experimental data of the liquid case (28).

In Fig.2.10, we vary the nutrient diffusion coefficient D_3 from 0 to 10 in log scale, in which interval between agar and liquid media are two extremes, to examine how the resource type determines the ratio of the motile strain to the immotile strain and extinction times of both strains. The ratio of the motile strain to the immotile strain at $t = 15$ decreases as D_3 increases. The extinction time of the motile strain decreases and that of the immotile strain increases as D_3 increases, and the extinction times of both strains coincide when D_3 is large enough ($D_3 > 1$).

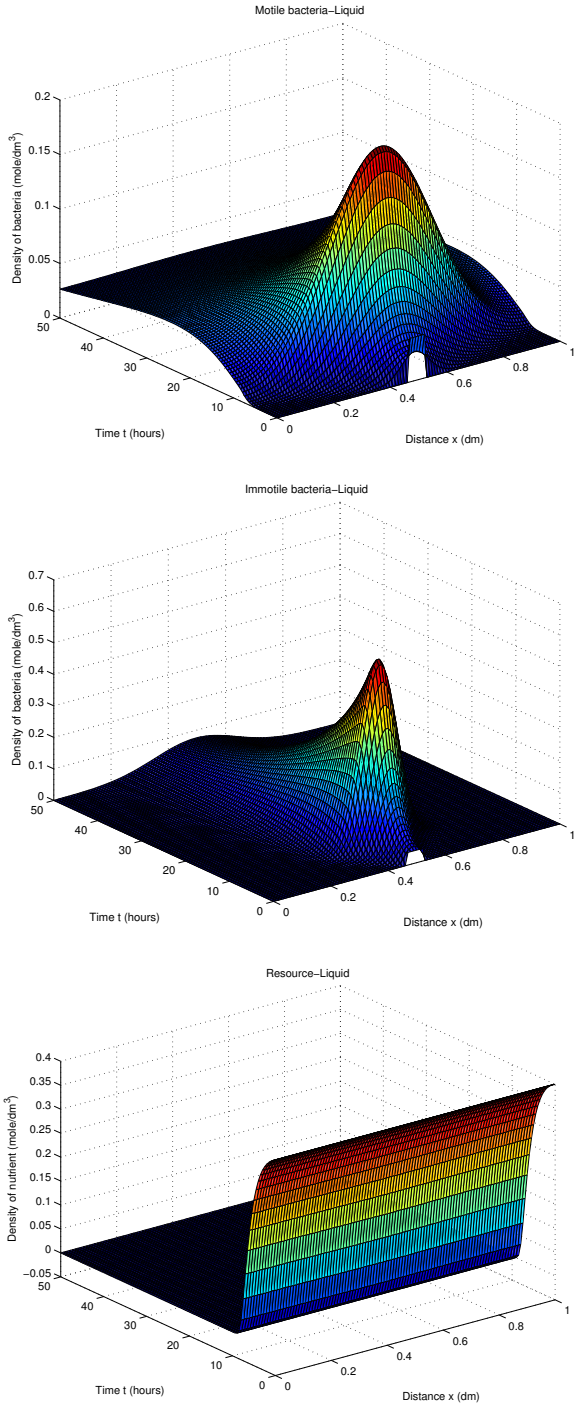

Figure 2.9: One dimensional simulation for the competition of motile and immotile strains in a homogeneous nutrient environment - liquid case. Chosen values of parameter are $\alpha_1 = \alpha_2 = 0.6h^{-1}$, $k_1 = k_2 = 0.04(dm)^{-3}$, $\delta_1 = \delta_2 = 0.03h^{-1}$, $\gamma_1 = \gamma_2 = 0.5$, $D_1 = 0.002(dm)^2h^{-1}$, $D_2 = 0.0002(dm)^2h^{-1}$, $D_3 = 4(dm)^2h^{-1}$.

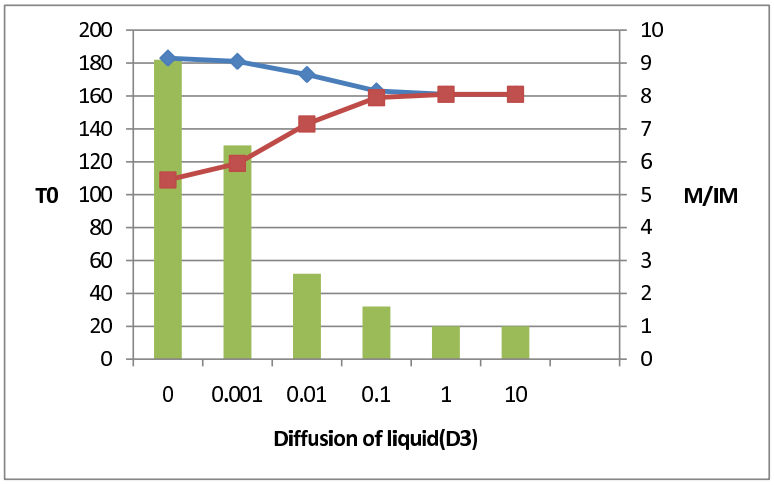

Figure 2.10: The dependence of the density ratio M/IM and the extinction times on the nutrient diffusion rate D_3. The two curves plot extinction times of motile strain (diamond) and immotile strain (square). The bars plot the ratios of motile/immotile strains at $t = 15$ under different nutrient diffusion rates.

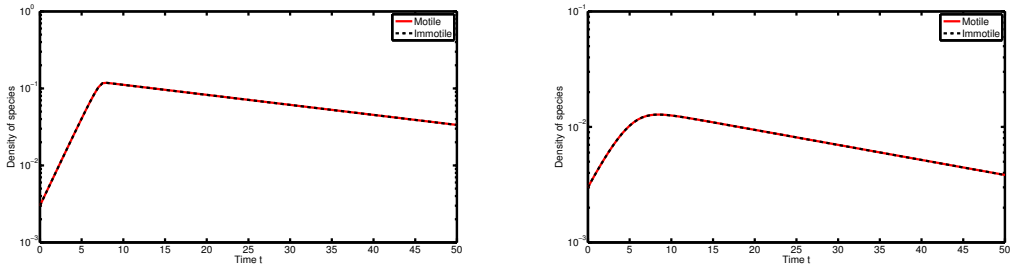

(a) high resource-liquid

(b) low resource-liquid

Figure 2.11: Total density of motile and immotile strains in one dimensional liquid case. Red and black colors represent total density of motile and immotile strains. (a) high resource. (b) low resource. Chosen values of parameters are $\alpha_1 = \alpha_2 = 0.6h^{-1}$, $k_1 = k_2 = 0.04(dm)^{-3}$, $\delta_1 = \delta_2 = 0.03h^{-1}$, $\gamma_1 = \gamma_2 = 0.5$, $D_1 = 0.002(dm)^2h^{-1}$, $D_2 = 0.0002(dm)^2h^{-1}$, $D_3 = 4(dm)^2h^{-1}$.

Var/Par	Definition	Unit	Value	Reference
B_1	Density of motile bacteria	$\mathrm{M}(dm)^{-3}$	-	-
B_2	Density of immotile bacteria	$\mathrm{M}(dm)^{-3}$	-	-
N	Density of nutrient	$\mathrm{M}(dm)^{-3}$	-	-
D_1	Diffusion coefficient of motile bacteria	$(dm)^2h^{-1}$	$D_2 - 0.36$	(14; 11)
D_2	Diffusion coefficient of immotile bacteria	$(dm)^2h^{-1}$	$0 - 0.036$	(14; 11)
α_i	Resource uptake rates	h^{-1}	$0.02 - 0.86$	(14; 3; 26; 13)
δ_i	Bacterial mortality rates	h^{-1}	$0.01 - 0.07$	(14; 3)
γ_i	Yield constants	-	0.5	(14; 11)
k_i	Half-saturation constants	$\mathrm{mole}(dm)^{-3}$	$0.001 - 0.08$	(14; 19; 1)
D_3	Diffusion coefficient of nutrient	$(dm)^2h^{-1}$	$>> D_1$ (liquid) 0 (agar)	(12)

Table 2.1: Variables and Parameters

Chapter 3

Phage-Bacteria Interactions in a Petri Dish

3.A Introduction

The identification of antibiotic resistance as a major medical problem has led to alternative antimicrobial treatments, including phage therapy. Previous experimental studies have proved the efficiency of phage therapy in treating bacterial infections as it appears to be a better alternative than traditional antibiotic treatment that has resulted in increased resistance to bacteria (42; 44). The specificity of phages is a potential disadvantage when the particular species of infecting bacteria is unidentified (49). However, the specificity of bacteriophages might reduce the chance that useful bacteria are killed when fighting an infection. Each phage has a host range, a limited number of host cells that it can infect. In general, there are some very important differences to favor phages in this context related to antibiotics.

In this chapter, we will concentrate on the mathematical and numerical analysis of bacteria-phage interaction using reaction-diffusion equations. A few studies discuss the spread of phage infection on bacteria in a petri dish and the co-evolutionary arms races between bacteria and phage in a chemostat environment. Jones et al.' paper (40) showed that phage infection spreads at a constant speed and that traveling wave solutions represent a wave of phage infection. Based on Jones et al.' (40) paper, Smith et al. (41) analyzed a model in its natural setting of a bounded domain. They both assume that host bacteria in agar do not grow or diffuse but in reality, we cannot neglect bacterial growth and movements. Therefore, we assume that it can grow and diffuse. Weitz et al.' model (48) described the population dynamics of bacteria and virulent phage in continuous culture and the changes in phenotypic trait space that control host resource consumption and phage adsorption. They found that multiple quasi species of bacteria and phage can coexist in a homogeneous medium with a single resource. Moreover, we suggest that the better model should incorporate nutrient explicitly in a closed system.

Our main goal of this chapter is to explore how phages affect bacterial population in a nutrient- limited environment. To obtain a theoretical understanding, we modify and extend an existing reaction-diffusion model of bacteria-phage interaction incorporating nutrient explicitly. Thus, on the basis of the work in ((40),(41)), section $3.B$ aims at presenting a general minimum model for bacteria-phage interaction in a homogeneous nutrient environment on the bounded domains. We assume that the phage can diffuse, while bacteria and nutrients may or may not diffuse. In sections $3.C$ and $3.D$, we will study the mathematical results for ODE and phage-only moving models. Guided by a

reaction diffusion model with bounded domain that represents the surface of a petri dish, we lead our analysis to basic issues of persistence and extinction of bacteria and phages. Mathematically, we can show that phages' mortality rate determines the persistence or extinction of phages and bacteria. In section 3.E, we will provide simulation results exhibit the role of phage in controlling the bacterial population in a homogeneous resource-limited environment. In addition, we show the existence of traveling wave solutions of our model system in one space dimension, the effect of burst size, which is the number of phage that are produced per phage-infected bacterium, extinction time of bacteria and the relation between threshold value of burst size for bacterial extinction and infection rate or yield constant. In section 3.F, we discuss two extended models that incorporate infected and resistant bacterial populations.

3.B Mathematical Model

Following Weitz et al. (48) and Smith (41), we assume that host bacteria in agar can grow and diffuse and once a bacterium becomes infected by a phage, it no longer competes with bacteria for resources. Using these assumptions, we construct a reaction diffusion model, which incorporates nutrient explicitly. Also, we incorporate bacterial growth and movement to make our model more realistic than Smith model (41).

For this model, $N(t,x)$, $B(t,x)$, $V(t,x)$ represent the density of nutrient, host bacteria and phage respectively. Bacteria multiply via binary fission at a per capita rate that is a function of the resource concentration in the petri dish. A minimum mathematical model for bacteria-phage interactions in a petri dish

is

$$\begin{aligned}\frac{\partial N}{\partial t} =& D_N \Delta N - \frac{1}{\gamma} h(N) B, \\ \frac{\partial B}{\partial t} =& D_B \Delta B + h(N) B - kBV, \\ \frac{\partial V}{\partial t} =& D_V \Delta V + \beta kBV - kBV - \delta V,\end{aligned} \tag{3.1}$$

where Δ ia a Laplacian, D_N, D_B, D_V are diffusion coefficients of nutrient, bacteria and phage respectively, k is the infection rate, $\beta > 1$ is the burst size, δ is the mortality rate of phage, α is a maximum specific growth rate, K is the half saturation constant, $\gamma < 1$ is the yield constant, and $h(N) = \frac{\alpha N}{k+N}$ is the nutrient consumption function that satisfies $h(0) = 0, h'(t) > 0, h''(t) \leq 0$, for example, $h(N) = \alpha N$ or $h(N) = \frac{\alpha N}{K+N}$. The model has initial and homogeneous Neumann boundary (zero flux) conditions: $N(0, x) = N_0$ for $x \in \Omega$, $B(0, x) = B_0$ for $x \in \Omega$, and $V(0, x) = V_0$ for $x \in \Omega_\epsilon$ (where Ω_ϵ is a small disk with radius ϵ, it can be centered at the center of petri dish or at any point); $\nabla N = 0, \nabla B = 0, \nabla V = 0$ on $\partial\Omega$, where n is an outward normal vector to the boundary $\partial\Omega$.

In the next few sections, we will study mathematical analysis for the simple ODE model (3.2) and the phage only moving model in one and two-dimensional spaces. We perform rigorous mathematical analyses including uniform and non-uniform steady states and traveling wave solutions.

3.C Mathematical Analysis of ODE Model

For simplicity, we first consider the ODE model. We use this model to study the steady state results. The model is provided by

$$\begin{aligned} \frac{dN}{dt} =& -\frac{1}{\gamma}h(N)B, \\ \frac{dB}{dt} =& h(N)B - kBV, \\ \frac{dV}{dt} =& \beta kBV - kBV - \delta V, \end{aligned} \tag{3.2}$$

with initial conditions:

$$N(0,x) = N_0,$$

$$B(0,x) = B_0,$$

$$V(0,x) = V_0 \qquad \text{(small and supported in a small disk)}.$$

Our first theorem determines the steady state result for the ODE model.

Theorem 3.1: *The model (3.2) admits infinitely many steady states* $(N_s, 0, 0)$ *and* $(0, B_s, 0)$*, where* $N_s \geq 0$*,* $B_s \geq 0$*.*

Proof: For spatially uniform steady states where solutions are independent of time and space, we have following algebraic equations

$$\begin{aligned} h(N)B &= 0, \\ (h(N) - kV)B &= 0, \\ k(\beta - 1)BV - \delta V &= 0. \end{aligned} \tag{3.3}$$

The first equation of (3.3) implies $B = 0$ or $N = 0$.

If $N = 0$, substituting it into the second equation of (3.3) leads to $V = 0$.

If $B = 0$, then $N \geq 0$ and $V \geq 0$.

If $B = 0$, substituting it into the third equation of (3.3) leads to $V = 0$.

Therefore, $(N_s, 0, 0)$ and $(0, B_s, 0)$ are the steady states.

Biologically, there is no meaning for the steady state $(0, B_s, 0)$ and this is an artifact of the model assumption wherein there is no intrinsic death rate of bacteria but infected rate. And $(N_s, 0, 0)$ is a viral steady state.

3.D Mathematical Analysis of Phage only Moving Model

In this model, we assume that environment is a semi-solid agar which essentially makes the bacteria and nutrients immobile (41). However, the phage can diffuse. The following reaction-diffusion equations relate the concentrations of resource (N), bacteria (B), and phage (V):

$$\begin{aligned} \frac{\partial N}{\partial t} &= -\frac{1}{\gamma} h(N) B, \\ \frac{\partial B}{\partial t} &= h(N) B - kBV, \\ \frac{\partial V}{\partial t} &= D_V \Delta V + \beta k B V - kBV - \delta V. \end{aligned} \tag{3.4}$$

If we substitute $V = 0$ to (3.4) implies

$$N_t = -\frac{1}{\gamma} B_t.$$

Integrating it with respect to t yields

$B = \gamma N + C$, where C is an arbitrary constant.

Therefore, $V = 0$ is an invariant set for (3.4).

Our second theorem determines the steady state result for the phage only moving model in one and two-dimensional spaces.

Theorem 3.2: *The model (3.4) with Neumann boundary conditions admits infinitely many steady states* $(N_s, 0, 0)$ *and* $(0, B_s, 0)$*, where* $N_s \geq 0$*,* $B_s \geq 0$*.*

Proof: For spatially non-uniform steady states for the one-dimensional case, where solutions are independent of time, we have the following equations

$$\begin{aligned} h(N))B =& 0, \\ (h(N) - kV)B =& 0, \\ D_V \frac{d^2V}{dx^2} + (\beta - 1)BV - \delta V =& 0. \end{aligned} \tag{3.5}$$

The first equation of (3.5) implies $B = 0$ or $N = 0$.

If $N = 0$, substituting it into the second equation of (3.5) leads to $V = 0$.

If $B = 0$, then $N \geq 0$ and $V \geq 0$.

If $B = 0$, then substituting it into the third equation of (3.5) leads to

$$D_V \frac{d^2V}{dx^2} - \delta V = 0. \tag{3.6}$$

From steady states we can see that $V(x) = 0$ is always a solution of the above equation. Therefore we shall look for solutions other than the trivial zero solution. Let $V = e^{wx}$, where w is a constant ready to be determined, then equation (3.6) leads to $w^2 - \frac{\delta}{D_V} = 0$, and thus the solution is

$$V = C_1 e^{wx} + C_2 e^{-wx}.$$

For equation (3.6), there is no solution when $\delta/D_V > 0$. We can prove this as follows:

Suppose there is a solution, then it must be

$$V = C_1 e^{\sqrt{\frac{\delta}{D_V}}x} + C_2 e^{-\sqrt{\frac{\delta}{D_V}}x}$$

for some constants C_1 and C_2 and we can solve the constants using boundary conditions $\frac{\partial V}{\partial x}(0,t) = \frac{\partial V}{\partial x}(L,t) = 0$. Thus $C_1 = C_2 = 0$. Therefore equation (3.6) has only zero solution ($\delta > 0$, $D_V > 0$).

For spatially non-uniform steady states for the two-dimensional case, where solutions are independent of time, we have the following equations:

$$\begin{aligned} h(N)B &= 0, \\ (h(N) - kV)B &= 0, \\ D_V\left(\frac{\partial^2 V}{\partial x^2} + \frac{\partial^2 V}{\partial y^2}\right) + (\beta - 1)BV - \delta V &= 0, \end{aligned}$$

or equivalently in polar coordinates

$$\begin{aligned} h(N)B &= 0, \\ (h(N) - kV)B &= 0, \\ D_V\left(V_{rr} + \frac{1}{r}V_r + \frac{1}{r^2}V_{\theta\theta}\right) + (\beta - 1)BV - \delta V &= 0. \end{aligned} \tag{3.7}$$

The first equation of (3.7) implies $B = 0$ or $N = 0$.

If $N = 0$, substituting it into the second equation of (3.7) leads to $V = 0$.

If $B = 0$, then $N \geq 0$ and $V \geq 0$.

If $B = 0$, then substituting it into the third equation of (3.7) leads to

$$V_{rr} + \frac{1}{r}V_r + \frac{1}{r^2}V_{\theta\theta} - \frac{\delta}{D_V}V = 0. \tag{3.8}$$

That is,

$$\begin{aligned} \Delta V &= \frac{\delta}{D}V \quad \text{in} \quad \Omega, \\ \frac{\partial V}{\partial n} &= 0 \quad \text{in} \quad \partial\Omega. \end{aligned} \tag{3.9}$$

Then the equation (3.9) has only zero solution. □

From one and two dimensional cases: For the bacteria (and for the nutrients), there are two distinct equilibrium, corresponding to the absence of the phage population.

In order to find the reproduction number of phage, we consider the growth rate of phage population,

$$\frac{dV}{dt} = ((\beta - 1)kB - \delta)V = rV.$$

Thus, we have

$$r = (\beta - 1)kB - \delta = \delta(\frac{(\beta - 1)kB}{\delta} - 1) = \delta(R(B) - 1)$$

where $R(B) = \frac{(\beta-1)kB}{\delta}$.

At the phage free equilibrium $(0, \tilde{b}, 0)$

$$R_0 = \frac{(\beta - 1)k\tilde{b}}{\delta}.$$

If $R_0 < 1$ then the phage population will die out and there is no epidemic.
If $R_0 > 1$ then there is an epidemic or traveling wave occurs.
The existence of traveling wave solutions is an interesting characteristic in population dynamics of bacteria and phage. It plays an important role in understanding the long term asymptotic properties of such systems. Here we are looking for traveling wave solutions for the reaction-diffusion model (3.4) in a homogeneous nutrient environment.

Let $B(t,x) = B(x-ct)$, $V(t,x) = V(x-ct)$, and $N(t,x) = N(x-ct)$, then the equations become

$$\begin{aligned} -cN' &= -\frac{1}{\gamma}h(N)B, \\ -cB' &= h(N)B - kBV, \\ -cV' &= D_V V'' + (\beta - 1)kBV - \delta V, \end{aligned} \tag{3.10}$$

where the dependent variable is $s = x - ct$. We can assume without loss of generality that $c > 0$. If $N > 0$ implies N is strictly increasing on a traveling-wave solution as s increases. The first equation of (3.10) says $N' > 0$. Let $N(-\infty) = \tilde{n}$ and $N(+\infty) = \tilde{N}$.
A traveling wave solution should connect to equilibria at $s = -\infty$ and at $s = +\infty$. The equilibria are

$$(N, B, V) = (\tilde{n}, 0, 0)$$

for arbitrary $\tilde{n} \geq 0$, and

$$(N, B, V) = (0, \tilde{b}, 0)$$

for arbitrary $\tilde{b} \geq 0$.

Obviously, the appropriate equilibrium approach as $s \to +\infty$ must be $(N, B, V) = (\tilde{N}, 0, 0)$.

The first equation of (3.10) says that

$$\int_{-\infty}^{\infty} B(s)ds = c\gamma \int_{-\infty}^{\infty} \frac{N'(s)}{h(N(s))}ds = c\gamma \int_{\tilde{n}}^{\tilde{N}} \frac{du}{h(u)}.$$

Assuming $h(0) = 0$ and $h'(0) > 0$, we see that $\tilde{n} = 0$ implies the integrals diverge.

If $\tilde{n} > 0$, then the equilibrium approached as $s \to -\infty$ is clearly $(N, B, V) = (\tilde{n}, 0, 0)$ and the integrals both converge, telling us how much bacteria in the wave is related to $\tilde{n}, \tilde{N}$ and c.

If $\tilde{n} = 0$, then both integrals diverge. In this case, the equilibrium approach as $s \to -\infty$ is probably $(N, B, V) = (0, \tilde{b}, 0)$, since the amount of bacteria in the wave is infinite. However, this could also happen if the equilibrium is $(N, B, V) = (0, 0, 0)$.

It is reasonable to expect that, since $V(\pm\infty) = 0$, we have $V'(\pm\infty) = 0$. Then, integrating the third equation of (3.10), we get

$$(\beta - 1) \int_{-\infty}^{\infty} kBVds = \delta \int_{-\infty}^{\infty} Vds.$$

Multiplying the first equation of (3.10) by γ and adding to the second equation of (3.10) gives

$$-c(\gamma N + B)' = -kBV.$$

Thus, $\gamma N + B$ is strictly increasing. Integrating, we get

$$c\left(\gamma(\tilde{N} - \tilde{n}) + (B(+\infty) - B(-\infty))\right) = \int_{-\infty}^{\infty} kBV ds.$$

We know that $B(+\infty) = 0$ but we are not sure about whether the same holds for $B(-\infty) = 0$.

Putting the two integrals together, we have

$$c(\beta - 1)\left(\gamma(\tilde{N} - \tilde{n}) - B(-\infty)\right) = \delta \int_{-\infty}^{\infty} V ds.$$

Now let $V' = P$ then the system (3.10) can be written as a system of first-order ODEs as follows

$$\begin{aligned} N' &= \frac{1}{\gamma c} h(N) B, \\ B' &= -\frac{1}{c} h(N) B + \frac{kBV}{c}, \\ P' &= -\frac{cP}{D_V} - \frac{(\beta - 1) kBV}{D_V} + \frac{\delta V}{D_V}, \\ V' &= P. \end{aligned} \tag{3.11}$$

A traveling wave solution to (3.4), is a trajectory in the 4-dimensional phase space of (3.11), which goes from the equilibrium $(0, \tilde{b}, 0, 0)$ to the other equilibrium point, $(\tilde{n}, 0, 0, 0)$.

The following theorem summarizes the necessary and sufficient condition for the existence of traveling-wave solutions for the system (3.4).

A traveling wave should start from $(\tilde{n}_1, 0, 0, 0)$ to $(\tilde{n}_2, 0, 0, 0)$ where $\tilde{n}_1 < \tilde{n}_2$, or from$(0, \tilde{b}, 0, 0)$ to $(\tilde{n}, 0, 0, 0)$.

Theorem 3.3: *Assume that* $R_0 = \frac{(\beta-1)k\tilde{b}}{\delta} > 1$, *then for every* $c \geq c^* = 2\sqrt{D_V((\beta-1)k\tilde{b}-\delta)}$, *model (3.4) has a traveling wave solution connecting* $(0,\tilde{b},0)$ *and* $(\tilde{n},0,0)$.

Proof:

The equation (3.11) has two equilibria $E_n = (\tilde{n},0,0,0)$ and $E_b = (0,\tilde{b},0,0)$. We call the nonnegative solutions of (3.11) satisfying

$$\lim_{s\to-\infty}(N(s),B(s),V(s)) = (0,\tilde{b},0),$$

$$\lim_{s\to\infty}(N(s),B(s)V(s)) = (\tilde{n},0,0).$$

We first linearize (3.11) about the critical point $(n,0,0,0)$, $\tilde{n} \geq 0$, to get the eigenvalues. The Jacobian matrix is

$$J_N = \begin{pmatrix} 0 & \frac{h_s}{\gamma c} & 0 & 0 \\ 0 & -\frac{h_s}{c} & 0 & 0 \\ 0 & 0 & -\frac{c}{D_V} & \frac{\delta}{D_V} \\ 0 & 0 & 1 & 0 \end{pmatrix}$$

and thus the characteristic polynomial is given by

$$\chi(\lambda) = \begin{vmatrix} 0-\lambda & \frac{h_s}{\gamma c} & 0 & 0 \\ 0 & -\frac{h_s}{c}-\lambda & 0 & 0 \\ 0 & 0 & -\frac{c}{D_V}-\lambda & \frac{\delta}{D_V} \\ 0 & 0 & 1 & 0-\lambda \end{vmatrix}.$$

The characteristic equation $\chi(\lambda) = 0$ is

$$\lambda\left(\lambda + \frac{h_s}{c}\right)\left(\lambda^2 + \frac{c}{D_V}\lambda - \frac{\delta}{D_V}\right) = 0.$$

We have the following eigenvalues:

$\lambda_1 = 0,$ $\lambda_2 = -\frac{h_s}{c},$

$\lambda_3 = -\frac{c}{2D_V} + \frac{1}{2}\sqrt{\frac{c^2}{D_V^2} + \frac{4\delta}{D_V}}\ ,$ $\lambda_4 = -\frac{c}{2D_V} - \frac{1}{2}\sqrt{\frac{c^2}{D_V^2} + \frac{4\delta}{D_V}}.$

There are two negative eigenvalues, one positive eigenvalue and one zero eigenvalue. This implies that at $(\tilde{n}, 0, 0, 0)$, there is a 2-dimensional stable manifold and 1-dimensional unstable manifold.

We now linearize (3.11) about the critical point $(0, \tilde{b}, 0, 0)$, $\tilde{b} \geq 0$, to get the eigenvalues. The Jacobian matrix is

$$J_B = \begin{pmatrix} \frac{h'(0)\tilde{b}}{\gamma c} & 0 & 0 & 0 \\ -\frac{h'(0)\tilde{b}}{c} & 0 & 0 & \frac{k\tilde{b}}{c} \\ 0 & 0 & -\frac{c}{D_V} & \frac{\delta}{D_V} - \frac{(\beta-1)k\tilde{b}}{D_V} \\ 0 & 0 & 1 & 0 \end{pmatrix}$$

and thus the characteristic polynomial is given by

$$\chi(\lambda) = \begin{vmatrix} \frac{h'(0)\tilde{b}}{\gamma c} - \lambda & 0 & 0 & 0 \\ -\frac{h'(0)\tilde{b}}{c} & 0 - \lambda & 0 & 0 \\ 0 & 0 & -\frac{c}{D_V} - \lambda & \frac{\delta}{D_V} - \frac{(\beta-1)k\tilde{b}}{D_V} \\ 0 & 0 & 1 & 0 - \lambda \end{vmatrix}.$$

The characteristic equation $\chi(\lambda) = 0$ is

$$\lambda\left(\lambda - \frac{h'(0)\tilde{b}}{\gamma c}\right)\left(\lambda^2 + \frac{c}{D_V}\lambda + \frac{(\beta-1)k\tilde{b}}{D_V} - \frac{\delta}{D_V}\right) = 0.$$

The set of eigenvalues are given by

$\lambda_1 = 0, \qquad \lambda_2 = \frac{h'(0)\tilde{b}}{\gamma c},$

$\lambda_3 = -\frac{c}{2D_V} + \frac{1}{2}\sqrt{\frac{c^2}{D_V^2} - 4\frac{(\beta-1)k\tilde{b}-\delta}{D_V}}$,

$\lambda_4 = -\frac{c}{2D_V} - \frac{1}{2}\sqrt{\frac{c^2}{D_V^2} - 4\frac{(\beta-1)k\tilde{b}-\delta}{D_V}}$.

There are two negative eigenvalues, one positive eigenvalue and one zero eigenvalue. This implies that at $(0, \tilde{b}, 0, 0)$, there is a two-dimensional stable manifold and one-dimensional unstable manifold, as long as $c^2 > 4D_V((\beta-1)k\tilde{b}-\delta)$. Since J_N and J_B have real eigenvalues, it is reasonable to look for monotone traveling waves.

The necessary condition for the existence of traveling wave solutions of system (3.11) connects the unstable manifold at $(0, \tilde{b}, 0, 0)$ and the stable manifold at $(\tilde{n}, 0, 0, 0)$, which is called the waves of invasion. Therefore, the minimum traveling wave speed c^* for the existence of traveling wave solutions is
$c > 2\sqrt{D_V((\beta-1)k\tilde{b} - \delta)} = c^*$, where $R_0 = \frac{(\beta-1)k\tilde{b}}{\delta} > 1$.
Until now, we only know that $c \geq 2\sqrt{D_V((\beta-1)k\tilde{b} - \delta)}$ is necessary, we do not know, if it is also a sufficient condition. But, indeed, by constructing the Lyapunov function, using Lasalle's Invariance Principle, we can show that the solution curve which leaves the unstable manifold $(0, \tilde{b}, 0, 0)$ ends up in the

stable manifold $(\tilde{n}, 0, 0, 0)$. This corresponds to a heteroclinic orbit.

Now, we show the existence of traveling wave solutions via a heteroclinic orbit connecting two steady states $(0, \tilde{b})$ and $(\tilde{n}, 0)$ in the plane $\{(N, B, P, V) : V = 0, P = 0\}$.

Consider the system

$$\begin{aligned} N' =& \frac{1}{\gamma c} h(N) B, \\ B' =& -\frac{1}{c} h(N) B. \end{aligned} \tag{3.12}$$

The solution of (3.11) in $\{(N, B, P, V) : V = 0, P = 0\}$ plane is given by $(N(s), B(s), 0, 0)$, where $(N(s), B(s))$ is the solution of (3.12), so the unstable manifold is contained in the largest invariant manifold.

The equilibrium point $(0, \tilde{b})$ corresponding to the bacteria at carrying capacity in the absence of nutrient is an unstable and $(\tilde{n}, 0)$ corresponding to the nutrient at carrying capacity in the absence of bacteria is a stable. There is a zone of transition from the state $(0, \tilde{b})$ to the state $(\tilde{n}, 0)$ with decreased bacteria level and increased nutrient level. That is, the wave $N(s)$ connecting 0 and $\tilde{n}$ should be increasing and moving right or decreasing and moving left but $c > 0$ so that $N(s)$ should be increasing. Likewise, the wave $B(s)$ should be decreasing.

We try to look for solutions of (3.11) in the set

$W = \{(N, B, P, V) : V = 0, P = 0, 0 < N < \tilde{n}, 0 < B < \tilde{b}\}$ in $\mathbb{R}^4$.

Consider the function $L = \frac{1}{2} B^2 \geq 0$ which is defined and differentiable on W. Then

$$\frac{dL}{dt} = \frac{dB}{dt} B = -\frac{1}{c} h(N) B^2 \leq 0$$

in $\overline{W}$. Thus L is a Lyapunov function on W. We define

$$E = \{(N, B, P, V) \in \overline{W} : \frac{dL}{dt} = 0\}.$$

The set E can be simplified as follows: $\frac{dL}{dt} = 0$ for all t implies $N = 0$ or $B = 0$.

$N = 0$ corresponds to the equilibrium $(0, \tilde{b})$ which is unstable and $B = 0$ corresponds to the equilibrium $(\tilde{n}, 0)$ which is stable. Since $(N(s), B(s), 0, 0)$ lies in W for $s \geq 0$ and is bounded. By Lasalle's theorem, every trajectory approaches $(\tilde{n}, 0)$.

The unstable manifold of $(0, \tilde{b})$ will have $N > 0$ near the equilibrium by positivity. Thus, the heteroclinic orbit exists by connecting the positive branch of the unstable manifold of $(0, \tilde{b})$ to the globally attracting $(\tilde{n}, 0)$.

Biologically, the phage population interacting with bacterial population creates a symbiosis with nutrient source leading to the formation of traveling waves. In our case, the phage population invades an area of the petri dish where the nutrient is sufficient.

In Fig. 3.1, we numerically show traveling-wave solutions for different phage diffusion rates and different time periods. As the diffusion rate increases, traveling waves propagate faster, thus it takes less time for phages to spread all over the petri dish. □

To investigate long-term behavior of phage and bacteria for cases $\delta > 0$ and $\delta = 0$. We define the total population of phages, nutrients and bacteria as follows:

$$\widetilde{V}(t) = \int_\Omega V(t, x)dx, \qquad \widetilde{N}(t) = \int_\Omega N(t, x)dx, \quad \text{and} \quad \widetilde{B}(t) = \int_\Omega B(t, x)dx.$$

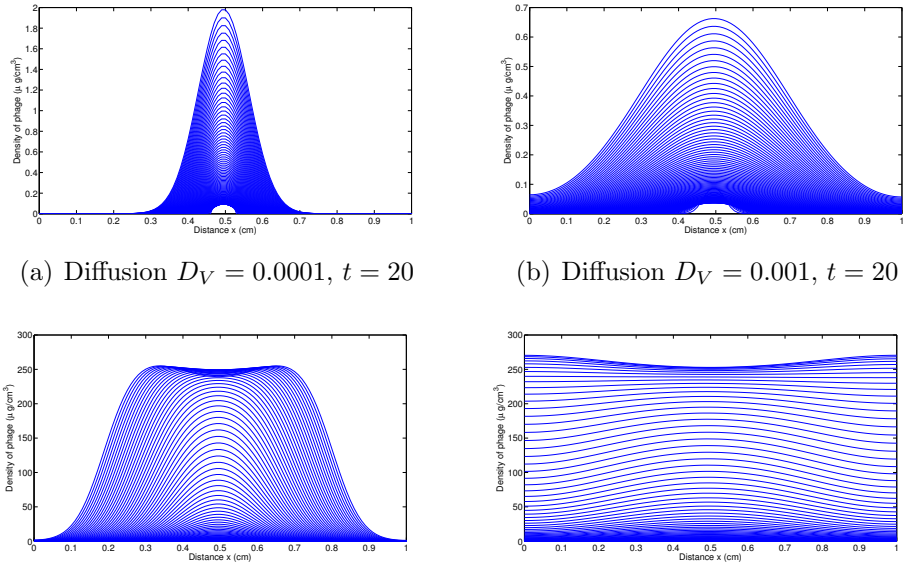

(a) Diffusion $D_V = 0.0001$, $t = 20$

(b) Diffusion $D_V = 0.001$, $t = 20$

(c) Diffusion $D_V = 0.0001$, $t = 60$

(d) Diffusion $D_V = 0.001$, $t = 60$

Figure 3.1: Numerical simulations show the existence of traveling-wave solutions for the system (3.4) with $D_V = 0.0001$ or $D_V = 0.001$. We run simulations for the time ($t = 20$) and ($t = 60$). Different curves represent different times. If we make a cross-section, the distances between any two consecutive curves are the same.

Theorem 3.4: *If* $\delta > 0$, $V(t,x) \to 0$, $B(t,x) > 0$ *as* $t \to \infty$, *for* $x \in \Omega$.

Proof: Differentiating $\widetilde{V}(t)$ yields

$$\frac{d\widetilde{V}(t)}{dt} = \int_\Omega D_V \triangle V dx - \delta \widetilde{V}(t) - (\beta - 1)(\gamma \frac{d\widetilde{N}(t)}{dt} + \frac{d\widetilde{B}(t)}{dt}).$$

The integral is zero by the zero flux hypothesis and Stoke's theorem. We thus obtain the ODE

$$\frac{d\widetilde{V}(t)}{dt} + \delta \widetilde{V}(t) = -(\beta - 1)(\gamma \frac{d\widetilde{N}(t)}{dt} + \frac{d\widetilde{B}(t)}{dt}).$$

By the Method of Variation of Parameters, the solution can be written as

$$\begin{aligned}\widetilde{V}(t) = \widetilde{V}(0)e^{-\delta t} - (\beta-1)\gamma \int_0^t e^{-\delta(t-s)} \frac{d\widetilde{N}(s)}{ds} ds \\ -(\beta-1)\int_0^t e^{-\delta(t-s)} \frac{d\widetilde{B}(s)}{ds} ds.\end{aligned} \tag{3.13}$$

We decompose the integral from 0 to t into two sub integrals $[0, \sqrt{t}]$ and $[\sqrt{t}, t]$. Integrating by parts we obtain

$$-\int_0^{\sqrt{t}} e^{-\delta(t-s)} \frac{d\widetilde{N}(s)}{ds} ds = -e^{-\delta(t-\sqrt{t})}\widetilde{N}(\sqrt{t}) + e^{-\delta t}\widetilde{N}(0) + \delta \int_0^{\sqrt{t}} \widetilde{N}(s) e^{-\delta(t-s)} ds,$$

and

$$-\int_0^{\sqrt{t}} e^{-\delta(t-s)} \frac{d\widetilde{B}(s)}{ds} ds = -e^{-\delta(t-\sqrt{t})}\widetilde{B}(\sqrt{t}) + e^{-\delta t}\widetilde{B}(0) + \delta \int_0^{\sqrt{t}} \widetilde{B}(s) e^{-\delta(t-s)} ds.$$

Since $N(t,x)$ and $B(t,x)$ are monotone decreasing in t, it follows that $\widetilde{N}(t)$ and $\widetilde{B}(t)$ are also monotone decreasing in t, and thus

$$-\int_0^{\sqrt{t}} e^{-\delta(t-s)} \frac{d\widetilde{N}(s)}{ds} ds \leq -e^{-\delta(t-\sqrt{t})}\widetilde{N}(\sqrt{t}) + e^{-\delta t}\widetilde{N}(0) + \delta\sqrt{t}\widetilde{N}(0) e^{-\delta(t-\sqrt{t})},$$

and

$$-\int_0^{\sqrt{t}} e^{-\delta(t-s)} \frac{d\widetilde{B}(s)}{ds} ds \leq -e^{-\delta(t-\sqrt{t})}\widetilde{B}(\sqrt{t}) + e^{-\delta t}\widetilde{B}(0) + \delta\sqrt{t}\widetilde{B}(0) e^{-\delta(t-\sqrt{t})}.$$

All terms on the right hand side of both equations approach zero as $t \to \infty$.

Estimating the second integral is even easier, since

$$-\int_{\sqrt{t}}^{t} e^{-\delta(t-s)}\frac{d\widetilde{N}(s)}{ds}ds \leq -\int_{\sqrt{t}}^{t}\frac{d\widetilde{N}(s)}{ds}ds = -(\widetilde{N}(t)-\widetilde{N}(\sqrt{t})), \tag{3.14}$$

and

$$-\int_{\sqrt{t}}^{t} e^{-\delta(t-s)}\frac{d\widetilde{B}(s)}{ds}ds \leq -\int_{\sqrt{t}}^{t}\frac{d\widetilde{B}(s)}{ds}ds = -(\widetilde{B}(t)-\widetilde{B}(\sqrt{t})). \tag{3.15}$$

Since $\widetilde{N}(t)$ and $\widetilde{B}(t)$ are monotone decreasing in t and bounded from below, the limits of $\widetilde{N}(t)$ and $\widetilde{N}(\sqrt{t})$ as t approaches infinity coincide, the difference is zero, and thus the second sub integral approaches zero as $t \to \infty$. Similarly for $\widetilde{B}(t)$ and $\widetilde{B}(\sqrt{t})$.

Now equation (3.13) implies

$$\begin{aligned} 0 \leq \lim_{t\to\infty}\widetilde{V}(t,x) = \lim_{t\to\infty}\widetilde{V}(0)e^{-\delta t} &- (\beta-1)\gamma\int_0^t e^{-\delta(t-s)}\frac{d\widetilde{N}(s)}{ds}ds \\ &-(\beta-1)\int_0^t e^{-\delta(t-s)}\frac{d\widetilde{B}(s)}{ds}ds \end{aligned}$$

$$\begin{aligned} &= \lim_{t\to\infty}\widetilde{V}(0)e^{-\delta t} - \lim_{t\to\infty}(\beta-1)\gamma\left(\int_0^{\sqrt{t}} e^{-\delta(t-s)}\tfrac{d\widetilde{N}(s)}{ds}ds + \int_{\sqrt{t}}^t e^{-\delta(t-s)}\tfrac{d\widetilde{N}(s)}{ds}ds\right) \\ &\quad - \lim_{t\to\infty}(\beta-1)\left(\int_0^{\sqrt{t}} e^{-\delta(t-s)}\tfrac{d\widetilde{B}(s)}{ds}ds + \int_{\sqrt{t}}^t e^{-\delta(t-s)}\tfrac{d\widetilde{B}(s)}{ds}ds\right) \\ &\leq \lim_{t\to\infty}\widetilde{V}(0)e^{-\delta t} \\ &\quad + \lim_{t\to\infty}(\beta-1)\gamma\left(-e^{-\delta(t-\sqrt{t})}\widetilde{N}(\sqrt{t}) + e^{-\delta t}\widetilde{N}(0) + \delta\sqrt{t}\widetilde{N}(0)e^{-\delta(t-\sqrt{t})}\right) \\ &\qquad + \lim_{t\to\infty}(\beta-1)\gamma\left(-\widetilde{N}(t)+\widetilde{N}(\sqrt{t})\right) \\ &\qquad\quad - \lim_{t\to\infty}(\beta-1)\left(-e^{-\delta(t-\sqrt{t})}\widetilde{B}(\sqrt{t}) + e^{-\delta t}\widetilde{B}(0) + \delta\sqrt{t}\widetilde{B}(0)e^{-\delta(t-\sqrt{t})}\right) \\ &\qquad\qquad + \lim_{t\to\infty}(\beta-1)\left(-\widetilde{B}(t)+\widetilde{B}(\sqrt{t})\right) = 0. \end{aligned}$$

Therefore, $\widetilde{V}(t,x) \to 0$ as $t \to \infty$, for $x \in \Omega$.

Hence, $V(t,x) \to 0$ as $t \to \infty$, for $x \in \Omega$.

The first equation of (3.4) implies

$$N(t,x) = N_0 e^{-\frac{\alpha}{\gamma}\int_0^t B(s,x)ds}.$$

Since $V(t,x) \to 0$ as $t \to \infty$, the second equation of (3.4) implies

$$\lim_{t\to\infty} B_t = \lim_{t\to\infty} h(N)B = \lim_{t\to\infty} -\gamma N_t.$$

Integrating from 0 to t implies

$$\int_0^t \lim_{t\to\infty} B_t dt = \int_0^t \lim_{t\to\infty} -\gamma N_t dt,$$

$$\lim_{t\to\infty} \int_0^t B_t dt = \lim_{t\to\infty} \int_0^t -\gamma N_t dt,$$

$$\lim_{t\to\infty} B(t,x) - B_0 = \lim_{t\to\infty} -\gamma(N(t,x) - N_0),$$

$$\lim_{t\to\infty} B(t,x) = B_0 - \lim_{t\to\infty} \gamma N_0 e^{-\frac{\alpha}{\gamma}\int_0^t B(s,x)ds} - \gamma N_0,$$

$$\liminf_{t\to\infty} B(t,x) = B_0 + \gamma N_0 > 0.$$

Therefore, $B(t,x) > 0$ as $t \to \infty$, for $x \in \Omega$.

Hence, $\widetilde{B}(t,x) > 0$ as $t \to \infty$, for $x \in \Omega$.

Theorem 3.5: *If* $\delta = 0$, $\widetilde{V}(t) \to V_\infty \in (0,\infty)$, as $t \to \infty$, for $x \in \Omega$.

Proof: Consider the equation

$$V_t = D_V \Delta V + \beta k B V - k B V - \delta V.$$

Letting $\delta = 0$ implies

$$V_t = D_V \Delta V + \beta k B V - k B V.$$

That is,

$$\frac{d\widetilde{V}}{dt} = \int_\Omega D_V \Delta V d\bar{x} + \int_\Omega (\beta - 1) k B V d\bar{x} = \int_\Omega (\beta - 1) k B V d\bar{x} \geq 0,$$

since $\beta >> 1$.

Therefore, $\widetilde{V}(t) \to V_\infty \in (0, \infty)$ as $t \to \infty$, for $x \in \Omega$.

Note: If $\delta = 0$, $B(t, x) \to 0$ as $t \to \infty$, for $x \in \Omega$.

In case $\delta = 0$, the model neglects phage decay, and the only loss of phage is due to adsorption to bacteria.

In case $\delta > 0$, the phage will eventually disappear, leaving behind some of uninfected bacteria.

3.E Numerical Simulations

We consider a closed system (like a petri dish) that contains a population of phage, a population of bacteria, and potentially limiting bacterial nutrients. We run simulations in one-dimensional and two-dimensional spaces. Simulation results in one-dimensional space are obtained using MATLAB. Similar

to the one-dimensional space initial condition, we use the following initial condition for phages (V) to run the simulation in two-dimensional space in FLEXPDE:

$$V(0, x, y) = \exp[(-(x - 0.5)^2 - (y - 0.5)^2)/0.01].$$

We use that initial condition to mimic one 'drop' of phage in the petri dish. Actually after a very short time, one drop will become that initial function for phages density.

For all simulations, zero flux boundary conditions are used. We estimate reasonable ranges of parameters from literature to run simulations (see Table 3.1). Furthermore, we compute the effect of burst size and the long term behavior of bacteria and phages.

Var/Par	Definition	Unit	Value	Reference
B	Density of bacteria	$\mu g(cm)^{-3}$	-	-
V	Density of phage	$\mu g(cm)^{-3}$	-	-
N	Density of nutrient	$\mu g(cm)^{-3}$	-	-
D_B	Diffusion coefficient of bacteria	$(cm)^2h^{-1}$	$0 - 0.03$	(45)
D_V	Diffusion coefficient of phage	$(cm)^2h^{-1}$	$0 - 0.002$	(45)
D_N	Diffusion coefficient of nutrient	$(cm)^2h^{-1}$	$0 - 10$	(45)
α	Resource uptake rate	h^{-1}	$0.7 - 0.8$	(45; 46; 47)
δ	Phage mortality rate	h^{-1}	$0.003 - 0.03$	(46)
γ	Yield constants	-	0.5	(14; 11)
K	Half-saturation constant	$\mu g(cm)^{-3}$	$4 - 5$	(46; 47)
β	burst size	-	$50 - 150$	(47; 39; 40)
k	Infection rate	h^{-1}	$(6.24)10^{-8} - (6.24)10^{-6}$	(39; 46)
q	Decompose rate	h^{-1}	$0 - 0.01$	

Table 3.1: Variables and Parameters

3.E.1 Phage-only Moving Model

We start with the simulations in one-dimensional space and place a 'drop' of phage in the middle of the semi-solid agar petri dish and observe the outcomes (see Fig.3.2). Here, we assume the bacteria are immotile. We select parameter values from ranges given in Table 3.1:

$\alpha = 0.738,\ K = 4,\ k = 0.000624,\ \beta = 70,\ \delta = 0.03\ \gamma = 0.5,\ D_B = 0,$ $D_V = 0.0001,\ D_N = 0$ and the initial conditions for $x \in [0, 1]$ are:

$$V(0,x) = \begin{cases} 0.1, |x - 0.5| \leq 0.03; \\ 0, \quad |x - 0.5| > 0.03; \end{cases},$$

$B(0, x) = 1$, and $N(0, x) = 10$.

Initially, the bacterial population start to increase but then diminishes as the phage population increases. And finally both die out due to the nutrient-closed system (see Fig.3.2). Fig.3.3 illustrates that all bacterial populations are converted to phage after a certain time.

3.E.2 In the Absence of Phages

If we assume that there are no phages, i.e. $V(0) = 0$, the bacteria grow and maintain a stable density that is limited by the nutrients (see Fig.3.4(b)). In this case, when there is no interaction of phages with bacteria, the figure shows that although bacterial population is not yet controlled by phage, it can be seen through the total density of bacterial populations (see Fig.3.4).

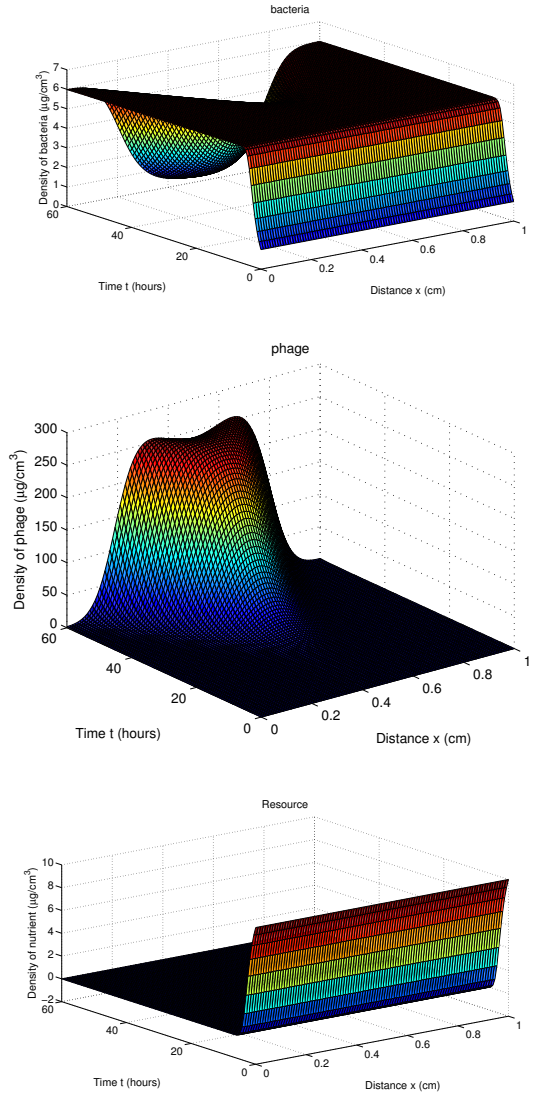

Figure 3.2: One dimensional simulation in a homogeneous nutrient environment - phage-only moving model. Chosen values of parameters are $\alpha = 0.738$, $K = 4$, $k = 0.000624$, $\beta = 70$, $\delta = 0.03$ $\gamma = 0.5$, $D_B = 0$, $D_V = 0.0001$, $D_N = 0$.

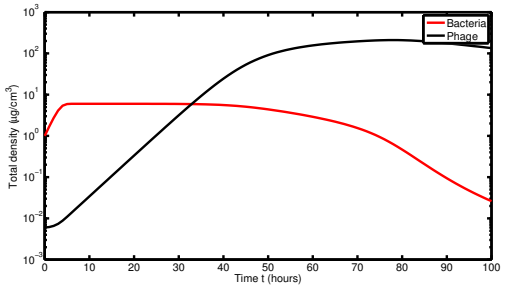

Figure 3.3: One dimensional simulation in a homogeneous nutrient environment for total population of bacteria and phage - phage-only moving model. Chosen values of parameters are $\alpha = 0.738$, $K = 4$, $k = 0.000624$, $\beta = 70$, $\delta = 0.03$ $\gamma = 0.5$, $D_B = 0$, $D_V = 0.0001$, $D_N = 0$.

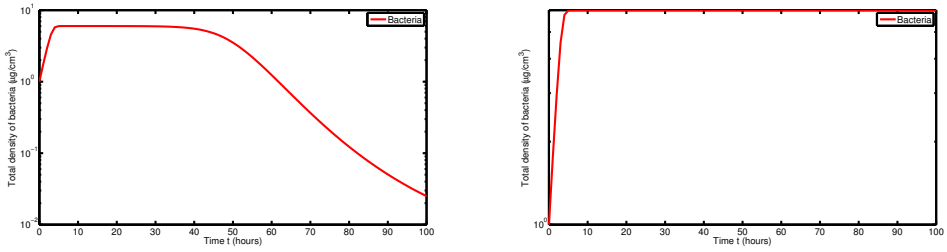

(a) with phage (b) without phage

Figure 3.4: Compare bacterial population with and without phage. Chosen values of parameters are $\alpha = 0.738$, $K = 4$, $k = 0.000624$, $\beta = 70$, $\delta = 0.003$ $\gamma = 0.5$, $D_B = 0$, $D_V = 0.0001$, $D_N = 0$.

3.E.3 Soft Agar Model

We assume that host bacteria in agar grow and diffuse but agar itself does not diffuse. In this case, we consider the environment as soft agar which essentially makes the bacteria diffuse. In order to obtain the soft agar model, we expand our phage-only moving model (3.4), which incorporates diffusion term for bacteria. The model is provided by

$$\begin{aligned}\frac{\partial N}{\partial t} =& -\frac{1}{\gamma}h(N)B,\\ \frac{\partial B}{\partial t} =& D_B\frac{\partial B}{\partial x} + h(N)B - kBV,\\ \frac{\partial V}{\partial t} =& D_V\frac{\partial V}{\partial x} + \beta kBV - kBV - \delta V.\end{aligned} \tag{3.16}$$

We start with the simulations in one-dimensional space. We place a 'drop' of phage in the middle of the soft agar petri dish and observe the outcomes (see Fig. 3.5). In this case our parameter values are given in Table 3.1.

Initially, bacterial density starts to increase fast while there is no increase on the phage density. After a latent period, the bacterial density gets steady and then decreases, while the phage density starts to increase. And finally both go extinct due to the nutrient-closed system and the phage mortality (see Fig. 3.5). Fig. 3.6 illustrates that the entire bacterial population converts to phage after a long time. Finally, we compute the long term behavior of bacteria and phages in the agar media (see Fig. 3.7).

Fig. 3.7 shows a simulation running over 180 hours, assuming the replication rate of bacteria follows the exponential law over this period of time. Altogether, this simulation just gives us an idea of what could happen over a longer period of time which is that both bacteria and phage go extinct.

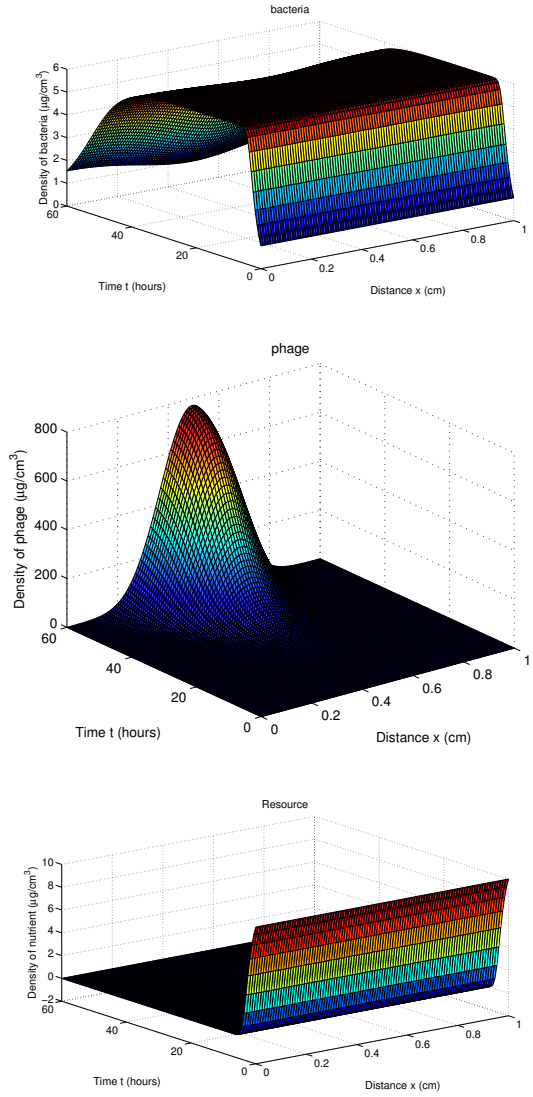

Figure 3.5: One dimensional simulation in a homogeneous nutrient environment - soft agar model. Chosen values of parameters are $\alpha = 0.738$, $K = 4$, $k = 0.000624$, $\beta = 70$, $\delta = 0.03$ $\gamma = 0.5$, $D_B = 0.02$, $D_V = 0.0001$, $D_N = 0$.

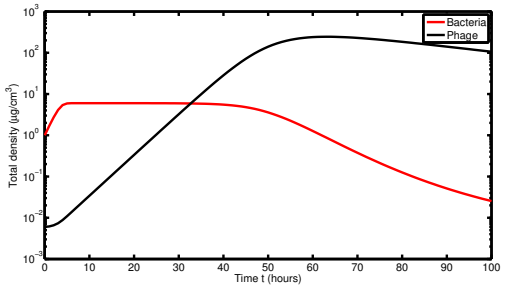

Figure 3.6: One dimensional simulation in a homogeneous nutrient environment for total population of bacteria and phage - general agar model. Chosen values of parameters are $\alpha = 0.738$, $K = 4$, $k = 0.000624$, $\beta = 71$, $\delta = 0.03$ $\gamma = 0.5$, $D_B = 0.02$, $D_V = 0.0001$, $D_N = 0$.

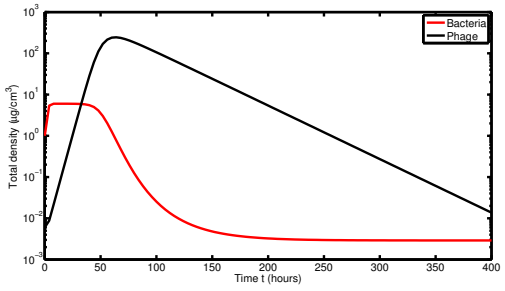

Figure 3.7: Long term behavior - soft agar model. Chosen values of parameters are $\alpha = 0.738$, $K = 4$, $k = 0.000624$, $\beta = 70$, $\delta = 0.03$, $\gamma = 0.5$, $D_B = 0.02$, $D_V = 0.0001$, $D_N = 0$.

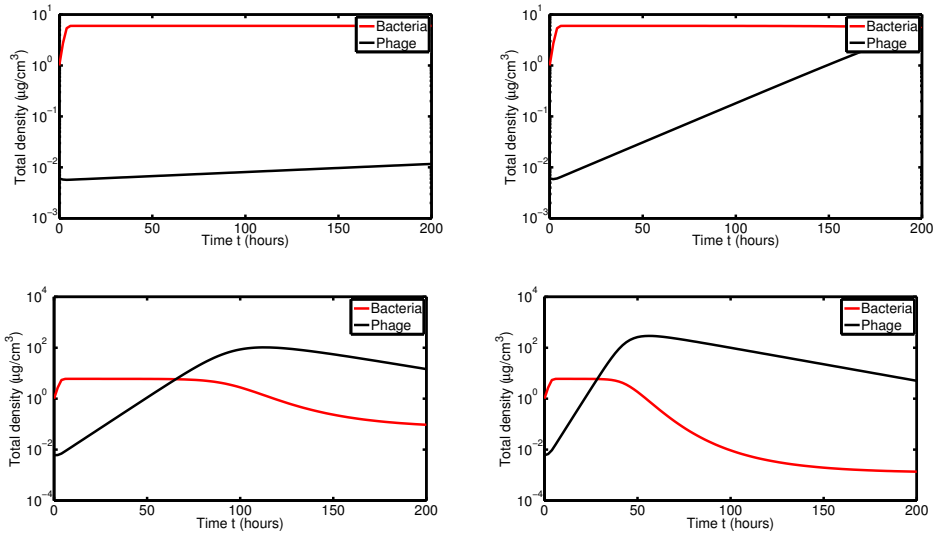

Figure 3.8: Effect of burst size - soft agar model. Chosen values of parameters are $\alpha = 0.738$, $K = 4$, $k = 0.000624$, $\beta = 10 - 100$, $\delta = 0.003$ $\gamma = 0.5$, $D_B = 0.02$, $D_V = 0.0001$, $D_N = 0$, (1) Top left : $\beta = 10$, (2) Top right : $\beta = 18$, (3) Bottom left : $\beta = 40$, (4) Bottom right : $\beta = 80$.

3.E.4 Effect of Burst Size

In this section, we compute the total density of bacteria and phages for different burst sizes. For example, we increase the burst size from 10 to 120 to see the effect on bacteria and phages. In addition, we compute the extinction time of bacteria and the maximum density of bacteria and phages for different burst size. We define extinction time as the time when bacterial density reduces to $0.0001 \mu g/cm^{-3}$.

The lower burst size can take a long time to infect and destroy bacteria (see Fig.3.8 panels (1),(2)) while the higher burst size can take a short time to destroy bacteria (see Fig.3.8 panels (3),(4)). According to Fig.3.9, higher burst size results in shorter survival of bacteria. Therefore, the bacteria will be controlled if the burst size of phages is greater than a certain threshold (see

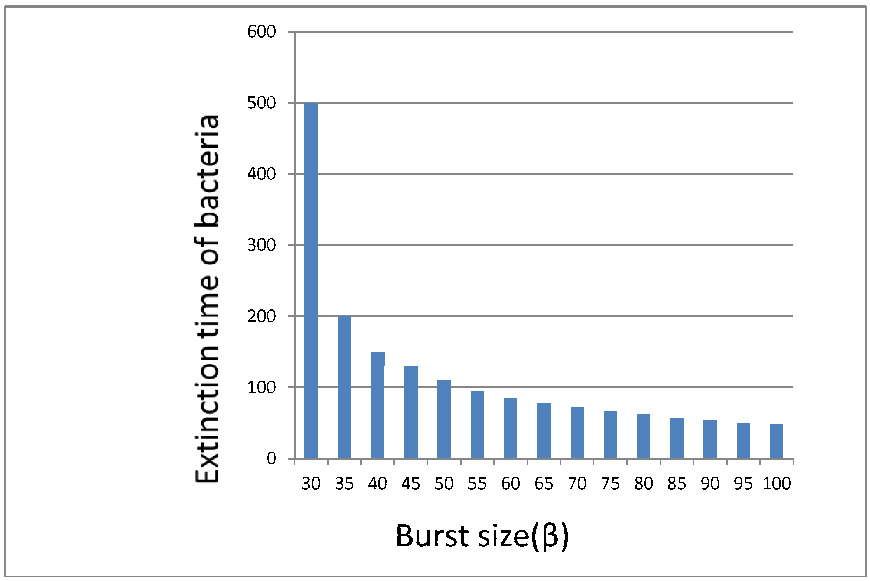

Figure 3.9: Extinction time of bacteria vs. burst size (β) - soft agar model case.

Fig.3.10). We define the threshold value of burst size as the minimum value of burst size above which bacteria go extinct after 200 hrs. Here, we choose 200 hrs which is approximately 8 days, as an effective recovery time from a bacterial infection. If we increase the infection rate or the yield constant, the threshold value of burst size is decreasing (see Fig.3.11, Fig.3.12). The threshold heavily depends on the parameters, such as infection rate and yield coefficient, but is independent of nutrient diffusion (see Fig.3.13).

3.E.5 General Minimum Model

In this section, we assume the environment is a water solution in which bacteria swim using flagella. Phages, on the other hand, do not swim (45) but diffuse like Brownian particles. In order to obtain a general minimum model, we

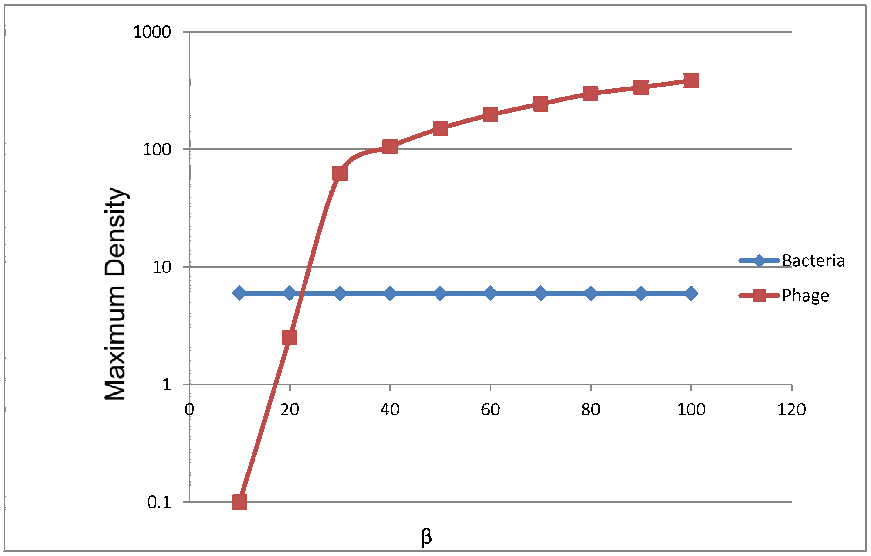

Figure 3.10: Bifurcation diagram for the burst size (β) and the maximum densities of bacteria and phages - soft agar model case.

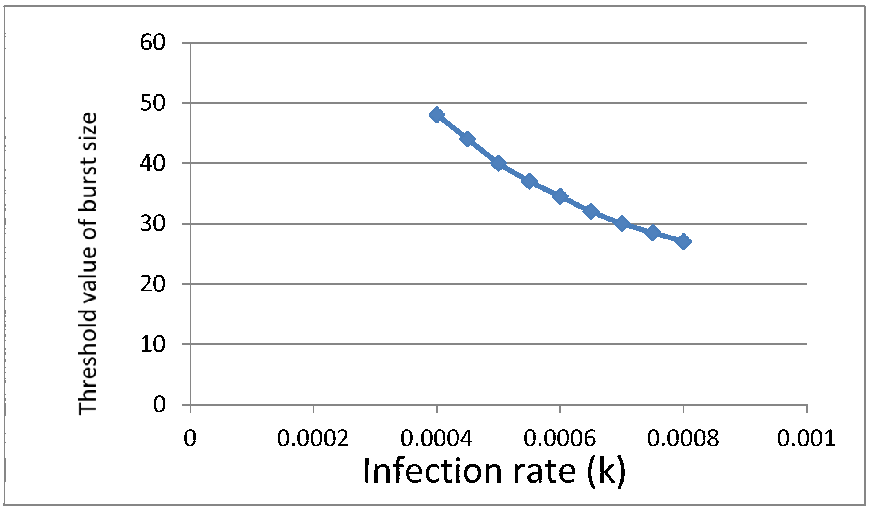

Figure 3.11: Threshold value of burst size for bacterial extinction time vs. infection rate (k) - general agar model case.

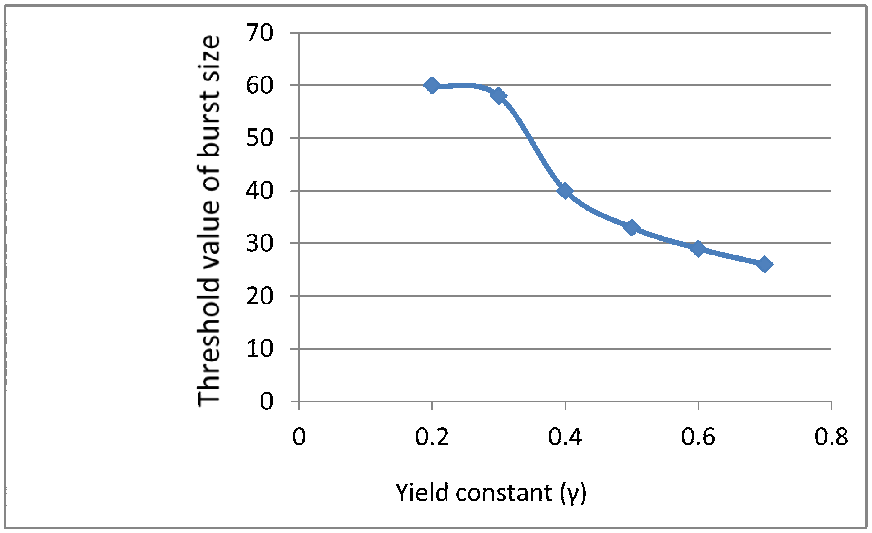

Figure 3.12: Threshold value of burst size for bacterial extinction time vs. yield constant (γ) - general agar model case.

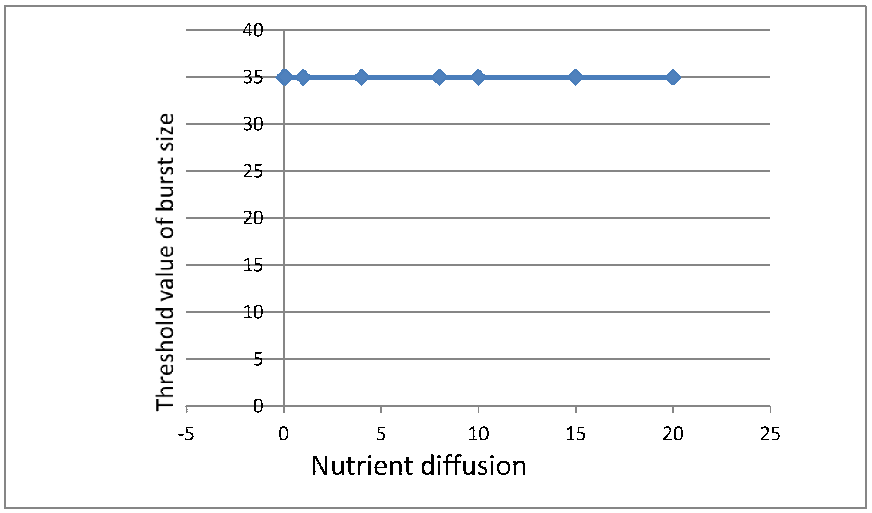

Figure 3.13: Threshold value of burst size for bacterial extinction time vs. nutrient diffusion (D_N) - general minimum model.

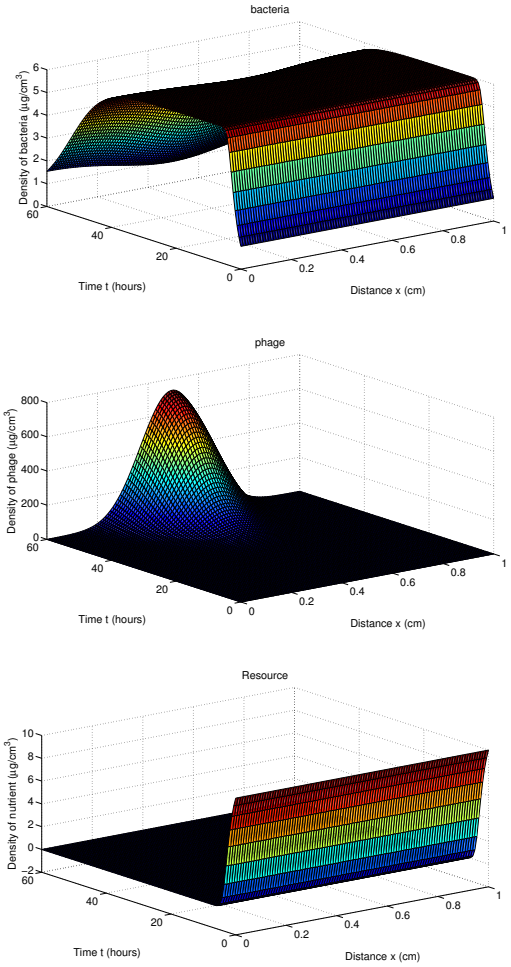

Figure 3.14: One dimensional simulation in a homogeneous nutrient environment - general minimum model case. Chosen values of parameters are $\alpha = 0.738$, $K = 4$, $k = 0.000624$, $\beta = 70$, $\delta = 0.03$ $\gamma = 0.5$, $D_B = 0.02$, $D_V = 0.0001$, $D_N = 1$.

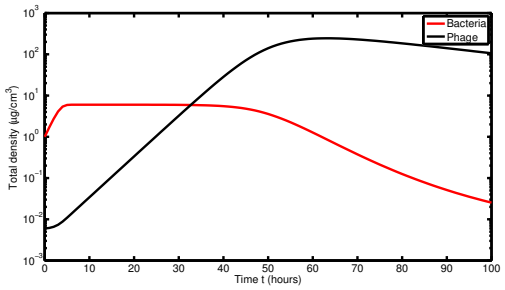

Figure 3.15: One dimensional simulation in a homogeneous nutrient environment for total population of bacteria and phage- general minimum model. Chosen values of parameters are $\alpha = 0.738$, $K = 4$, $k = 0.000624$, $\beta = 70$, $\delta = 0.03$, $\gamma = 0.5$, $D_B = 0.02$, $D_V = 0.0001$, $D_N = 1$.

expand the previous model (3.16), by incorporating the diffusion term for nutrients. The model is provided by

$$\begin{aligned} \frac{\partial N}{\partial t} &= D_N \frac{\partial N}{\partial x} - \frac{1}{\gamma} h(N) B, \\ \frac{\partial B}{\partial t} &= D_B \frac{\partial B}{\partial x} + h(N) B - kBV, \\ \frac{\partial V}{\partial t} &= D_V \frac{\partial V}{\partial x} + \beta kBV - kBV - \delta V. \end{aligned} \tag{3.17}$$

We start with simulations on one-dimensional space. We place a 'drop' of phage in the middle of the liquid petri dish and observe the outcomes (see Fig.3.14).

From figures 3.6 and 3.15, we predict that nutrient diffusion is not an important component to determine the population dynamics of bacteria and phages.

3.E.6 Two Dimensional General Agar Model

We place a very small quantity of virus at any point in the petri dish and spread the host bacteria evenly on a plate of agar. We then compute the density distributions of bacteria and pages over time, and record spatial distributions

at 0hr, 5hrs, 10hrs, and 40hrs in Fig. 3.16. We select parameter values from ranges given in Table 3.1.

We choose the following initial conditions to run simulations in FLEXPDE:

$$
\begin{aligned}
&B(0,x,y) = 1,\\
&V(0,x,y) = \exp[(-(x-0.5)^2 - (y-0.5)^2)/0.01],\\
&N(0,x,y) = 10.
\end{aligned}
$$

Our model in a soft agar medium is provided by

$$
\begin{aligned}
\frac{\partial N}{\partial t} =& -\frac{1}{\gamma} h(N)B,\\
\frac{\partial B}{\partial t} =& D_B\left(\frac{\partial^2 B}{\partial x^2} + \frac{\partial^2 B}{\partial y^2}\right) + h(N)B - kBV,\\
\frac{\partial V}{\partial t} =& D_V\left(\frac{\partial^2 V}{\partial x^2} + \frac{\partial^2 V}{\partial y^2}\right) + \beta kBV - kBV - \delta V.
\end{aligned}
\tag{3.18}
$$

Initially, without showing any growth in phage, bacteria start to grow fast around the petri dish. After a latent period (10 hours), the density of phage starts to increase very fast and the density of bacteria starts to decrease. At 40 hours, phages destroy all bacteria and dominate most of the petri dish. Finally, at 180 hours phages go extinct due to the absence of bacteria (see Fig. 3.16).

3.F Extended Models

We can easily extend the general minimum model by incorporating infected bacteria and resistant bacteria. We use the functions, $k(N) = (1-x)k_{max} + xk_{max}\frac{N}{N+K}$, $\beta(N) = (1-x)\beta_{max} + x\beta_{max}\frac{N}{N+K}$, $0 \le x \le 1$, to run the simula-

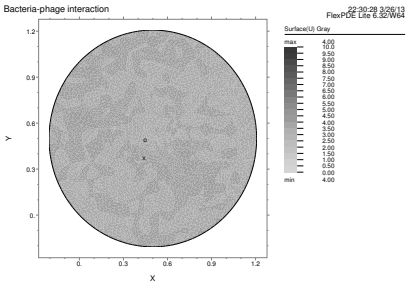

(a) Density of B at $t = 0$

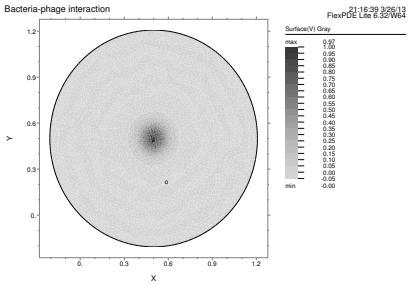

(b) Density of V at $t = 0$

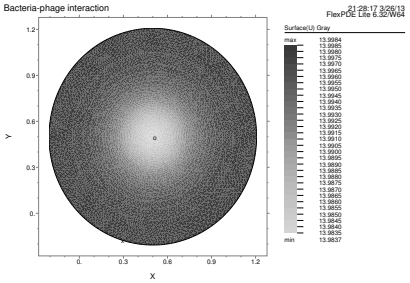

(c) Density of B at $t = 5$

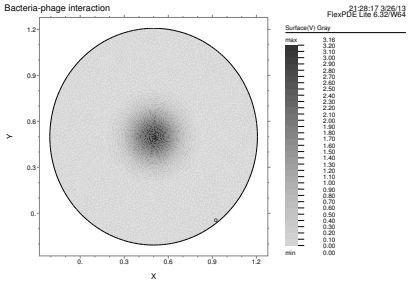

(d) Density of V at $t = 5$

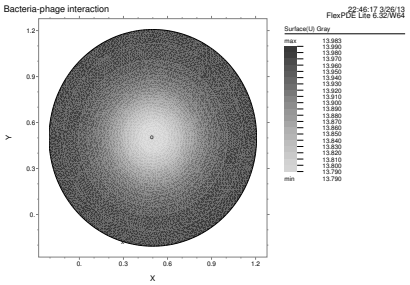

(e) Density of B at $t = 10$

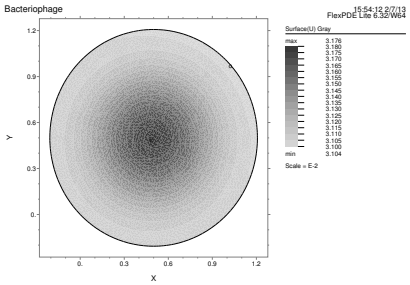

(f) Density of V at $t = 10$

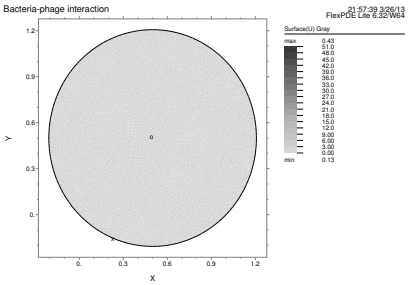

(g) Density of B at $t = 40$

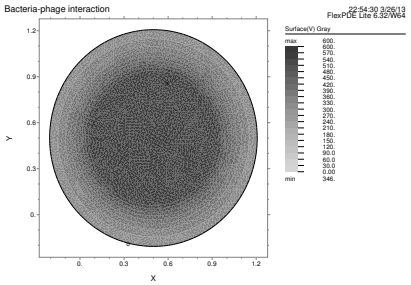

(h) Density of V at $t = 40$

Figure 3.16: Two dimensional simulations at $t = 0, 5, 10, 40$. In these figures, the color changing from dark grey to light grey represents the density changing from high to low.

tions that was used in (39) but, our simulation results predict that the average values of k and β also admit the same results as those functions results. Therefore, we present the simulation results with the average values of k and β. We select parameter values from ranges given in Table 3.1:

$\alpha_1 = 0.738$, $\alpha_1 = 0.538$, $K = 4$, $k = 0.000624$, $\beta = 70$, $\delta = 0.03$, $q = 0.02$ $\gamma = 0.5$, $D_B = D_I = 0.02$, $D_V = 0.0001$, $D_N = 1$ and the initial conditions:
$V(0,x) = \begin{cases} 0.1, |x-0.5| \leq 0.03; \\ 0, \quad |x-0.5| > 0.03; \end{cases}$,
$B(0,x) = 1$, and $N(0,x) = 10$.

3.F.1 NBVI Model

Susceptible (B) and infected (I) bacteria are assumed to have the same moving ability. The following reaction diffusion equations express the concentrations of nutrients (N), uninfected bacteria (B), infected bacteria (I), and phage (V):

$$\begin{aligned} \frac{\partial N}{\partial t} &= D_N \Delta N - \frac{1}{\gamma} h(N) B, \\ \frac{\partial B}{\partial t} &= D_B \Delta B + h(N) B - kBV, \\ \frac{\partial I}{\partial t} &= D_I \Delta I + kBV - qI, \\ \frac{\partial V}{\partial t} &= D_V \Delta V + \beta q I - kBV - \delta V, \end{aligned} \tag{3.19}$$

where D_N,D_B, D_I, D_V are diffusion coefficients of nutrient, bacteria, infected bacteria and phage respectively, k is the infection rate, $\beta > 1$ is the burst size, δ is the mortality rate of phage, α is a maximum specific growth rate, K is

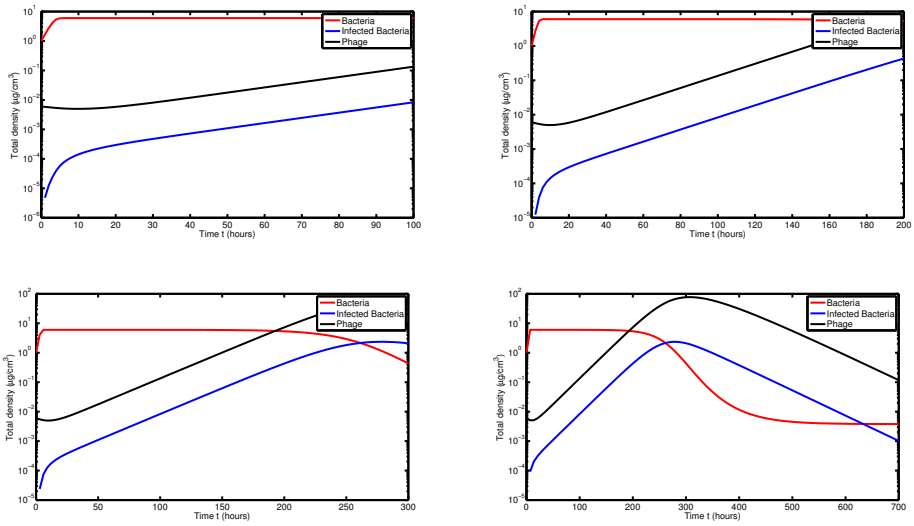

Figure 3.17: NBVI model-(1) Top left : t=100, (2) Top right: t =200, (3) Bottom left: t=300, (4) Bottom right: t=700. Chosen values of parameters are $\alpha = 0.738$, $K = 4$, $k = 0.000624$, $\beta = 60$, $\delta = 0.03$ $\gamma = 0.5$, $D_B = D_I = 0.02$, $D_V = 0.001$,$D_N = 10$, $q = 0.02$.

the half saturation constant, $\gamma < 1$ is the yield constant, q is the decompose rate, and $h(N)$ is the nutrient consumption function that satisfies $h(0) = 0, h'(t) > 0, h''(t) \leq 0$. The model has initial and homogeneous Neumann boundary (zero flux) conditions: $N(0,x) = N_0$ for $x \in \Omega$, $B(0,x) = B_0$ for $x \in \Omega$, $I(0,x) = 0$ and $V(0,x) = V_0$ for $x \in \Omega_\epsilon$ (where Ω_ϵ is a small disk with radius ϵ, it can be centered at the center of petri dish, or at any other point); $\nabla N = 0, \nabla B = 0, \nabla I = 0, \nabla V = 0$ on $\partial\Omega$, where n is an outward normal vector to the boundary $\partial\Omega$.

From Fig.3.17, after a certain time, infected bacterial populations start to grow and then go extinct due to lack of nutrients.

3.F.2 NBVR Model

It is reasonable to assume that the resistant bacteria suffers a cost of resistance to phage infection in the form of a reduced growth rate. Also, they are not attacked by phages and can be considered as a mutant of the susceptible bacteria. The following reaction diffusion equations express the concentrations of nutrients (N), bacteria (B), resistant bacteria (R), and phage (V):

$$\begin{aligned}
\frac{\partial N}{\partial t} &= D_N \Delta N - \frac{1}{\gamma} h_1(N) B - \frac{1}{\gamma} h_2(N) R, \\
\frac{\partial B}{\partial t} &= D_B \Delta B + h_1(N) B - kBV, \\
\frac{\partial R}{\partial t} &= D_R \Delta R + h_2(N) R, \\
\frac{\partial V}{\partial t} &= D_V \Delta V + \beta kBV - kBV - \delta V,
\end{aligned} \tag{3.20}$$

where D_N,D_B, D_R, D_V are diffusion coefficients of nutrient, bacteria, resistant bacteria and phage respectively, k is the infection rate, $\beta > 1$ is the burst size, δ is the mortality rate of phage, α is a maximum specific growth rate, K is the half saturation constant, $\gamma < 1$ is the yield constant, and $h(N)$ is the nutrient consumption function that satisfies $h(0) = 0, h'(t) > 0, h''(t) \leq 0$. The model has initial and homogeneous Neumann boundary (zero flux) conditions: $N(0, x) = N_0$ for $x \in \Omega$, $B(0, x) = B_0$ for $x \in \Omega$, $R(0, x) = R_0$ and $V(0, x) = V_0$ for $x \in \Omega_\epsilon$ (where Ω_ϵ is a small disk with radius ϵ, it can be centered at the center of petri dish, or at any other point); $\nabla N = 0, \nabla B = 0, \nabla R = 0, \nabla V = 0$ on $\partial\Omega$, where n is an outward normal vector to the boundary $\partial\Omega$. And $h_1(N) > h_2(N)$, which implies that sensitive-bacteria B(t) is superior to resistant-bacteria R(t) with respect to taking up of the resource.

From Fig.3.18, we can see that susceptible bacterial populations are controlled

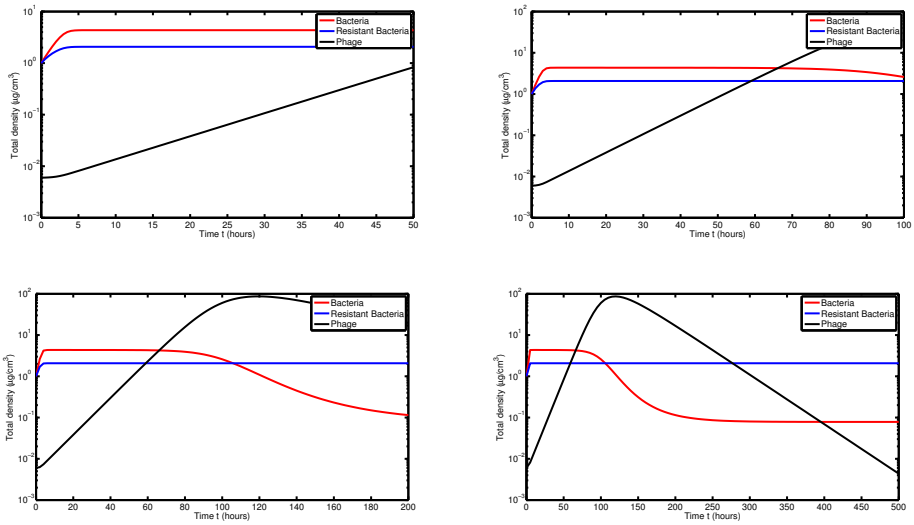

Figure 3.18: NBVR model-(1) Top left : t=50, (2) Top right: t =100, (3) Bottom left: t=200, (4) Bottom right: t=500. Chosen values of parameters are $\alpha = 0.738$, $K = 4$, $k = 0.000624$, $\beta = 50$, $\delta = 0.03$ $\gamma = 0.5$, $D_B = D_R = 0.02$, $D_V = 0.001$, $D_N = 1$.

by phages infection but not resistant bacteria populations. The model also predicts that the susceptible bacteria can dominate the resistant bacteria in the absence of phage.

Chapter 4

Competition of Fast and Slow Movers for Renewable and Diffusive Resources

4.A Introduction

Movement of animals is a characteristic feature for species. The role of moving speed in species competition has been studied recently in many papers. Applying the Lotka-Volterra competition model with diffusion, previous studies showed that the slow mover excludes the fast mover after a long time (34; 36; 33). However, it is actually possible to have the coexistence case or the case that the fast mover excludes the slow mover (35; 37; 38). The well-known Lotka-Volterra competition model with diffusion is a phenomenological model which incorporates the effect of a resource implicitly. A better model should incorporate resource dynamics explicitly.

In this chapter, we will concentrate on the analysis of competition of fast and

slow moving animals for renewable and diffusive resources using the reaction-diffusion equation. The competition results were studied in the context of previous study by Dockery et al. (34). Their work assumes that fast movers excluded by slow movers under strong evolutionary force. However, They used Lotka-Volterra competition model to study their results but in reality we have to incorporate nutrients explicitly to get the better results. Thus, on the basis of the work in (34), section 4.B aims at presenting a mechanistic but simple model to examine the competition of fast and slow moving species in the presence of renewable and diffusive resources. These two species are assumed to be genetically identical except for their moving speeds. The environment is assumed to be continuous but not homogeneous. Using these assumptions, we construct a resource-explicit model with linear or nonlinear resource uptake functions. In section 4.C, we run numerical simulations for linear and nonlinear models and discuss how the nonsymmetric resource uptake rates affect the results. Simulations of our linear model show two cases: the fast mover goes extinct but the slow mover survives at a positive constant level, or both species go extinct. These are consistent with the previous results (34). Simulations of our nonlinear model show two new outcomes: the fast mover goes extinct but the slow mover survives at oscillations, or both species survive at oscillations. The coexistence scenario can definitely appear in nature; thus, our resource-explicit competition model with nonlinear resource uptake functions is a more realistic model than the Lotka-Volterra type models or our model with linear resource uptake functions.

4.B Mathematical Model

We consider the competition of two species with different moving speeds. These two species compete for renewal and diffusive resources, and they are genetically identical except for their diffusion coefficients. Our model has three variables: F (density of the fast mover), S (density of the slow mover), and R (density of renewable resources):

$$\begin{aligned}
\frac{\partial F}{\partial t} &= D_1 \Delta F + [h_1(R) - \delta_1]\, F, \\
\frac{\partial S}{\partial t} &= D_2 \Delta S + [h_2(R) - \delta_2]\, S, \\
\frac{\partial R}{\partial t} &= D_3 \Delta R + R(m(x) - R) - \frac{1}{\gamma_1} h_1(R) F - \frac{1}{\gamma_2} h_2(R) S,
\end{aligned} \tag{4.1}$$

where $\Delta = \frac{\partial^2}{\partial x^2}$, the resource uptake functions $h_i(R)$ satisfy the conditions $h_i(0) = 0$, $h_i'(t) > 0$, and $h_i''(t) \leq 0$, $i = 1, 2$. For example, $h_i(R) = \alpha_i R/(k_i + R)$ or $h_i(R) = \alpha_i R$. Here, α_i's are maximum specific growth rates, k_i's are half-saturation constants for resource uptake (representing resource uptake efficiencies), δ_i's are mortality rates, γ_i's are yield constants, and D_i's are diffusion coefficients. According to the definitions of F and S, we should have $D_1 >> D_2$. In our simulations, we apply zero flux boundary conditions. We choose the resource renewal rate (or carrying capacity) function $m(x) = r(1 + \tanh(x - 0.5)/0.1)$, or $r \exp((x - 0.5)^2)/0.1$, or $r \exp(-(x - 0.5)^2)/0.1$. The first function $(\tanh(x - 0.5)/0.1)$ is monotone, the second function $(\exp((x - 0.5)^2)/0.1)$ has its minimum in the middle, and the third function $(\exp(-(x - 0.5)^2)/0.1)$ has its maximum in the middle. Environments are heterogeneous across space and time. The function $m(x)$ represents their natural growth rates and it reflects the quality and quantity

of resources available at position x. We vary two key resource parameters r and D_3 to discuss the competition results of fast and slow movers (see Tables 4.1-4.6).

We integrate both variables F and S over space to obtain the (total) densities of the two competing species. All possible competition outcomes of the (total) densities are listed below:

1. $C_1 \rightarrow$ both go extinct;
2. $C_2 \rightarrow$ the fast mover goes extinct but the slow mover survives at a positive constant level;
3. $C_3 \rightarrow$ the fast mover goes extinct but the slow mover survives at oscillations;
4. $C_4 \rightarrow$ the fast mover survives at a positive constant level but the slow mover goes extinct;
5. $C_5 \rightarrow$ the fast mover survives at oscillations but the slow mover goes extinct;
6. $C_6 \rightarrow$ both survive at an internal steady state;
7. $C_7 \rightarrow$ both survive at oscillations.

4.C Numerical Simulations

We run simulations in one-dimensional space for linear and nonlinear models. Finally, we study the simulation results for nonsymmetric resource uptake rates. Simulation results are obtained using MATLAB.

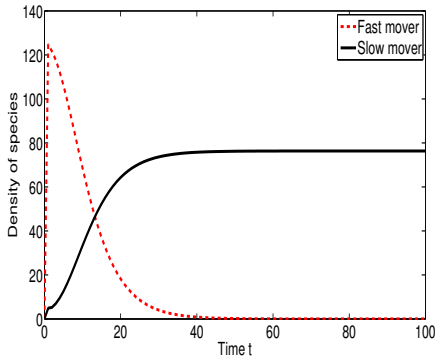

(a) $m(x) = r(1+\tanh(x-0.5)/0.1)$, $r = 10$

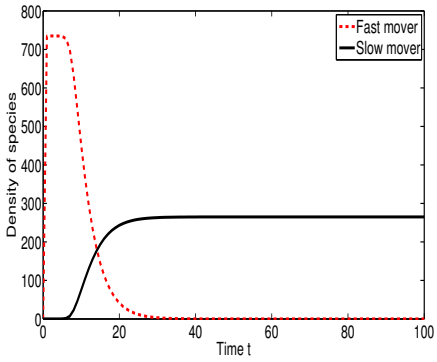

(b) $m(x) = r\exp((x-0.5)^2/0.1)$, $r = 10$

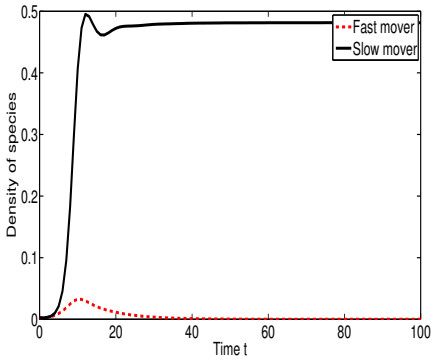

(c) $m(x) = r(1+\tanh(x-0.5)/0.1)$, $r = 1$

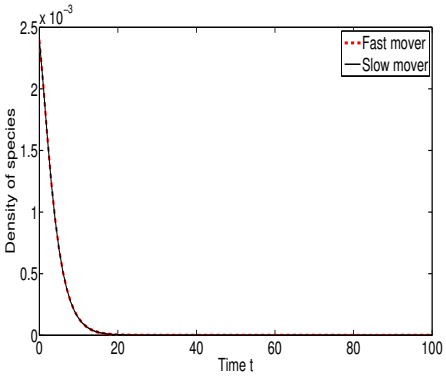

(d) $m(x) = r(1+\tanh(x-0.5)/0.1)$, $r = 0.1$

Figure 4.1: Plots of total density as a function of time for linear case with different values of the parameter r and different forms of the function $m(x)$. Chosen values of parameters are: $D_1 = 1$, $D_2 = 0.01$, $D_3 = 0.001 - 10$, $\alpha_1 = \alpha_2 = 0.7$, $\delta_1 = \delta_2 = 0.4$, $\gamma_1 = \gamma_2 = 0.49$.

4.C.1 Linear Model

The model with linear resource uptake functions is mathematically tractable, especially for stability analysis. The linear resource uptake functions apply the well-mixing assumption, which is widely accepted in many biological in-

D_3/r	0.01	0.1	1	10
0.001	C_1	C_1	C_2	C_2
0.01	C_1	C_1	C_2	C_2
0.1	C_1	C_1	C_2	C_2
1	C_1	C_1	C_2	C_2
10	C_1	C_1	C_2	C_2

Table 4.1: Linear case with $m(x) = r(1+\tanh\frac{x-0.5}{0.1})$- The possible competition outcomes according to the total density of fast and slow movers.

D_3/r	0.01	0.1	1	10
0.001	C_1	C_1	C_2	C_2
0.01	C_1	C_1	C_2	C_2
0.1	C_1	C_1	C_2	C_2
1	C_1	C_1	C_2	C_2
10	C_1	C_1	C_2	C_2

Table 4.2: Linear case with $m(x) = r\exp[\frac{(x-0.5)^2}{0.1}]$- The possible competition outcomes according to the total density of fast and slow movers.

teractions. The linear model is provided by

$$\begin{aligned}
\frac{\partial F}{\partial t} &= D_1\Delta F + [\alpha_1 R - \delta_1]\, F, \\
\frac{\partial S}{\partial t} &= D_2\Delta S + [\alpha_2 R - \delta_2]\, S, \\
\frac{\partial R}{\partial t} &= D_3\Delta R + R(m(x) - R) - \frac{1}{\gamma_1}\alpha_1 RF - \frac{1}{\gamma_2}\alpha_2 RS,
\end{aligned} \tag{4.2}$$

where $m(x) = r(1 + \tanh(x - 0.5)/0.1)$ or $m(x) = r\exp[\frac{(x-0.5)^2}{0.1}]$ or $m(x) = r\exp[-\frac{(x-0.5)^2}{0.1}]$, $D_1 = 1$, $D_2 = 0.01$, $D_3 = 0.001 - 10$, $\alpha_1 = \alpha_2 = 0.7$, $\delta_1 = \delta_2 = 0.4$, $\gamma_1 = \gamma_2 = 0.49$, and $r = 0.01 - 10$.

We run a group of simulations for three different forms of the function $m(x)$. Comparing Fig.4.1(a) with Fig.4.1(b) for different forms of $m(x)$, we find that the density of the slow mover quickly increases from the very beginning in panel (a), but the density of the slow mover starts to increase after a while in panel (b). The asymptotic behaviors are about the same in these two

D_3/r	0.01	0.1	1	10
0.001	C_1	C_1	C_2	C_2
0.01	C_1	C_1	C_2	C_2
0.1	C_1	C_1	C_1	C_2
1	C_1	C_1	C_1	C_2
10	C_1	C_1	C_1	C_2

Table 4.3: Linear case with $m(x) = r\exp[-\frac{(x-0.5)^2}{0.1}]$- The possible competition outcomes according to the total density of fast and slow movers.

panels: the fast mover goes extinct and the slow mover survives at a positive constant level. Comparing panel (a) with panel (c), the fast mover dominates the community in the beginning in panel (a), but when we choose smaller values for the parameter r in panel (c), the slow mover seems dominant all the time. When we choose the parameter r as being extremely small in panel (d), then both species go extinct due to the shortage of resources. We vary the resource related parameters r and D_3 in Tables 4.1-4.3, which provide more thorough results. From these tables, we observe that both species go extinct when r is small, while the fast mover goes extinct and slow mover survives at a positive constant level when r is large. These two outcomes are consistent to Lotka-Volterra type models (34).

Because of the resource equation has faster dynamics than the equations of the competing species, we apply the quasi-steady state approximation to obtain

$$R = k(x) - \frac{r}{\gamma}(F + S)$$

which implies

$$\frac{\partial F}{\partial t} = D_1 F_{xx} + (rk(x) - d - \frac{r^2}{\gamma}F - \frac{r^2}{\gamma}S)F,$$
$$\frac{\partial S}{\partial t} = D_2 S_{xx} + (rk(x) - d - \frac{r^2}{\gamma}F - \frac{r^2}{\gamma}S)S.$$

This is the same model as the Lotka-Volterra competition model with diffusion (34). Hence, the results of our linear model are qualitatively the same as Lotka-Volterra type models.

4.C.2 Nonlinear Model

The linear resource uptake function goes to infinity as the resource availability tends to infinity. This is obviously unrealistic. The Monod function gives a saturation level of the resource uptake function when the resource availability is sufficiently high. This nonlinear nutrient uptake function can lead to more realistic predictions. The nonlinear model is provided by

$$\begin{aligned}
\frac{\partial F}{\partial t} &= D_1 \Delta F + \left[\frac{\alpha_1 R}{k_1 + R} - \delta_1\right] F, \\
\frac{\partial S}{\partial t} &= D_2 \Delta S + \left[\frac{\alpha_2 R}{k_2 + R} - \delta_2\right] S, \\
\frac{\partial R}{\partial t} &= D_3 \Delta R + R(m(x) - R) - \frac{1}{\gamma_1}\frac{\alpha_1 R}{k_1 + R}F - \frac{1}{\gamma_2}\frac{\alpha_2 R}{k_2 + R}S,
\end{aligned} \tag{4.3}$$

where $m(x) = r(1 + \tanh(x - 0.5)/0.1)$ or $m(x) = r\exp[\frac{(x-0.5)^2}{0.1}]$ or $m(x) = r\exp[-\frac{(x-0.5)^2}{0.1}]$, $D_1 = 1$, $D_2 = 0.01$, $D_3 = 0.001 - 10$, $\alpha_1 = \alpha_2 = 0.7$, $\delta_1 = \delta_2 = 0.4$, $\gamma_1 = \gamma_2 = 0.49$ and $r = 0.01 - 10$.

We plot representative simulation results for the nonlinear model in Fig.4.2. If we fix r and increase D_3 from panel (a) to panel (b), we have the transition

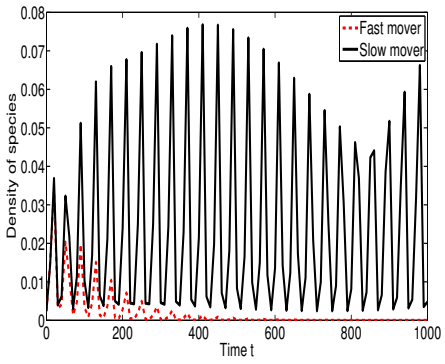

(a) $r = 0.1$, $D_3 = 0.01$

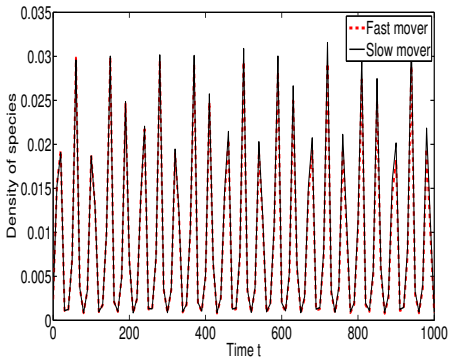

(b) $r = 0.1$, $D_3 = 0.1$

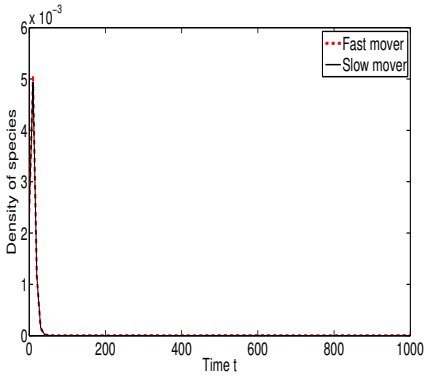

(c) $r = 0.01$, $D_3 = 0.001$

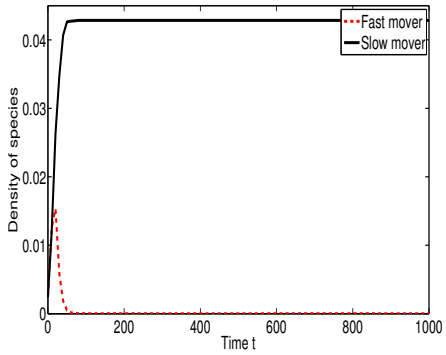

(d) $r = 0.1$, $D_3 = 0.001$

Figure 4.2: Plots of total density as a function of time for nonlinear case with different values of r and D_3. Chosen values are $D_1 = 1$, $D_2 = 0.01$, $D_3 = 0.001 - 10$, $\alpha_1 = \alpha_2 = 0.7$, $\delta_1 = \delta_2 = 0.4$, $k_1 = k_2 = 0.06$, $\gamma_1 = \gamma_2 = 0.49$.

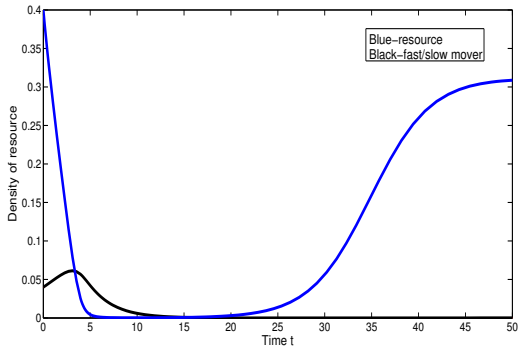

(a) $r = 0.1$, $D_1 = D_2 = 0$

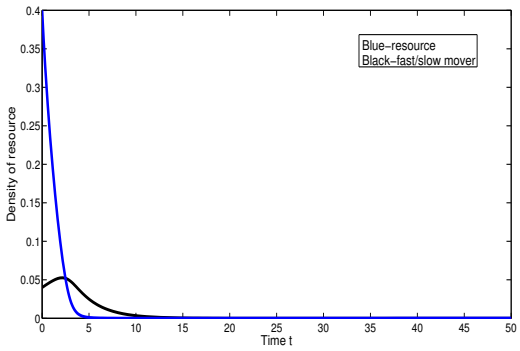

(b) $r = 0.01$, $D_1 = D_2 = 0$

Figure 4.3: ODE case. Chosen values are $D_1 = 0$, $D_2 = 0$, $D_3 = 0$, $\alpha_1 = \alpha_2 = 0.7$, $\delta_1 = \delta_2 = 0.4$, $k_1 = k_2 = 0.06$, m=3.12228 r.

D_3/r	0.01	0.1	1	10
0.001	C_1	C_2	C_1	C_1
0.01	C_1	C_2	C_1	C_1
0.1	C_1	C_2	C_1	C_1
1	C_1	C_2	C_1	C_1
10	C_1	C_2	C_1	C_1

Table 4.4: Nonlinear case with $m(x) = r(1 + \tanh \frac{x-0.5}{0.1})$- The possible competition outcomes according to the total density of fast and slow movers.

D_3/r	0.01	0.1	1	10
0.001	C_1	C_2	C_2	C_2
0.01	C_1	C_3	C_2	C_2
0.1	C_1	C_7	C_1	C_2
1	C_1	C_7	C_1	C_1
10	C_1	C_7	C_1	C_1

Table 4.5: Nonlinear case with $m(x) = r \exp[\frac{(x-0.5)^2}{0.1}]$- The possible competition outcomes according to total density of fast and slow movers.

from the case when the fast mover goes extinct and the slow mover survives at oscillations, to the oscillatory coexistence case. If we fix D_3 and increase r from panel (c) to panel (d), we have a transition from the extinction case to the case when the fast mover goes extinct and the slow mover survives at a positive constant level.

We vary r and D_3 for different forms of the function $m(x)$ in Tables 4.4-4.6, which provides more thorough results. When we choose the monotone $m(x)$, the possible outcomes are the same as the linear model or Lotka-Volterra type models. When we choose the other two types of $m(x)$ (min or max in the middle), the nonlinear model leads to two new outcomes: the fast mover goes extinct and the slow mover survives at oscillations, or both survive at oscillations. These new observations seem to occur in the intermediate values of r (between 0.1 and 1). These possibilities can never be obtained from the

D_3/r	0.01	0.1	1	10
0.001	C_1	C_1	C_3	C_2
0.01	C_1	C_1	C_3	C_1
0.1	C_1	C_1	C_7	C_1
1	C_1	C_1	C_7	C_1
10	C_1	C_1	C_7	C_1

Table 4.6: Nonlinear case with $m(x) = r\exp[-\frac{(x-0.5)^2}{0.1}]$- The possible competition outcomes according to total density of fast and slow movers.

linear model or Lotka-Volterra type models.

Following the same logic as in the linear model, we apply the quasi-steady state approximation to obtain

$$m(x) - R = \frac{1}{\gamma}\left(\frac{\alpha F}{k+R} + \frac{\alpha S}{k+R}\right)$$

which implies

$$R^2 + (k - m(x))R + (\frac{\alpha}{\gamma}(F+S) - m(x)k) = 0$$

whose roots are

$$R = \frac{m(x) - k \pm \sqrt{(k-m(x))^2 - 4(\frac{\alpha}{\gamma}(F+S) - m(x)k)}}{2}.$$

If we replace R with one of these roots in the first two equations of the model (4.3), we will obtain a very complicated model that is quite different from the Lotka-Volterra competition model with diffusion (34). This is one possible way to explain the appearance of the two new outcomes from the nonlinear model.

In addition, we consider a special case for the effect of the consumption func-

tion h_i in the nonlinear model. First we plot the solution for resource without being eaten by the fast and slow movers (consumption function $h_1 = h_2 = 0$). For different $m(x)$, we can see different shapes (Fig.4.4). Then we plot the solution with resource being eaten by only the fast mover or only the slow mover or both to see the outcomes. After 50 hours, the resource renewal happens in resource only eaten by fast movers more than one time but only one time in resource only eaten by slow mover (Fig.4.5). Also, the total density of resource renewal is getting slower in resource eaten by only fast mover than only slow mover. For example, At 100 hours, the total density of resource is higher in resource only eaten by slow mover than fast mover.

Remark: ODE Case

In this section, we set $D_1 = D_2 = D_3 = 0$, and simulate ODE equations to compare with reaction diffusion PDE simulation results . We choose the average value for m and higher and lower resource parameter r to plot the figures (Fig.4.3). In this case, the resource parameter r is independent on the growth of fast and slow movers but for the higher resource parameter r, we can observe the resource renewal faster then the lower resource parameter r.

4.C.3 Nonsymmetric Resource Uptake Rates

The fast mover has a higher energy cost, which leads to a higher resource uptake rate than the slow mover, that is, $\alpha_1 > \alpha_2$. We apply this non-symmetric nutrient uptake rates for the linear model in Fig.4.6 and Fig.4.7. Fig.4.6 shows the new outcome that the fast mover survives at a positive constant level and the slow mover goes extinct. In Fig.4.7, we vary α_1 from $\alpha_2(= 0.7)$ to 1.8. The switch occurs at $\alpha_1 = 1.1$ from the case that the slow mover wins to the

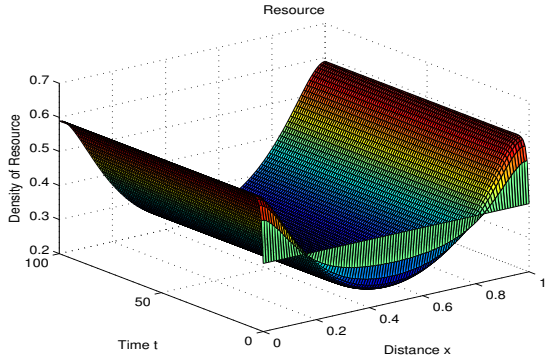

(a) $m(x) = r\exp((x-0.5)^2/0.1)$

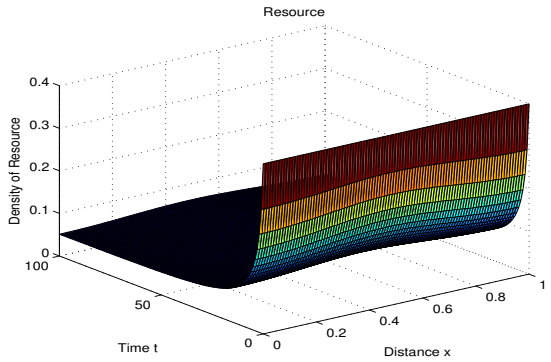

(b) $m(x) = r\exp(-(x-0.5)^2/0.1)$

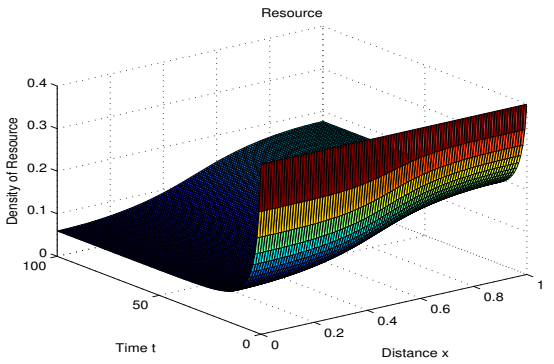

(c) $m(x) = r(1+\tanh(x-0.5)/0.1)$

Figure 4.4: Resource without being eaten by fast and slow movers ($h_1 = h_2 = 0$) along space and time for different $m(x)$. Chosen values are $D_1 = 1$, $D_2 = 0.01$, $D_3 = 0.01$, $\alpha_1 = \alpha_2 = 0.7$, $\delta_1 = \delta_2 = 0.4$, $k_1 = k_2 = 0.06$, $r = 0.1$.

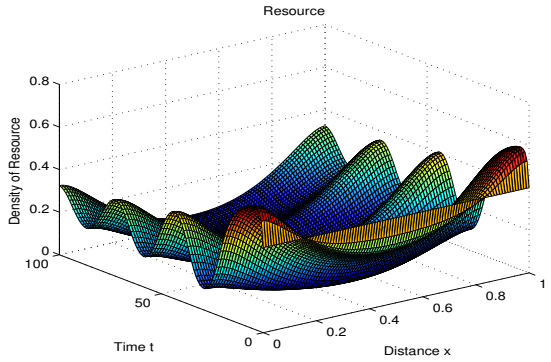

(a) Resource and fast mover ($h_2 = 0$)

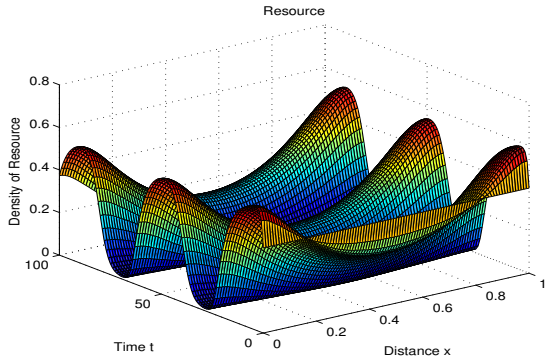

(b) Resource and slow mover ($h_1 = 0$)

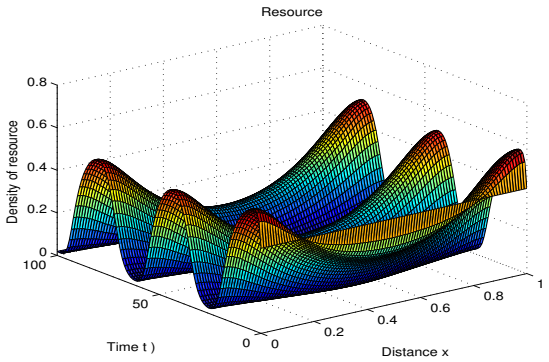

(c) Resource, fast mover and slow mover

Figure 4.5: Resource being eaten by (a) only fast mover, (b) only slow mover, (c) both. Chosen values are $D_1 = 1$, $D_2 = 0.01$, $D_3 = 0.01$, $\alpha_1 = \alpha_2 = 0.7$, $\delta_1 = \delta_2 = 0.4$, $k_1 = k_2 = 0.06$, $\gamma_1 = \gamma_2 = 0.49$, $r = 0.1$ $m(x) = r\exp((x-0.5)^2/0.1)$.

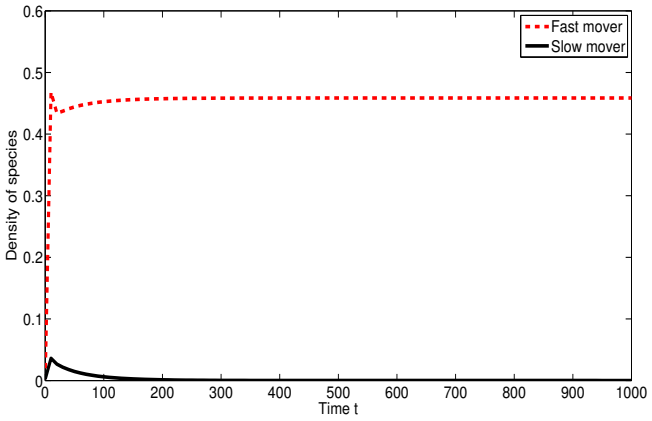

Figure 4.6: Nonsymmetric resource uptake rates $\alpha_1 > \alpha_2$ with $r = 1$, $D_3 = 0.01$.

case that the fast mover wins. For the nonlinear model, we can see the similar switch as the linear model, although the fast mover can survive not only at a positive constant level but also at oscillations.

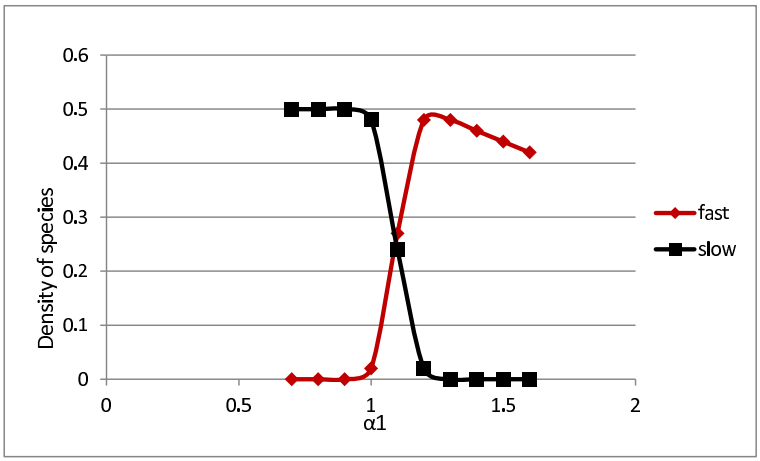

Figure 4.7: Bifurcation diagram with $m(x) = r(1 + \tanh(x - 0.5)/0.1)$, $r = 1$, $D_3 = 0.01$.

Chapter 5

Concluding Remarks

We presented a reaction diffusion model of resource-limited population growth, competition, and interaction based on biologically realistic assumptions regarding the relationship between resources and movement of bacteria or animals and the interaction of bacteria with phages. The common properties of this model were discussed and some specific cases were studied, including the role of random motility in bacterial competition, phages spread on host bacteria, and fast and slow moving animals competition. We approached these models mathematically and numerically using different techniques. To study its validity, we compared the mathematical and numerical results with the experimental results from previous literature.

In this thesis, we examined three different reaction-diffusion models that can be used to study species competition, movement, and infection. The first model used to interpret bacterial competition and movement in a homogeneous environment. On the basis of the work by Wei et al. (28), we presented, in chapter 2, an exposition of how bacterial random motility is influenced in bacterial competition in a petri dish. We simplified the mathematical analysis by

choosing one-dimensional domain. This allowed us to compare the behavior of higher dimensional cases. The second model used to interpret bacteria-phage interaction is the system of reaction-diffusion equations, which incorporates nutrient explicitly. In chapter 3, the model was analyzed under different assumptions. The third model used to interpret fast and slow moving species competition for renewable and diffusive resources. On the basis of the work by Dockery et al. (34), we presented, in chapter 4, an exposition of how linear and nonlinear resource uptake rates are played in the competition of fast and slow moving animals.

5.A Major Conclusions

First, we studied and analyzed a mathematical model for competition of motile and immotile bacterial strains in a homogeneous nutrient environment, in order to explore the role of nutrient and random (undirected) motility in bacterial competition. Our theoretical framework shows that bacteria always go extinct eventually due to lack of nutrients, while some nutrients will always be remaining. If we incorporate a nutrient input as chemostat-type models (nutrient-open), then the bacterial community can be sustained. We showed the existence of traveling-wave solutions by additionally providing their minimum and maximum traveling speeds. This result seems novel because almost all of the previous models have showed that traveling-wave solutions have a minimum traveling speed. Using numerical simulations, we showed that in agar media the motile strain grows on the boundary after a few hours; but in liquid media it always grows in the middle. In both media the immotile strain grows in the middle, and it has much higher total density in liquid media than

in agar media. In agar media the motile strain is dominant in total density, while in liquid media bacterial motility is not that important. The simulation and experimental results illustrate the advantage of undirected motility in agar media in the absence of chemotaxis.

Antibiotic resistance has inspired a novel treatment, phage therapy, for bacterial disease. Phage therapy is more effective for bacterial infections that are already resistant. We attempt to answer how efficient phage spread and replication control can eliminate malignant bacteria. Focussing on the lytic phage life cycle rather than the lysogenic cycle, we introduce reaction-diffusion models to describe the elimination of bacteria by phage and their spread. The main feature of our models is to incorporate nutrients explicitly for bacterial consumption and growth.

Theoretical framework suggests that phage population densities will exceed bacterial densities after a certain period of time and eventually go extinct due to lack of bacterial densities. We provide rigorous mathematical conditions for persistence/extinction of bacteria or phage. From existence of traveling wave solution, we can observe the wave of phage transition between steady states. Also, We determine how the extinction time of bacteria depends on the phage burst size, thus our theoretical framework can estimate how long a patient will recover under a selected phage therapy. The threshold heavily depends on other parameters, such as infection rate and yield coefficient, but is independent of nutrient diffusion coefficient. We suggest that the efficiency of phage therapy for bacterial infection depends on its infection rate, burst rate and initial dose. Finally, Our model has implications for the use of phage as antibiotic therapeutic agents.

Finally, for the competition of fast and slow movers for renewable and diffusive

resources, Lotka-Volterra type models only suggest two possibilities: the slow mover excludes the fast mover or both species go extinct. Our linear mechanistic model demonstrated similar results. Our nonlinear mechanistic model, a more realistic framework, also suggests two new possibilities: the slow mover excludes the fast mover in an oscillatory way or both species coexist in oscillatory way. If the nutrient uptake rate of the fast mover is larger than that of the slow mover, it is possible for the fast mover to exclude the slow mover. The possibility that the fast mover wins can also be caused by stochasticity (extinction of the slower mover in the early stage) or predation (the slow mover is easily to be caught by predators). In our model, results are obtained by the differences in the diffusion rates (D_i) because the per-capita rates (h_i) of increase are the same for both species. In reality the winner should be those who eat and grow fast but not the ones that run fast since resource is diffusive.

5.B Discussion

In chapter 2, in liquid media, if we assume that immotile strain utilizes nutrient more efficiently than the motile strain ($k_1 > k_2$) due to energy cost of movement, then the total density ratio of motile strain to immotile strain is far less than one. Models in two-dimensional space are enough to mimic the petri dish experiment (28), although some applications such as biofilm on teeth and bath tub may need three-dimensional space.

Recent bacteria-phage models have tended to focus more on ecological and evolutionary issues than on the effectiveness of a particular phage treatment in controlling a bacterial population. Therefore, we have to focus on its practical issues and modify the model to get better results.

In chapter 4, our results are independent of the form of the scalar function $m(x)$, as long as it is not constant. Therefore, the function $m(x)$ is not important since resource is diffusive. When the function $m(x)$ is a constant function (degenerate case), we can observe that both species survive at steady state. This result is a new possibility. When the parameter r is large, we have accuracy problems to run the simulation program. Also, the nonsymmetric resource uptake rates case invites further bifurcation studies, like hopf bifurcation.

5.C Future Work

More theoretical work and lab experiments need to be accumulated to validate undirected motility in bacteria and its effects on competition. The assumptions of the existing models require further verification in experiments. Some well organized lab experiments in heterogeneous nutrient environments will be important to understand the significance of undirected (random) cell movement.

Bacteria and bacteriophage continually evolve with mutation. As bacteria evolve to resist the dominant phage population, phages evolve by mutation and can infect the dominant resistant bacteria population. Therefore, we plan to extend our model to study the bacteria-phage co-evolution.

For fast and slow moving animals, we plan to run simulations for mechanistic models on higher dimensional space. Mathematical analyses of the proposed models need to be done. Specific species should be discussed later for data fitting. In addition, we will expand our models to incorporate species' resting stage, which may provide more possibilities for the competition results.

Bibliography

[1] Asei S, Byers B, Eng A, James N, Leto J. Bacterial Chemostat Model, 2007.

[2] Brazhnik PK and Tyson JJ. On traveling wave solutions of fisher's equation in two spatial dimensions. SIAM. J. Appl. Math 60:371-391, 2000.

[3] Chang I, Gilbert ES, Eliashberg N and Keasling JD. A three-dimensional stochastic simulation of biofilm growth and transport-related factors that affect structure. Micro. Bio. 149:2859-2871, 2003.

[4] Fontes M and Kaiser D. *Pnas*, Myxococcus cells respond to elastic forces in their substances. Proceedings of the National Academy of Sciences of the United States of America 96:8052-8057, 1999.

[5] Fujikawa H, Matsushita M. Fractal growth of Bacillus subtilis on agar plates. J. Phys. Soc. Jpn. 58:3875-3878, 1989.

[6] Fujikawa H and Matsushita M. Bacterial Fractal Growth in the Concentration Field of Nutrient. J. Phys. Soc. Jpn.60:88-94, 1991.

[7] Hibbing ME, Fuqua C, Parsek MR and Peterson BS. Bacterial competition: surviving and thriving in the microbial jungle. Nature Reviews Microbiology 8:15-25, 2010.

[8] Hzder DP, Hemmerbach R, Lebert M. Gravity and the bacterial unicellular organisms. Developmental and cell biology series 40, 2005.

[9] Kennedy CR, and Aris R. Traveling waves in a simple population model involving growth and death. Bull.of Math. Biol. 42:397-429, 1980.

[10] Keller E. Mathematical aspects of bacterial chemotaxis, Antibiotics and chemotherapy. 19:79-93, 1974.

[11] Kelly FX, Dapsis KJ, Lauffenburger DA. Effect of Bacterial Chemotaxis on Dynamics of Microbial Competition. Micro. Biol. 16:115-131, 1998.

[12] Khain E, Sander LM, and Stein AM. A model for Glioma Growth. Research Article 11:53-57, 2005.

[13] Krone SM, Lu R, Fox R, Suzuki H and Top EM. Modelling the spatial dynamics of plasmid transfer and persistence. Micro. Biol. 153:2803-2816, 2007.

[14] Lauffenburger D, Aris R, and Keller KH. Effects of Random Motility on growth of Bacterial Populations. Micro.Ecol. 7:207-227, 1981.

[15] Lauffenburger D, Aris R, and Keller KH. Effects of cell Motility and chemotaxis on growth of Bacterial Populations. Biophys.J. 40:209-219, 1982.

[16] Lauffenburger D and Calcagno P. Competition between two microbial populations in a nonmixed environment: Effect of cell random motility. Bio.tech. and Bio.eng. xxv:2103-1225, 1983.

[17] Matsushita M, Wakitaa J, Itoha H, Watanabea K, Araia T, Matsuyamab T, Sakaguchic H and Mimurad M. Formation of colony patterns by a bacterial cell population. Physica A: Statistical Mechanics and its Applications 274:190-199, 1999.

[18] Matsushita M, Hiramatsu F, Kobayashi N, Ozawa T, Yamazaki Y and Matsuyama T. Colony formation in bacteria:experiments and modeling. Biofilms 1:305-317, 2004.

[19] Mimura M, Sakaguchi HF, and Matsushita M. Reaction-diffusion modeling of bacterial colony patterns. Physica A stat mech Appl. 282:283-303, 2000.

[20] Murray JD. *USA TEX*, Mathematical Biology 1,3rd Ed., 2002.

[21] Nowaczyk K, Juszczak A, Domka F. Microbiological Oxidation of the waste Ferrous Sulphate. Polish Journal of Environmental Studies 6:409-416, 1999.

[22] Patlak CS. Random walk with persistence and external bias. Bull.Math.Biophys. 15:311-338, 1953.

[23] Saunders PT, Bazin MJ . On the stability of food chains. J.Theor. Biol. 52:121-142, 1975.

[24] Shepard RND and Sumner DY. Undirected motility of filamentous cyanobacteria produces reticulate mats. Geobiology 8:179-190, 2010.

[25] Skerker JM and Berger HC. Direct observation of extension and retraction of type IV pili. PNAS 98:6901-6904, 2001.

[26] Simonsen L. Dynamics of plasmid transfer on surfaces. J. general microbiology 136:1001-1007, 1990.

[27] Tokita R, Katoh T, Maeda Y, Wakita JI, Sano M, Matsuyama T, and Matsushita M. Pattern Formation of Bacterial Colonies by Escherichia coli. J. Phys. Soc.Jpn. 78:074005 (6 pages), 2009.

[28] Wei Y, Wang X, Liu J, Nememan L, Singh AH, Howie H, and Levin BR. The Population and Evolutionary of Bacteria in Physically Structured Habitats: The Adaptive Virtues of Motility. PNAS 108: 4047-4052, 2011.

[29] Wimpenny JT. CRC handbook of laboratory model systems for microbial ecosystems, 2, 1998.

[30] Youderian P. Bacterial motility: Secretory secrets of gliding bacteria. Current Biology 8:408-411, 1998.

[31] Ishihara A, Segal JE, Block SM and Berg HL (1983)Coordination of flagela on filgmentous cells of Escherichia Coli.. J.Bacteriology 155:228-237, 1983.

[32] Taylor BL and Koshlard DE. Reversal of flagella rotation in Monotrichous and Peritrichous bacteria: Generation of changes in direction.J.Bacteriology 119:640-642, 1974.

[33] Cantrell RS, Cosner C, and Lou Y. Evolutionary stability of ideal free dispersal strategies in patchy environments. J. Math. Biol. DOI: 10.1007/s00285-011-0486-5, 2011.

[34] Dockery J, Hutson V, Mischaikow K, and Pernarowski M. The evolution of slow dispersal rates: a reaction-diffusion model. J. Math. Biol. 37:61-83, 1998.

[35] Hutson V, Mischaikow K, and Polacik P. The evolution of dispersal rates in a heterogeneous time-periodic environment. J. Math. Biol. 43:501-533, 2001.

[36] Kirkland S, C.-K. Li C.K, and Schreiber S.J. On the evolution of dispersal in patchy environments. SIAM J. Appl. Math. 66:1366-1382, 2006.

[37] Lcenhour CR, Arnold J, Medvedovic M, Cushion MT. Competitive coexistence of two Pneumocystis species. Infect Genet Evol. 6(3):177-86, 2006.

[38] Pigolotti S, Cencini M. Coexistence and invasibility in a two-species competition model with habitat-preference. J. Theor. Bio. 265:609-617, 2010.

[39] Wei Y, Kirby A, and Levin BR. The Population and Evolutionary Dynamics of Vibrio cholerae and Its Bacteriophage: Conditions for Maintaining Phage-Limited Communities. The American Naturalist, 178(6), 715-728, 2011.

[40] Jones DA, Smith HL, Thieme HR, and Gergely Röst. On Spread of Phage Infection of Bacteria in a Petri Dish. SIAM J. Appl. Math., 72(2), 670-688, 2012.

[41] Smith HL and Thieme HR. A Reaction-diffusion system with time-delay modeling virus plaque formation. Canadian Applied Mathematics Quarterly, 19, 385-399, 2011.

[42] Sulakvelidze A, Alavidze Z,and Morris JG. Bacteriophage Therapy. Antimicrob Agents Chemother, 45(3): 649659, 2001.

[43] Smith HL and Thieme HR. Persistence of bacteria and phages in a chemostat. J. Math. Biol., 64:951979,2012.

[44] Brssow H. Phage therapy: the Escherichia coli experience. Microbiology, 151 : 7 2133-2140, 2005.

[45] Jones DA, Smith HL. Bacteriophage and Bacteria in a Flow Reactor. Bull Math Biol., 73(10): 2357-2383, 2011.

[46] Beretta E, Sakakibara H, and Takeuchi Y. Analysis of a Chemostat Model for Bacteria and Bacteriophage. Vietnam Journal of Mathematics, 30: 459-472, 2002.

[47] Lenski RE. Dynamics of Interactions between Bacteria and Virulent Bacteriophage. ADVANCES IN MICROBIAL ECOLOGY, 10: 1 - 44, 1988.

[48] Weitz JS, Hartman H, and Levin SA. Coevolutionary arms races between bacteria and bacteriophage. PNAS, 102: 9535-9540, 2005.

[49] Loc-Carrillo C and Abedon ST. Pros and cons of phage therapy. Bacteriophage, 1(2): 111-114, 2011.